ADVANCED MASTERS IN STRUCTURAL ANALYSIS
OF MONUMENTS AND HISTORICAL CONSTRUCTIONS

Master's Thesis

Oscar Minor García

The Impact of the Connection Stiffness on the Behaviour of a Historical Steel Railway Bridge

This Masters Course has been funded with support from the European Commission. This publication reflects the views only of the author, and the Commission cannot be held responsible for any use which may be made of the information contained therein.

Czech Republic | 2017

CZECH TECHNICAL UNIVERSITY IN PRAGUE
Faculty of Civil Engineering
Thákurova 7, 166 29 Prague 6, Czech Republic

MASTER'S THESIS PROPOSAL

study programme: Civil Engineering

study branch: Advanced Masters in Structural Analysis of Monuments and Historical Constructions

academic year: 2016/2017

Student's name and surname: Oscar Minor Garcia

Department: Department of Mechanics

Thesis supervisor: Pavel Ryjáček

Thesis title: The impact of the connection stiffness on the behaviour of a historical steel railway bridge.

Thesis title in English see above

Framework content: Analysis of the rotational stiffness of the connections in a steel bridge, and a parametric analysis to determine the impact in the general behaviour of the structure, of using either the calculated stiffnes, the pinned, or rigid assumptions for different types of elements.

Assignment date: 7/04/2017 Submission date: 06/07/2017

If the student fails to submit the Master's thesis on time, they are obliged to justify this fact in advance in writing, if this request (submitted through the Student Registrar) is granted by the Dean, the Dean will assign the student a substitute date for holding the final graduation examination (2 attempts for FGE remain). If this fact is not appropriately excused or if the request is not granted by the Dean, the Dean will assign the student a date for retaking the final graduation examination, FGE can be retaken only once. (Study and Examination Code, Art 22, Par 3, 4.)

The student takes notice of the obligation of working out the Master's thesis on their own, without any outside help, except for consultation. The list of references, other sources and names of consultants must be included in the Master's thesis.

.....
Master's thesis supervisor

.....
Head of department

Date of Master's thesis proposal take over: July 2017

OSCAR MINOR GARCIA
Student

This form must be completed in 3 copies – 1x department, 1x student, 1x Student Registrar (sent by department)

No later than by the end of the 2nd week of instruction in the semester, the department shall send one copy of BT Proposal to the Student Registrar and enter data into the faculty information system KOS.

DECLARATION

Name: Oscar Minor García

Email: ominorg@gmail.com

Title of the Msc Dissertation: The impact of the connection stiffness on the behavior of a historical steel railway bridge.

Supervisor(s): Pavel Ryjáček

Year: 2017

I hereby declare that all information in this document has been obtained and presented in accordance with academic rules and ethical conduct. I also declare that, as required by these rules and conduct, I have fully cited and referenced all material and results that are not original to this work.

I hereby declare that the MSc Consortium responsible for the Advanced Masters in Structural Analysis of Monuments and Historical Constructions is allowed to store and make available electronically the present MSc Dissertation.

University: Czech Technical University in Prague

Date: 05 of July, 2017

Signature: _____

This page is left blank on purpose.

A mi familia y amigos, 7 horas distantes pero siempre conmigo.

This page is left blank on purpose.

ACKNOWLEDGEMENTS

I would like to thank Pavel Ryjáček for the help and useful comments throughout this process, to Filip Kramolis for sharing the model, to Robert Jara for the technical help, to Filip Kutina for his ideas and kind remarks, to the staff in the front desk at čvut for struggling each day with me and the keys, to Brian for showing me a world from a different perspective, and to my partners in the SAHC master, always with a smile willing to help.

This work was possible thanks to the scholarship from the European Commission, in constant effort to increase and spread the knowledge to preserve the historic building heritage in all parts of the world, thank you.

Acknowledgment to Prof. Pere Roca for sharing his dedication and care for historical constructions.

This page is left blank on purpose.

ABSTRACT

Many of the steel railway bridges in Europe and other parts of the world were built in the 19th century and are still under service today. Truss structures were very popular for bridges. The considerations for its design were that the connections were pinned, so the elements are loaded only by axial forces. In reality, the connections were solved with rivets and large plates that prevent the rotation between elements, allowing the transmission of bending moments. In some cases, these second order forces induce important stresses in the structure.

In this work, the analysis of the stiffness of different types of joints is done by using the IDEA StatiCa software. Then, the results for each joint are applied in the general model of the bridge, built in CSI Bridge. Finally, a parametric analysis is done by changing the joints in different groups of elements, to determine the impact on the general behavior. The comparison is done on both, the truss and the deck; and the parameters used to compare are the maximum stresses and displacements. The bridge chosen as a typical example of this type of structures is the steel railway bridge over the Vltava River in Vyšehrad.

A linear relation between the stiffness and the number of rivets was observed from the analysis of the joints stiffness. Also, this linear behavior was observed for the moment of inertia of the section. The values of stiffness obtained, and the geometrical characteristics of the joint are also presented.

The connection condition with most impact in the general behaviour of the bridge is the crossbeam, affecting not only the deck but also the stresses in the truss.

This page is left blank on purpose.

ABSTRAKT

Mnoho ocelových železničních mostů v Evropě a dalších částech světa bylo postaveno v 19. století a je dodnes stále v provozu. jedná se zejména o příhradové konstrukce, které se navrhovaly jako zatížené pouze osovými silami. Ve skutečnosti se však styčníky řešily nýtováním a příložkami či styčníkovými deskami, které zabraňují otáčení mezi prvky, což umožňuje přenos ohybových momentů. V některých případech vyvolávají tyto momenty významná namáhání.

V této práci se analyzuje tuhost různých typů styčníků pomocí softwaru IDEA StatiCa. Výsledky pro každý spoj jsou pak použity v obecném modelu mostu, který je proveden v CSI Bridge. Následně se provádí parametrická analýza změnou tuhosti a sleduje se napětí a další veličiny na trámu i na mostovce. Zkoumání je založeno na příkladu železničního mostu přes řeku Vltavu ve Vyšehradě.

Dále byl odvozen lineární vztah mezi tuhostí a počtem nýtů a jsou uvedeny i výsledné tuhosti styčníků

This page is left blank on purpose.

RESUMEN

Gran cantidad de los puentes ferroviarios en Europa y otras regiones del mundo fueron construidos durante el siglo XIX y están en servicio hasta nuestros días. El uso de armaduras fue muy popular para la estructuración de puentes. Las consideraciones para el diseño fueron que las conexiones son articuladas de forma que los elementos están sujetos únicamente a fuerzas axiales. En la realidad, las conexiones fueron resueltas con remaches y grandes placas que previenen la rotación entre elementos, permitiendo la transmisión de momentos flexionantes. En algunos casos, estas fuerzas de segundo orden pueden provocar esfuerzos significativos en la estructura.

En este trabajo, el análisis de la rigidez en diferentes tipos de conexiones es hecho usando el software IDEA StatiCa. Los resultados para cada conexión fueron aplicados en el modelo general del puente, creado en CSI Bridge. Finalmente, un estudio paramétrico es hecho modificando las condiciones de conexión de algunos elementos, con el fin de determinar el impacto que tiene cada una en el comportamiento general de la estructura. Se hace la comparación tanto en la armadura como en la plataforma, usando los esfuerzos máximos y los desplazamientos como parámetros de comparación. El puente elegido para este análisis, por ser un ejemplo típico de este tipo de estructuras es el puente de acero sobre el Río Vlatava, en Vyšehrad.

Una relación lineal entre la rigidez y el número de remaches fue observada. Así mismo, un comportamiento lineal se obtuvo con el momento de inercia de la sección del elemento. Los valores de la rigidez obtenida y las características geométricas de las juntas analizadas también se presentan.

De igual forma, en este trabajo se observa que cada elemento es influenciado por la rigidez en su conexión, siendo las vigas transversales las que influyen en mayor medida en el comportamiento general de la estructura, influyendo no sólo en la plataforma sino también en las armaduras.

This page is left blank on purpose.

TABLE OF CONTENTS

This page is left blank on purpose.

LIST OF FIGURES

LIST OF TABLES

1. INTRODUCTION

The purpose of this work is to determine the impact of the stiffness of the connections in the general behaviour of a steel railway bridge. As a case study, the analysis is done for the connections on the steel railway bridge over the Vltava River in Vyšehrad.

This study is divided in two sections. The first part is focused on determining the rotational stiffness of various elements in the bridge: diagonals in the truss, and crossbeams and stringers in the deck of the bridge. The second part consists on applying the results obtained for each joint, in the general analytical model of the bridge. A parametric analysis is done on the general model to observe how the different conditions on the connections influence in the behaviour of the general bridge. Two zones are studied: the truss and the deck. In both zones the stresses and the displacements are checked. The analysis is done for static load cases only: self-weight, and a live load on three different locations.

A load test was performed on the bridge; therefore, the analytical model studied here may be in the future calibrated and compared with those results from the test. Additionally, this work is intended to serve as a help in the analysis of connections of similar steel bridges.

Historically, truss systems have been analysed as if the elements are loaded only by axial forces. This is true only if the connections are pinned, but in reality, especially for steel structures connected with rivets, connections restrain significantly the rotation between elements, allowing the transmission of bending forces. Second order stresses due to bending moment can be critical.

2. GOALS

The goals of this work are:

- To model different configurations of joints, and determine the rotational stiffness of the different elements.
- To apply the results of the stiffness for each joint in the general model of the bridge taken as a case study.
- To make a parametric analysis in order to determine the impact of the connection conditions of different elements in the behaviour of the complete bridge.

This page is left blank on purpose.

3. STATE OF THE ART

Truss systems became very popular in the nineteenth century to span long lengths without a substantial increment in the weight of the structure. This characteristic allowed a wide use of these systems for roofs on industrial buildings, and for bridges. Different configurations were proposed and patented, being each one more efficient for specific load conditions. For long span bridges, the most used configurations are parallel or polygonal chord trusses [Figure 1]. Normally, diagonals have a better performance when they are inclined 45 degrees. For deep trusses, configurations like K or diamond are used to achieve an inclination closer to 45 degrees. Besides the type of truss, the bridges can be deck type, with the way passing over the truss; trough type, where the carriage is resting in the lower chords, or semi-through type, where the deck is between lower and upper chords. In all cases, the span is divided into regular sections where crossbeams are connected to transfer the loads to the nodes. [1] [2]

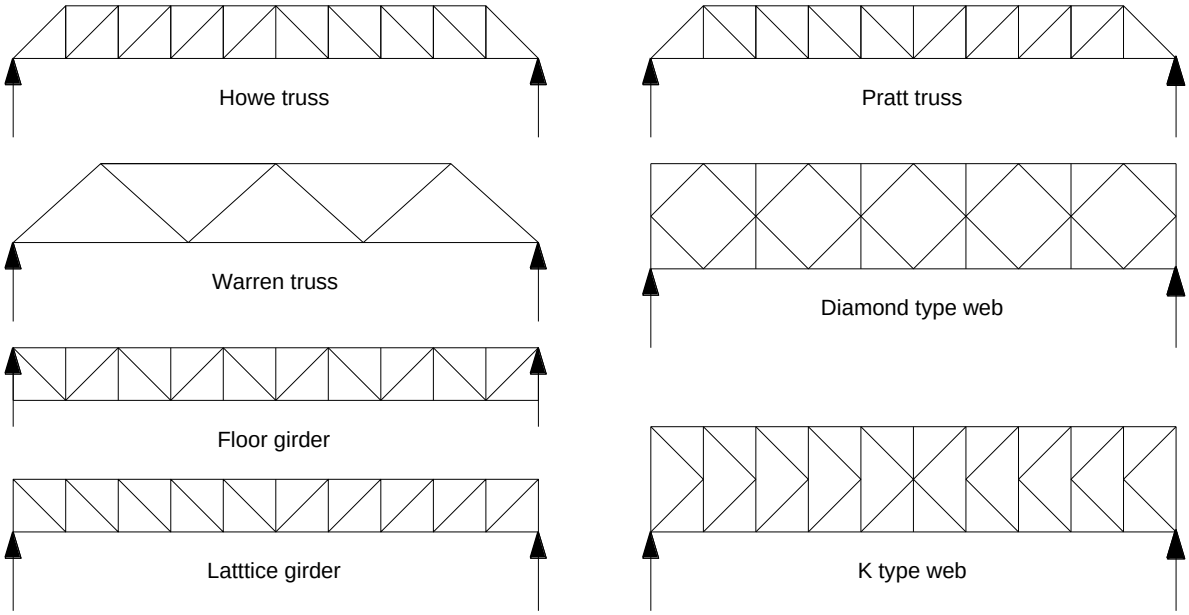

Figure 1. Types of parallel chord trusses [1] [2].

In a trussed structure, the members are subjected principally to axial forces: tension and compression, which results in a nearly uniform distribution of stresses throughout the entire section, maximizing the use of the properties of the material. This condition was only possible by taking certain assumptions for instance, the loads are applied on the nodes, and the members have pinned connections, with no transfer of shear force or flexural moment. Together with the correct supports, normally simply supported on the two ends, the result is an isostatic structure easy to calculate using the method of the joints or the method of the sections, both suitable for hand calculation.

In practice, the supports can be solved using a simply supported configuration that allows certain level of rotation, not far from the pinned assumption. But the connections between elements are usually made of more than one fastener. In fact, they are normally solved using large gusset plates with several fasteners that restrain the rotation between elements. Furthermore, to facilitate the construction, chords are typically made by continuous members, able to transmit flexural forces. The stiffness in joints, the continuity of the chord and the partial end fixity in connections are points that broaden the differences between the model used for analysis and the real behaviour [3]. The effect of these facts can be reflected on the stresses in the elements and in the deformation.

Moreover, in the nineteenth and the beginning of the twentieth centuries the connections were generally made with rivets. The riveting process consisted in heating the rivet until high temperatures, placing it on the holes on the plate, and hammering to form the second head. As the rivets cools, it shrinks and applies a clamping force on the connecting plates [4]. Thus, the joint can be considered as a solid piece of metal, as there is no relative displacement between plates. This characteristic also influences in the rotational properties of the joint [4]. In addition, riveted connections present a considerable amount of rigidity, but there are several uncertainties to account for this in the design of a joint [5].

Experiments to investigate the behaviour of riveted connections were done after the collapse of the first Quebec Bridge in 1907. A linear response for initial small load reversals was observed, followed by a low stiffness-slipping zone with higher load amplitude [6].

In the specific case of the Quebec Bridge, besides the buckling of members that was the main cause of failure, the connections played also an important role. They were bolted to allow small deflections before they were permanently riveted when the full load was applied [7].

The effect of restrain in joints was shown back in 1934 in reference [8]. Concrete structures brought back the discussion of connections being neither free nor continuous, as stated in reference [5], where it is mentioned that welded structures share the characteristic of continuity with concrete.

Several studies have been made on the effect of the stiffness in framed structures, where there is a relevant relation between the rigidity of the connection and the lateral deformation of the frame, and this is especially important in seismic design, where high ductility is taken into consideration as a dissipative mechanism by the plastic formation of hinges. A wide description of past investigation of semi-rigid connections can be found in reference [9]

The general behaviour of the semi-rigid connections in trusses is described in reference [9]. Pinned connections result in only axial force on the elements. Semi-rigid connection produces bending moment and shear force, therefore, secondary stresses. Moments and shear forces increase for increasing connection percentages being the most critical in the rigid connection. Axial forces are practically not affected by the connection percentage. Vertical displacements decrease by increasing

connection percentages. Finally, the higher the connection percentage, the higher the stresses in truss members.

Most of the fatigue damage observed on bridges is on the connections between the primary members, generally due to secondary effects [10]. As noted in [11] double angle shear connections can develop important bending stresses, contrary to the common assumption that these types of connections allow the rotation of the stringer end without developing appreciable moment. Furthermore, it has been observed that the angle fillet and the rivet head-to-shank junction are critical locations where cracks may start [10] [12]

There are many factors that influence in the study of fatigue of structures, especially in bridges. For instance, the characterization of the portion of the fatigue that is due to train loads in the past. In the past, the locomotive was the heaviest part of the train and it was followed for lighter wagons while in recent trains, the heavier wagons are those following the locomotive [13]

A significant number of bridges were built in the nineteenth and the beginning of the twentieth century, before standardisation and without concerning about fatigue behaviour. So far, most of the bridges seem to be able to resist the current load demands and traffic, but to avoid replacing the structures, and minimize the number of repairs, it is important to better understand the behaviour of these structures. [13]

3.1 The rotational stiffness

A connection is the part of the structure that transmits the forces from one member to another. These forces can be axial force, shear, bending moment, torsion or a combination of them as it is usually the real case. Each of these forces produces a deformation on the structure, but the largest deformation is the rotation caused by the bending moment. [14]

Historically, joints have been analysed and designed under the consideration that they are either pinned or fully rigid. These two hypothetical cases depend on the relative rotation that occurs between the connecting elements; but they represent two extreme conditions of the real behaviour. It is common to express the rotational deformation as a function of the bending moment applied in the connection, obtaining a moment-rotation curve as it is shown in Figure 2, with examples of curves for different types of connections. A fully pinned behaviour would be in the horizontal axis and, accordingly, the rigid behaviour in the vertical axis; but in real structures the behaviour falls always somewhere in between, as it can be observed for the different types of connections in Figure 2. The T-stub connection for example, is more rigid as it can resist high levels of moment with small rotation. On the other side, single web angle is close to the pinned connection allowing large rotation with minimal transmission of bending moment. [14]

Moment-curvature diagrams are usually obtained from physical tests, but for the analysis and design, it is possible to idealize the behaviour of the connection with a linear relation between moment and rotation, followed by a state in which the rotation increases without resisting any more bending moment. This linear relationship is defined as the rotational stiffness S_j [Figure 3-C].

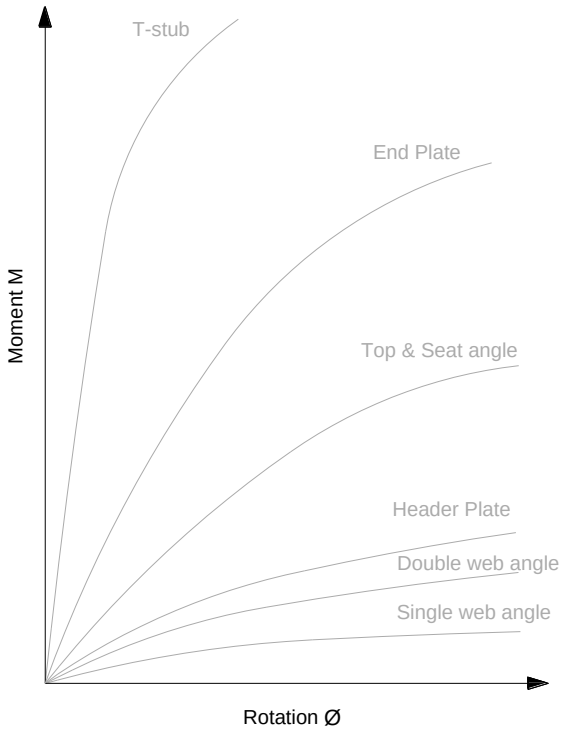

Figure 2. moment-rotation curves for different types of connectionns. [14]

3.2 Clasification of joints according to Eurocode

According to Eurocode EN 1993-1-8 [5.2.2.1] [15], the joints may be classified as rigid, normally pinned or semi-rigid, depending on its rotational stiffness [Figure 3-A]. The code provides boundaries between these classifications.

For a connection to be considered rigid it must satisfy:

$$S_{j,ini} \geq \frac{k_b \cdot E \cdot I_b}{L_b} \tag{1}$$

Where

- k_b = 8, for frames where bracing systems reducing horizontal displacements at least 80%
- k_b = 25, for other frames, in which in every storey K_b/K_c > 0.1

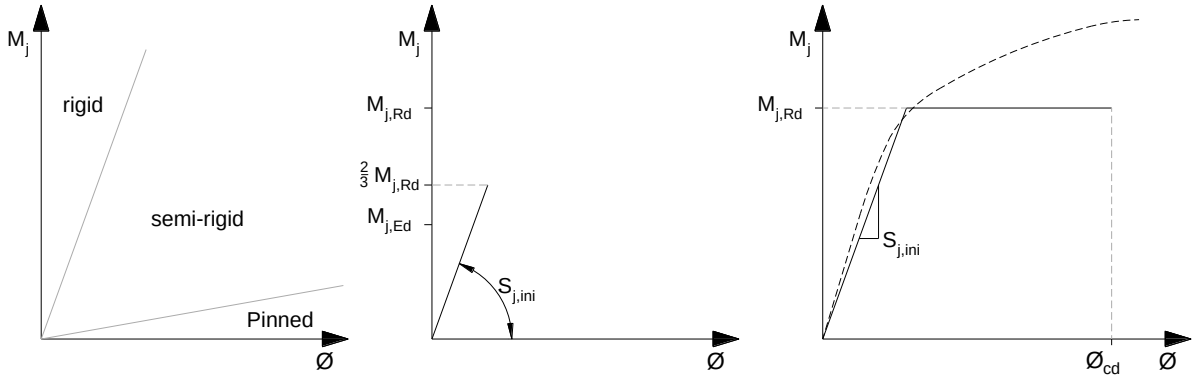

Figure 3. Typical diagram moment curvature showing the classification of connections according to the stiffness

For the case of the pinned connection, the rotational stiffness must be:

$$S_{j,ini} \leq \frac{0.5 \cdot E \cdot I_b}{L_b} \tag{2}$$

Where E is the elastic modulus, I_b the second moment of are of the beam, L_b the span center to center of the beam, K_b is the mean value of I_b/L_b for all the beams at the top of 'that storey' and K_c is the mean value of I_c/L_c for all the columns in 'that storey'.

As it can be seen from the parameter k_b, this classification was made for joints in structural frames. The behaviour in frames and braced frames is different; therefore, the classification should be different as noted in [16]. A truss connection can be seen as a particular case of a frame system, especially similar to a braced frame.

According to Eurocode EN 1993-1-8 [6.3.1 (1)] [15], 'the rotational stiffness should be determined from the flexibilities of its basic components, each represented by an elastic stiffness coefficient k_i'

The rotational stiffness Sj is computed as:

$$S_j = \frac{E \cdot z^2}{\mu \cdot \sum_i \frac{1}{k_i}} \tag{3}$$

Where the z is the lever arm, and μ is the stiffness ratio $S_{j,ini}/S_j$

Additionally, the Eurocode EN 1993-1-8 presents formulas to calculate the stiffness of basic joint components (table 6.111 of Eurocode EN 1993-1-8 [15]).

The philosophy for the determination of the bearing capacity and the stiffness of the joint included in the Eurocode EN 1993-1-8 is based on the Component Method (CM). This method considers the joint

as a system of interconnected components, and consists on: 1) the identification of the active components on the connection; say column web in shear, column web in compression, and column web in tension. 2) the response of each of the components is obtained using the corresponding formulas, and finally 3) the components are assembled to obtain the behaviour of the whole connection.

Figure 4 shows schematically the process of the component method for an end-plate connection with one beam and one row of bolts in compression and two rows of bolts in tension. The first part is the classification of the different components in the connections; in this case there are 8 components. The second step is the characterization of the stiffness of each element separately. In this step, a distribution of forces into each of the internal components needs to be done satisfying the equilibrium in the joint. Finally, the behaviour of the connection is obtained by assembling the individual components. [17]

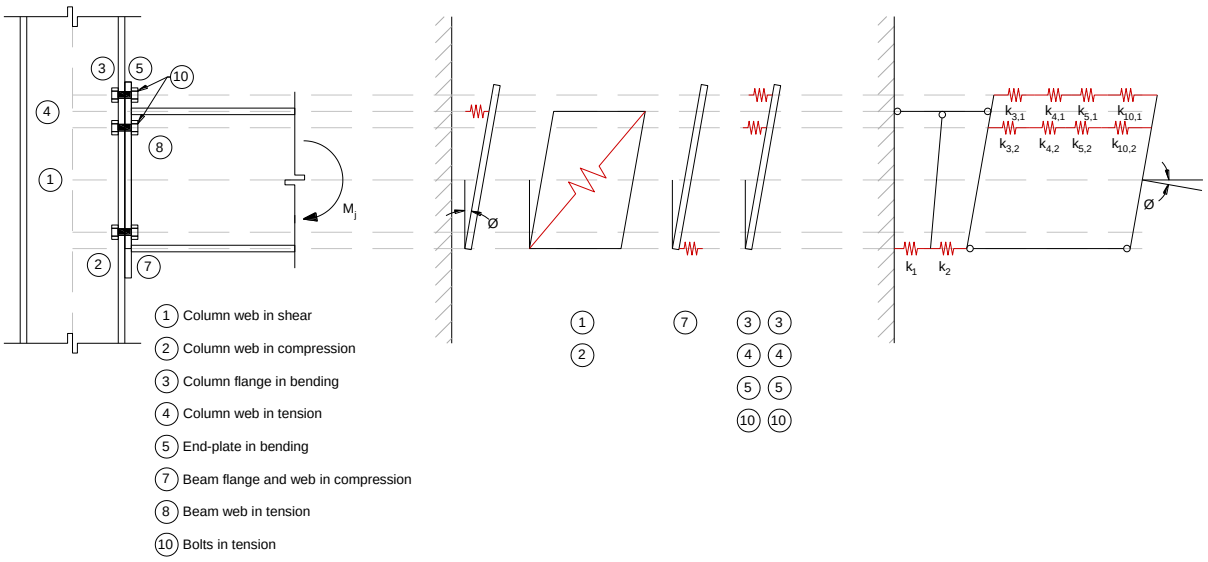

Figure 4. Schematical representation of the Component Method. Based on [17]

Eurocode provides rules for obtaining the strength, stiffness and rotation capacity for a limited number of components. The formulas proposed are specified for H and I sections and no procedure is proposed for hollowed sections. In the bridge used for the present analysis, the elements are neither H, I nor hollow but a mix of angles and plates.

3.3 Previous investigation on joint stiffness

A technical report studying the axial and rotational stiffness in the connections of a steel railway bridge was made by SUDOP on the bridge Tábor-Písek over the Vlatava River in the km 41,791. [18] This report includes the characterization of the connections and the modelling of the different joints on the software IDEA StatiCa version 5.

The bridge in which this report is focused on consists of three lattice trusses with a span of 84.4 m each, built in 1886. The elements are made of angles and plates. The connections are made with rivets and plates [Figure 5]. The results presented are the values of stiffness for the different elements and the calculation of the percentage of rigidity.

This report is the principal reference for the present study.

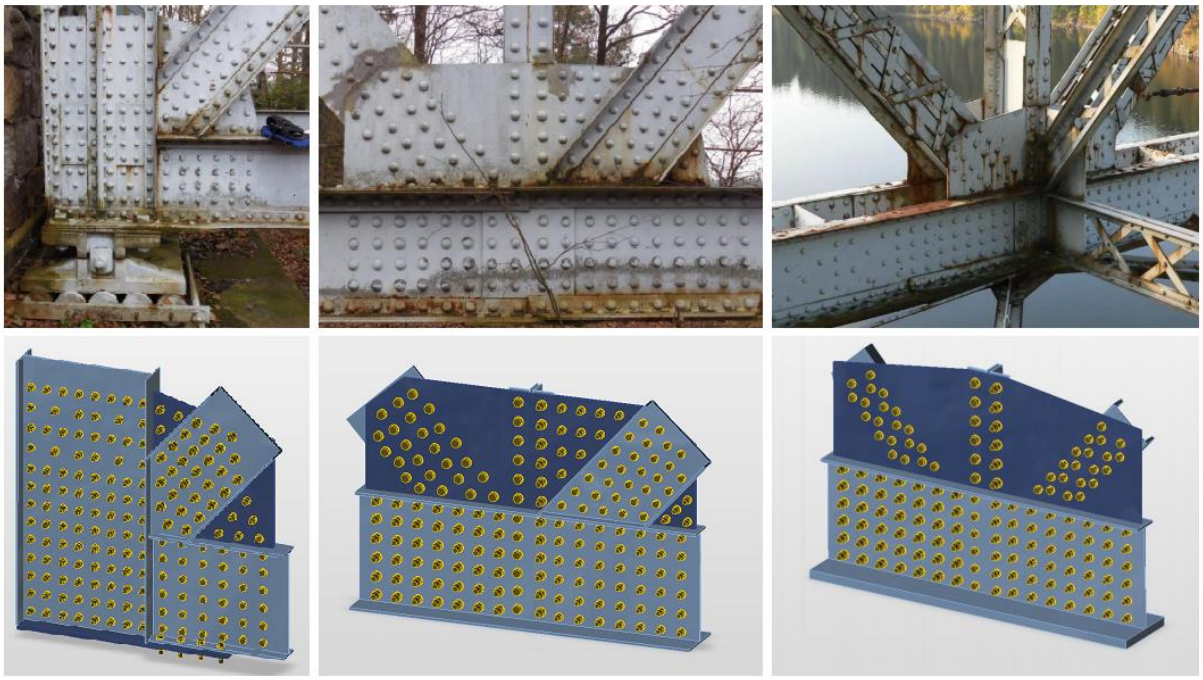

Figure 5. Types of connections analysed in the report on the Tábor – Písek bridge ref. [18]

This page is left blank on purpose.

4. ANALYSIS OF JOINTS STIFFNESS

Across Europe and other regions there are several number of bridges built around the same age during the boom of railways construction at the end of nineteenth century, many of which share characteristics of geometry, materials and type of connections. To investigate the joints and its influence on the general behaviour on steel railway bridges, the railway bridge located over the Vltava River near Vyšehrad is a representative example of the steel trussed structures connected with rivets, with a large variety of configuration of joints. Besides, the location and the availability of information facilitate the study of this structure.

4.1 Case study – Steel Railway Bridge

There is no official name for the steel railway bridge that connects Vyšehrad and Smichov, over the Vltava River in the center of Prague. It is usually referred to as *železničním mostu pod Vyšehradem*. The bridge has a total length of 218 m and is divided in three sections, each one formed by polygonal arched trusses supported on masonry pillars over the river bed. In the Vyšehrad end, the bridge is continued by 4 spans of 19 m each made of steel girders; while in the Smichov side, it is followed by an embankment. The structure allocates two railways between the trusses, and pedestrian ways in cantilever at both sides. Since its construction in 1901, it has become part of the urban landscape of the city [Figure 6].

The steel railway bridge presents its characteristic reddish colour caused by the constant process of rusting accumulated throughout more than hundred years of use. To analyse and determine the level of safety of the structure, different studies had been carried out recently, including general surveys, and one load test. The present work is intended to help in the construction of the model for the assessment of the current state of the bridge, which later is to be calibrated with the results from the load test.

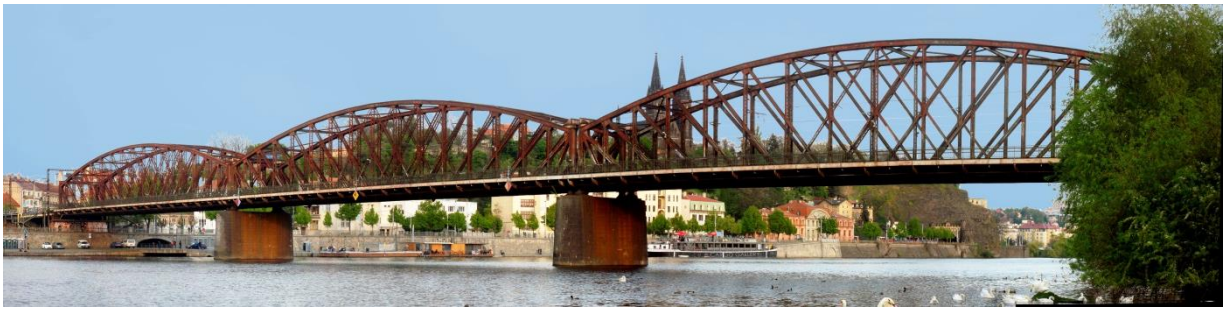

Figure 6. Steel Bridge near Vyšehrad

The analysis of the stiffness in the different types of connections is performed after they are grouped according to their geometrical configuration. The connections are analysed with models created in the software IDEA StatiCa. The results from the analysis of the connections are then used in the general model of the structure to investigate their impact on the behaviour of the bridge.

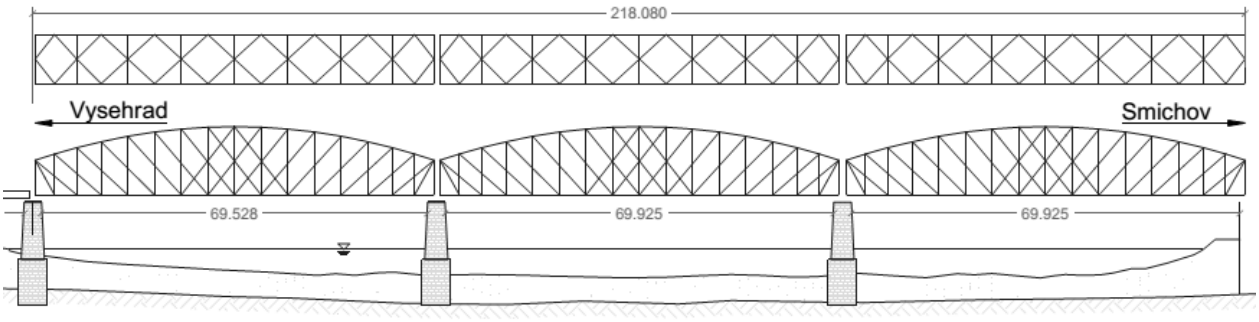

Figure 7. Longitudinal dimensions of the bridge

4.1.1 Historic background

Most of the railway system in the Czech Republic was built during the monarchy of the Austro-Hungarian Empire. The railway transportation was introduced in the Czech territory in the first third of the nineteenth century with a horse-drawn railway between Linz (Austria) and Ceske Budejovice, as an alternative to a proposal for a channel to join Vltava River with the Danube. The following decades other lines were proposed and constructed joining major cities to satisfy the need for transportation of freight, bringing economic development to the areas they crossed. The first formal train between Vienna and Prague was opened on 1845, and the route from Prague to Dresden was completed in 1851. The defeat of Austria against Prussia in 1866 proved the importance of transportation, thus the construction of new lines was promoted in order to build a national railway system throughout the empire. [19] [20]

The steel railway bridge over the Vltava river replaced a previous structure built around 1871 by the *Harkot's bridge building company* in Duisburg to connect the Franz Joseph I station (now the main station) with the Western Railway Station (now Smichov station). This bridge was made of steel in a

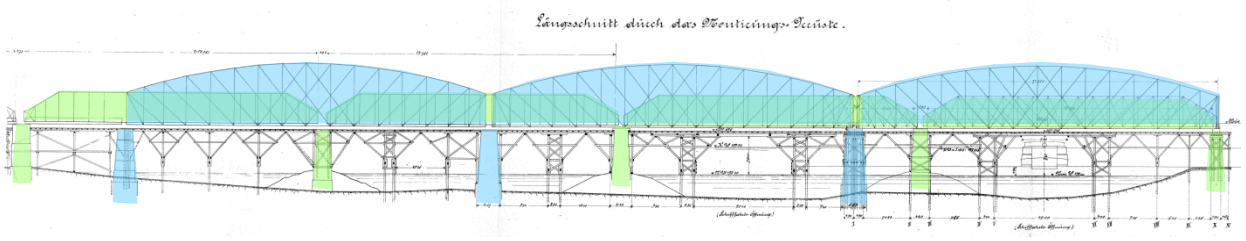

Figure 8. Original plan showing the superposition of the old and the new bridge.

Pratt trussed configuration with 5 spans and it allocated only one track, which was used at the beginning for transportation of goods. Passenger trains were not introduced until October 1888 and the gradually increase in the traffic soon exceeded the capacity of the single track bridge by the end of the nineteenth century and a new structure was proposed. [21]

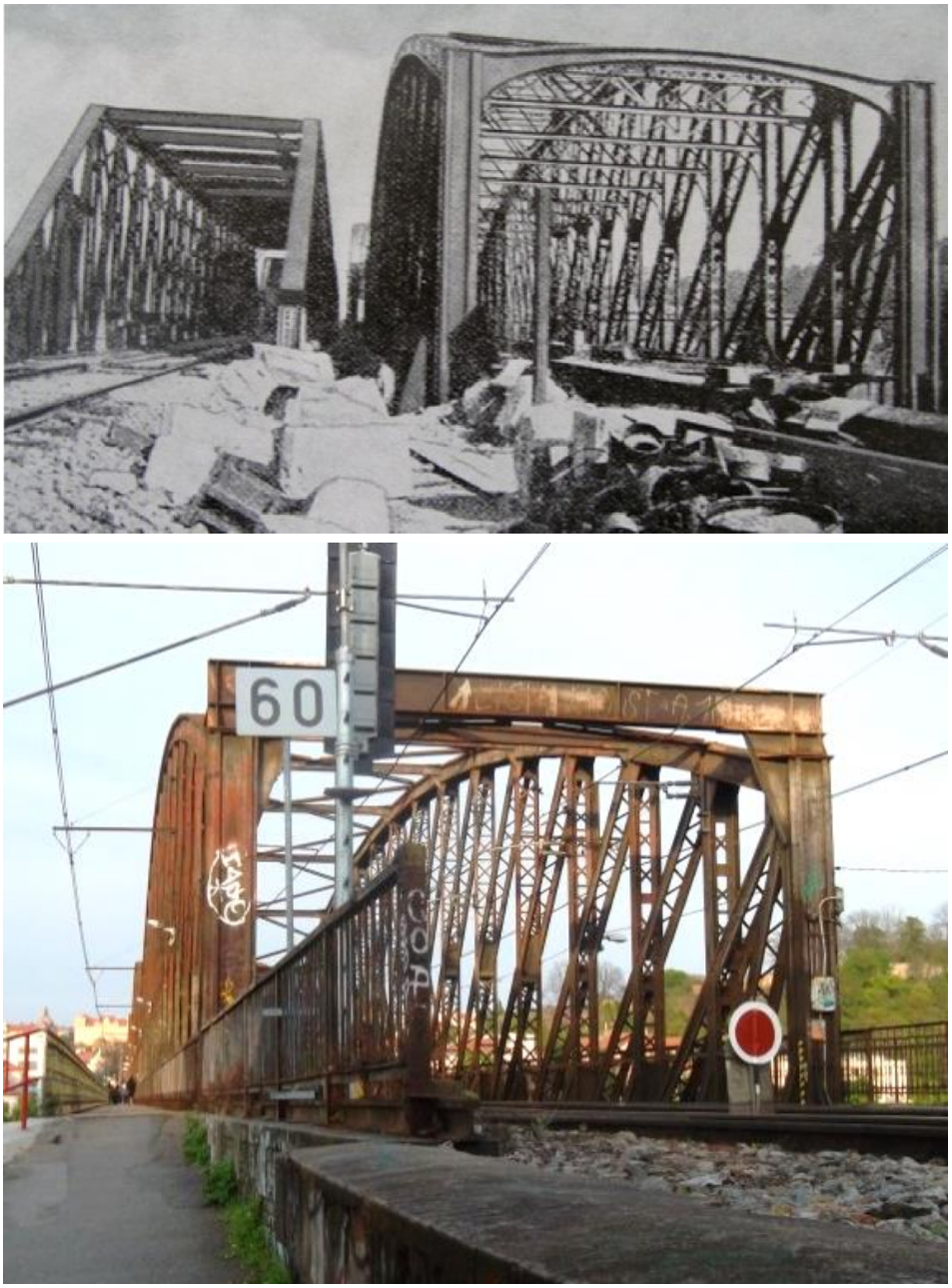

Figure 9.-A. Original single track bridge and the new bridge during the construction (ca. 1901) [21]. B. Current state of the bridge in the Smichov end

Figure 10 - A. Locomotive 498.009 1959; B. Locomotive 498.017 in the Smichov end in 1969; C. Locomotive T499.0002 Kyklop in1975; D. Locomotive 498.105 1971. All from ref [22].

The new bridge was planned in such a way that the replacement would take the minimal interruption of the railways traffic. To achieve this, the new structure consisted of three sections with larger spans, supported on two pillars, allowing their construction between the pillars of the old bridge. Figure 8 shows original drawings presenting the superposition of both bridges.

Each of the three sections of the bridge was supplied by different companies: *Czech-Morovian Machine Works*, *Prásilova brothers* and *Ruston's Engineering*, and they were assembled on an auxiliary structure next to the old bridge [Figure 9-A]. Some sources mention that the installation took only two days and three nights, with no interruption of the shipping traffic in the river and with a small pause of the railway traffic for only 60 hours. [21]

4.1.2 Past interventions

The original drawings specify the configuration of all the elements composing the bridge, the majority of which can be found in the present structure. However, there are two major interventions that can be identified after the inspection of the structure complemented with a careful examination of historical photographs.

The first of these modifications is the member that joins the trusses in the upper chord. Original drawings show the trusses being connected in the first frame (frame 0) by an arched beam with variable section, as the one seen in Figure 9-A. This beam was replaced for one I beam with higher depth observed in Figure 9-B. For the consecutive frames, the original drawings specify the upper chords of the trusses being connected with small beams and diagonals forming a transversal truss. This configuration is also observed in Figure 9-A, but in the present structure the connections are made with I beams.

According to reference [22], Figure 10-A is from 1959 and it shows the original configuration of beams in the upper part. Figure 10-B, from 1969 still shows original upper beams but it includes the electrification cables. Figure 10-C is from 1975 and the electric cables can be observed as well as the present beams. Figure 10-D, is dated in 1971 in the same reference, and it shows the current beams in the upper part, but no signs of the electric cables can be seen, which were introduced prior to 1969 if the other photograph date is correct. Taking aside these uncertainties, the upper beams on the bridge were changed around 1970, about the same period of time when the electrification of the line took place.

The second modification from the original drawings is in the deck, where complementary bracing (braking bracing) was added in the midspan and the end frames, as well as some elements restraining the stringers [Figure 12]. This seems to be reinforcement for the deck to allow the transit of heavier trains, and it was built probably not much after the initial construction of the bridge, considering the riveted connections. Unfortunately, no more information could be found in the consulted sources.

Moreover, in very few locations bolts were found, replacing damaged rivets. Figure 11-A shows one example of bolts adjacent to rivets that had lost the head due to the corrosion. Observe that the bolts have started to deteriorate, evidencing the high corrosion on this joint. Figure 11-B shows another location where bolts were observed.

The present study is intended to analyse the current configuration of the bridge, and for this, the geometry was obtained not only from the original drawings but also from the available survey made by SUDOP.

Figure 11. Bolts replacing rivets in different locations.

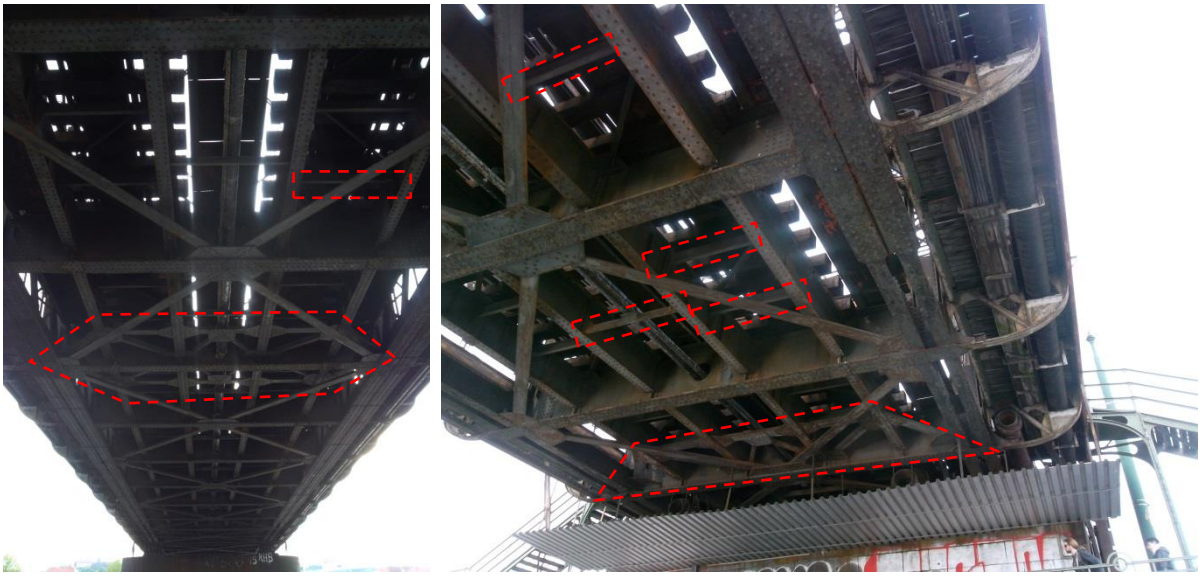

Figure 12. Brake Bracing in the deck.

4.1.3 Geometry

The static system of the steel bridge consists of a pair of trusses joined with perpendicular crossbeams over which the rails are supported.

Each section of the steel railway bridge has a span of 71.72 m and is formed by two trusses in a polygonal Pratt-like with center counter configuration. The height of the vertical elements varies to form the arch shape from 6.25 m in the supports (frame 0), to 12.25 m at the midspan (frame 8). Each truss is made with 17 vertical elements separated 4.80 m in the central part (frames 3 to 8), and 4.40, 4.00 and 3.46 m in the ends. The diagonals are parallel and join three frames, intersecting one vertical element in the middle. The exception is the diagonal 1, which joins only frames 0 and 1. Between frames 6 to 8, the diagonals change direction crossing each other [Figure 14].

Transversally, the trusses are separated 8.8 m, allocating both railways in between. There are pedestrian ways of 1.8 m in cantilever in both sides, resulting in a total width of 12.4 m [see Figure 13]. As discussed previously, the trusses are joined in the upper chords by I shaped sections and diagonal bracing forming diamonds. The deck is formed by the crossbeams of 1.03 m depth at every frame, and four perpendicular stringers of 0.69 m depth. The bracing in the deck is formed by double angles back-to-back.

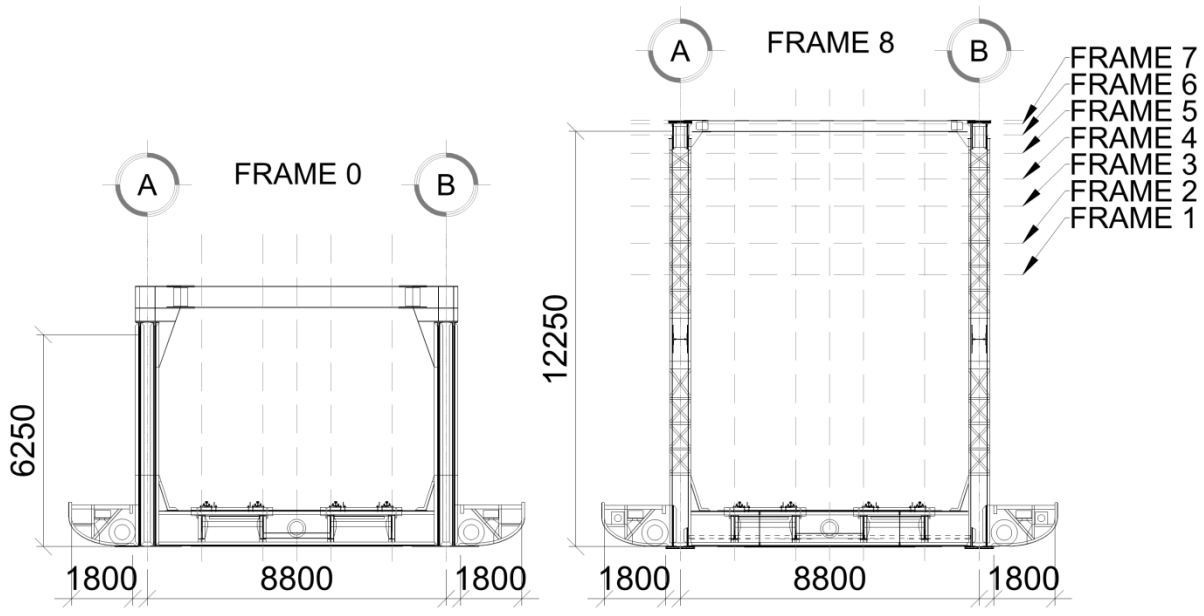

Figure 13. Transversal section of the steel railway bridge.

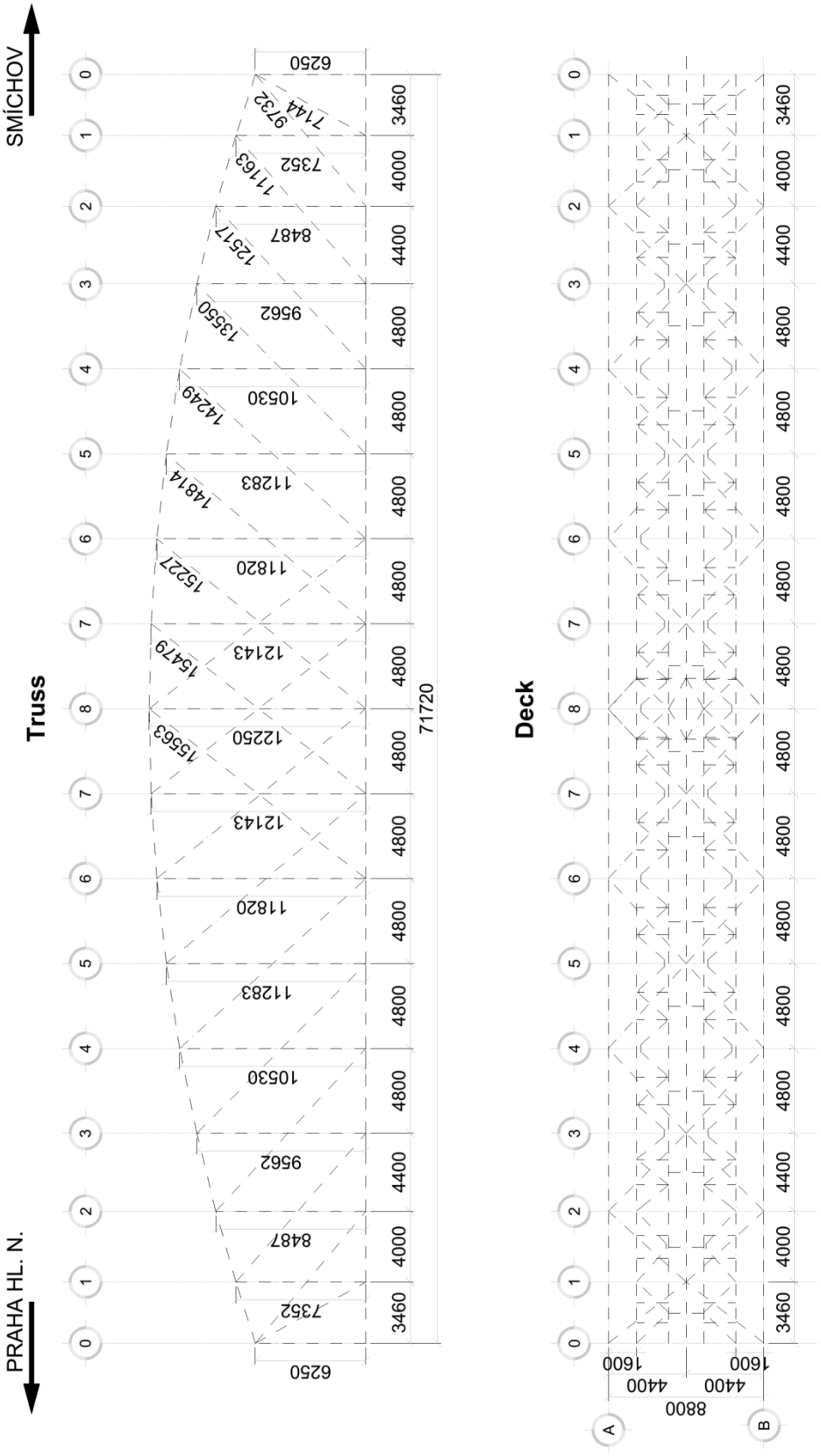

Figure 14. Longitudinal and plan view of the steel railway bridge.

All the original structure is made of angles and plates joined with rivets of three different diameters: 24, 22 and 20 mm. All the vertical elements are made of 4 angles back to back separated by strips forming crosses, except for the first vertical element that is formed by 16 angles and several continuous plates. [Figure 15]

Lower chords are made of a pair of continuous vertical plates of 0.56 m depth with two angles each at the bottom and horizontal plates, increased in number to increase the strength of the section in the central segment of the bridge. Upper chords are similar to the lower chords but with a depth of 0.48 m and a single plate at the top in an inverted U section. Similarly, additional plates are added at the top to get a stronger section in central segments. [Figure 15]

Diagonals are made typically of 4 pairs of back to back angles with perpendicular plates between them, and joined with strips in a cross manner such as in the columns. [see Figure 16]

The typical width of the members in the trusses is 0.44 mm, so the verticals and diagonals are wider or shorter allowing allocating the connecting plates.

The degree of optimization of the original design is such that most of the members are different from frame to frame.

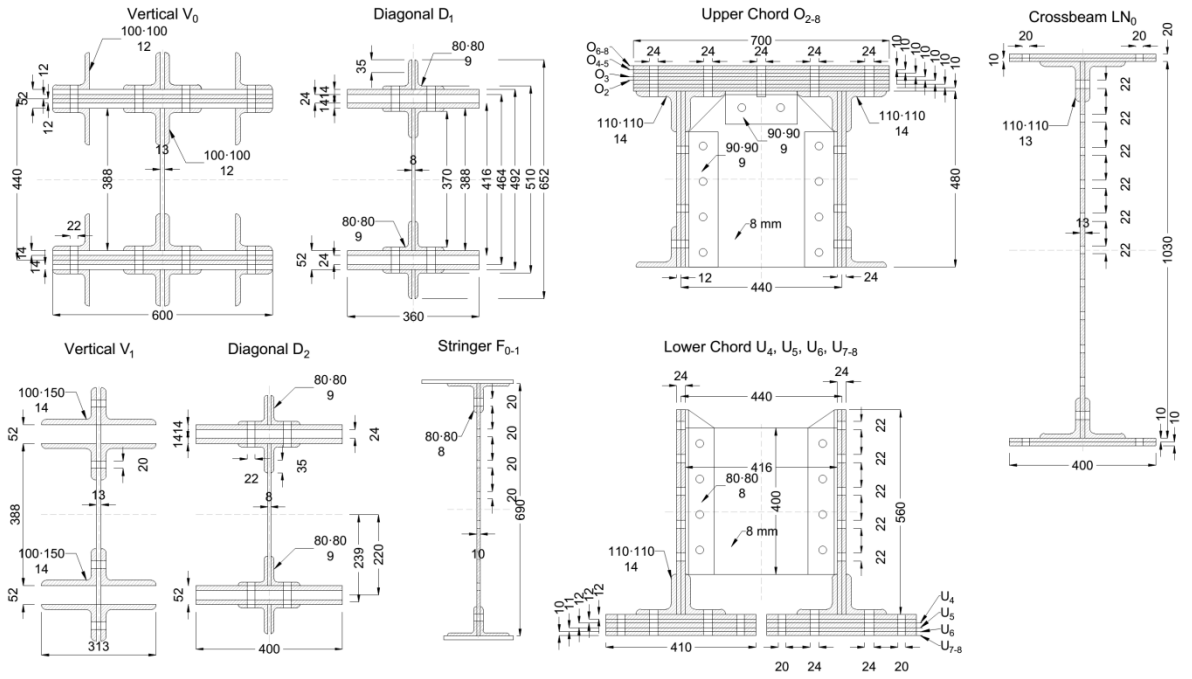

Figure 15. Typical transversal sections for the elements composing the bridge.

Figure 16. General view of the vertical elements and diagonals in the bridge.

4.1.4 Current state

From visual inspection, the most important source of degradation on the bridge is the rust accumulated during the course of the years, most likely contributed by an insufficient maintenance plan. Indications of painting can be observed in different sections, but either it was made long time ago or it did not cover the whole elements of the bridge. [Figure 17]

The effects of the action of rust can be observed in several forms, but the most important are: 1, reduction of the transversal section of certain elements, especially in connecting members [Figure 17-A], and 2, deformation of angles with the increment of volume and accumulation of material between them. This last effect look like local buckling of the flanges, but the plates restraining one of the flanges of the angles are stiff enough, so it is more likely that the deformation in the free flange is due to the accumulation of rust [Figure 17-B].

Only in pointed locations it is possible to observe damage on the rivets, like the one shown previously in Figure 11, the rest seems to be in a good state.

Figure 17 - Deterioration on the bridge. A, B (top) reduction of section in the connection elements. C,D (bottom) deformation on angles.

The rust damage seems to be general on the entire bridge, especially in the connections on lower chords, in the frames closer to the supports (0, 1 and 2). The section that looks more affected is the north truss of the Vyšehrad end. The upper connections were not accessible for inspection but they give the impression of being in a better state, explained perhaps for the fact that they are more exposed to the sunlight, which prevents the accumulation of moisture.

From the design stage some measures were taken to prevent the accumulation water or snow, for instance, the lower chords are not closed sections contrary to the upper chords that are inverted U sections. Nonetheless, the process of corrosion is difficult to avoid in exposed structures such as bridges, subjected to severe actions of the environment and for such a long period of time. This is why maintenance is extremely important to extend the life of a structure.

One more source of degradation but with lower impact is due to biological action. The different plates offer shelter for birds. It is not unusual to find pigeons forming nests between the plates [Figure 18]. The drops may contribute to the degradation of the steel elements as well as the accumulation of moisture by the nests and other materials.

Figure 18. Biological sources of decay on the bridge.

4.2 Groups of connections

In a typical bridge, the number of connections is normally large, especially in those with high degree of optimization of the elements where almost each joint is different in terms of dimensions of plates and number of fasteners. However, they can be grouped into families according to the type of elements that they join, for example, upper chord-diagonal-vertical. The groups of connections help to the characterization of joints and to decrease the number of connections to be analysed.

In this work the connections were divided in two families: connections in the truss and connections in the deck.

Each truss is formed by 16 vertical elements, resulting in 34 nodal connections. Additionally, there are 15 connections between diagonals and vertical elements, and 5 more connections between diagonals, resulting in 54 connections. [see Figure 21]. The following classification for groups of connection was made.

C-01 Support connection, vertical and inferior chord

C-02 Upper section of frame 0, joins vertical element with upper chord and two diagonals

C-03 Lower section of frame 1, joins vertical element with inferior chord and one diagonal.

C-04 Upper chord with vertical element and one diagonal. It includes the upper connections of frames 2 to 8, the difference besides the section of diagonals is the angle, from 39 to 51 degrees.

C-05 Connection of vertical element and diagonal. Similar to C 04, the variation besides the section of the angles is the angle of the diagonals.

C-06 Diagonal with vertical and lower chord. This includes frames 2 to 5.

C-07 Similar to C-06, but with double diagonals. Includes frames 6 to 8.

C-07 Upper chord with two diagonals. Includes frames 7 and 8.

In the case of the deck, the most important connections are between the crossbeams and the stringers. The classification of connections to be analysed in the deck is as follows:

C-09 Connection of crossbeam and truss.

C-10 Similar to C9, but with horizontal diagonals.

C-11 Connection of stringer with crossbeam.

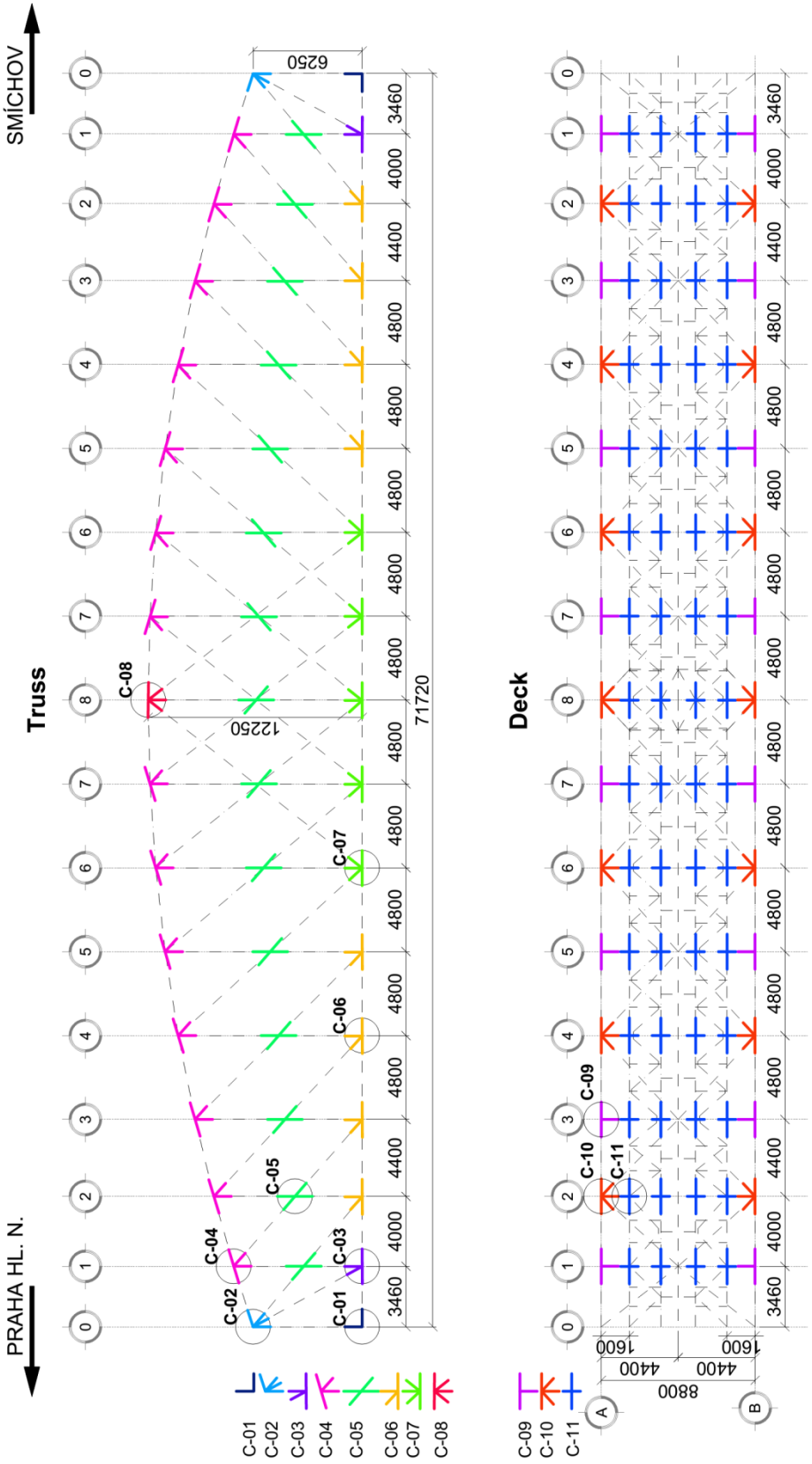

Figure 19. Connection groups. A) truss B) deck

Figure 19 presents graphically the classification of families of connections, its location on the bridge, and specifies the selected connections to be analysed for both, the truss and the deck. Figure 21 shows the typical variety of connections that constitute the bridge. Detailed drawings showing dimensions and sections of the elements are shown in Figure 20 for connection C-02 and the rest can be found in Annex A. Figure 22, Figure 23, and Figure 24 present a photograph of the connection, the drawing of the connection and the model prepared for the analysis.

Figure 21. Typical connections in the railway bridge.

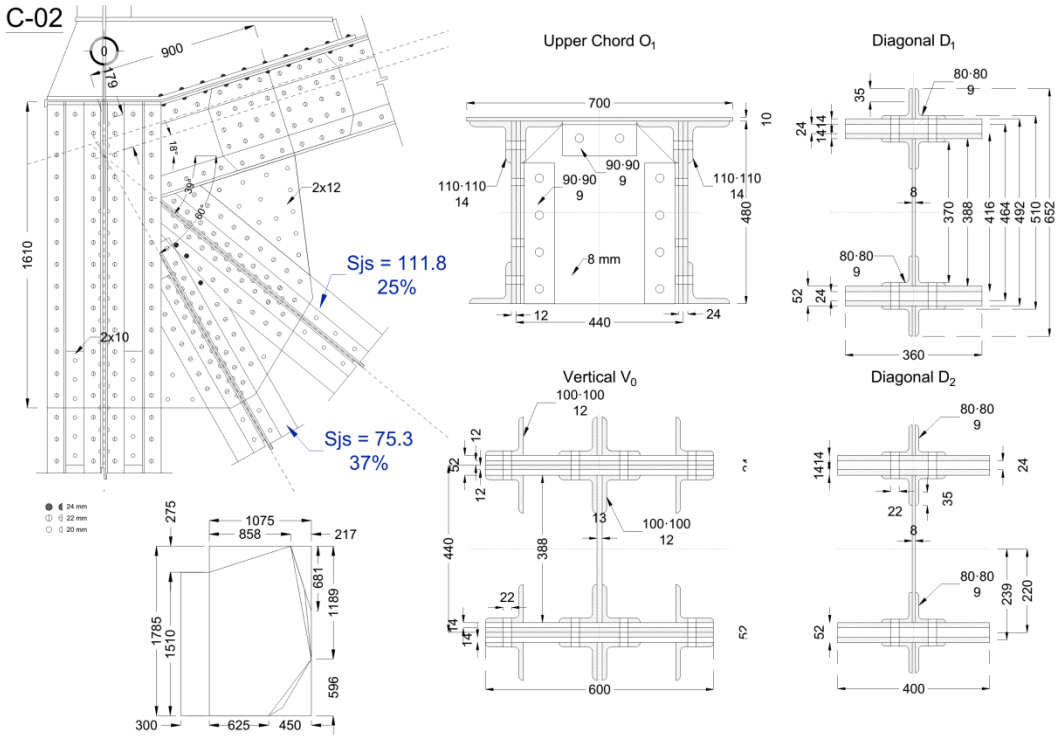

Figure 20. Detail of connection C-02. The complete details for all connections can be found in Annex A.

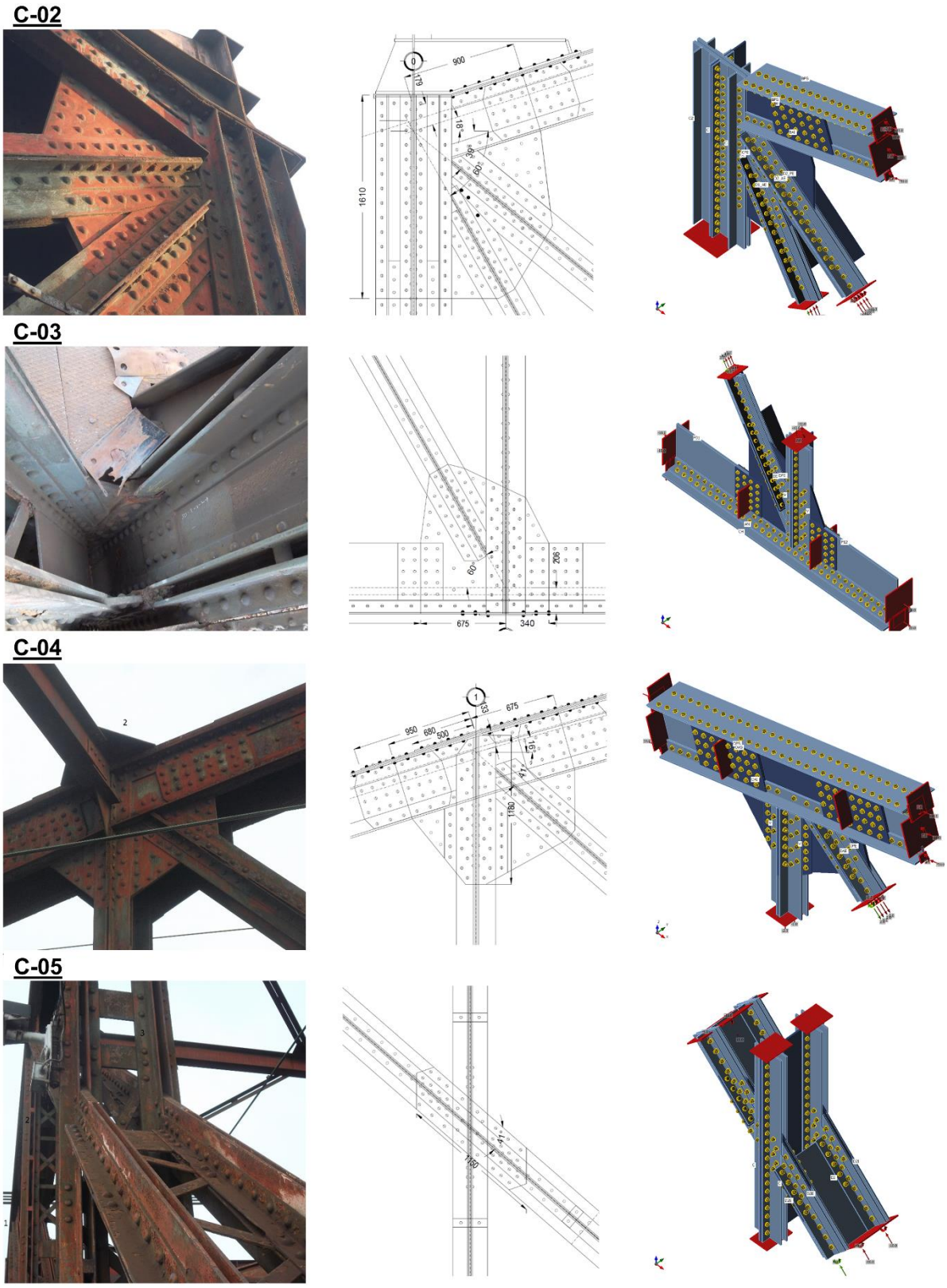

Figure 22. Connections on the bridge. [1/3]

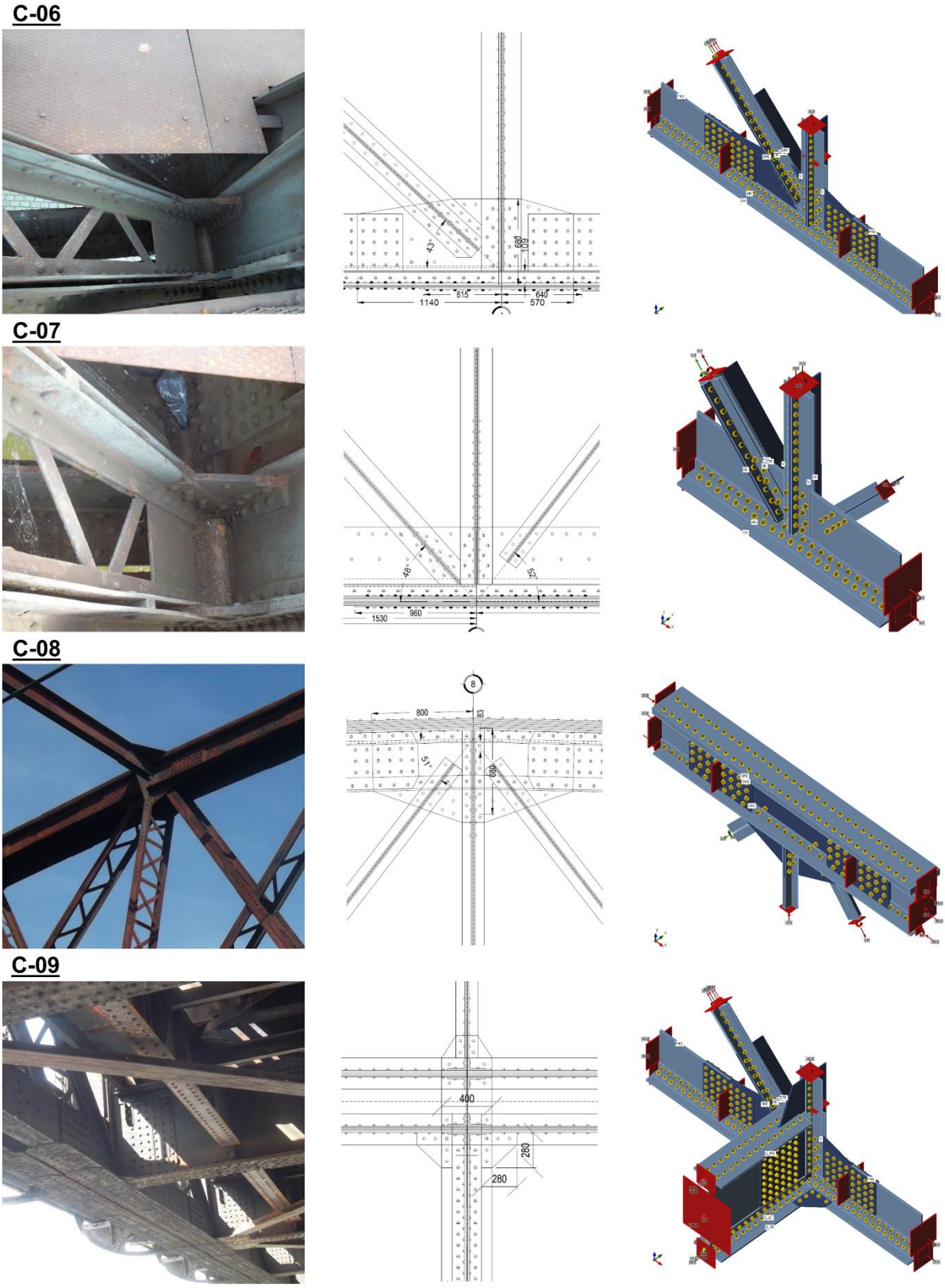

Figure 23. Connections on the bridge. [2/3]

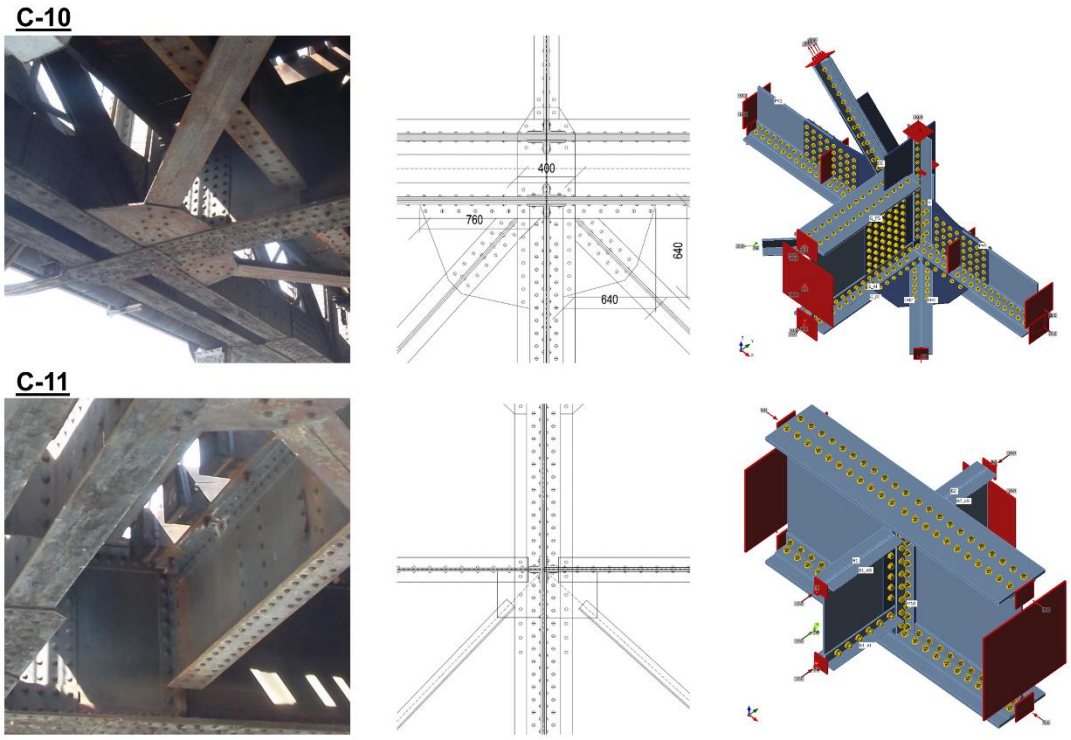

Figure 24. Connections on the bridge. [3/3]

4.3 Software specifications – IDEA StatiCa

The analysis of connections can be made with the component method described in section 3.2, or in specialized software, like ANSIS. The component method involves the calculation of the stiffness of several components for normal connections and is extremely complicated for riveted connections where hundreds of rivets are involved and with different plates. As an alternative, the connections can be modelled in finite element model software like ANSIS, but requires an elevated number of hours to obtain the complicated geometry. For these reasons, the software that suits better for the type of analysis intended in this work is IDEA StatiCa, which allows modelling any type of connection with the tools within the software, and the results obtained are either stresses in the connection, or directly the analysis of stiffness of the elements.

The software used for the evaluation of the stiffness in the connections is IDEA StatiCa version 8.0.15.43212. The Connection Evaluation Module is specialized in the 3D modeling of steel joints and the analysis of stress, deformations, fasteners and rigidity of the connection. This version is able to perform four type of analysis; these are:

- **Stress/strain**, response of the joint to applied design load
- **Stiffness analysis**, stiffness of connection of selected member of the joint

- **Member capacity design**, Joint is designed not on design load, but on maximal capacity of connected member,
- **Joint design resistance**, ratio between design load and maximal load is determined for the whole joint.

IDEA StatiCa is based on the Component Based Finite Element Modeling (CBFEM) on both finite element modeling (FEM) and components theory, and uses a nonlinear calculation.

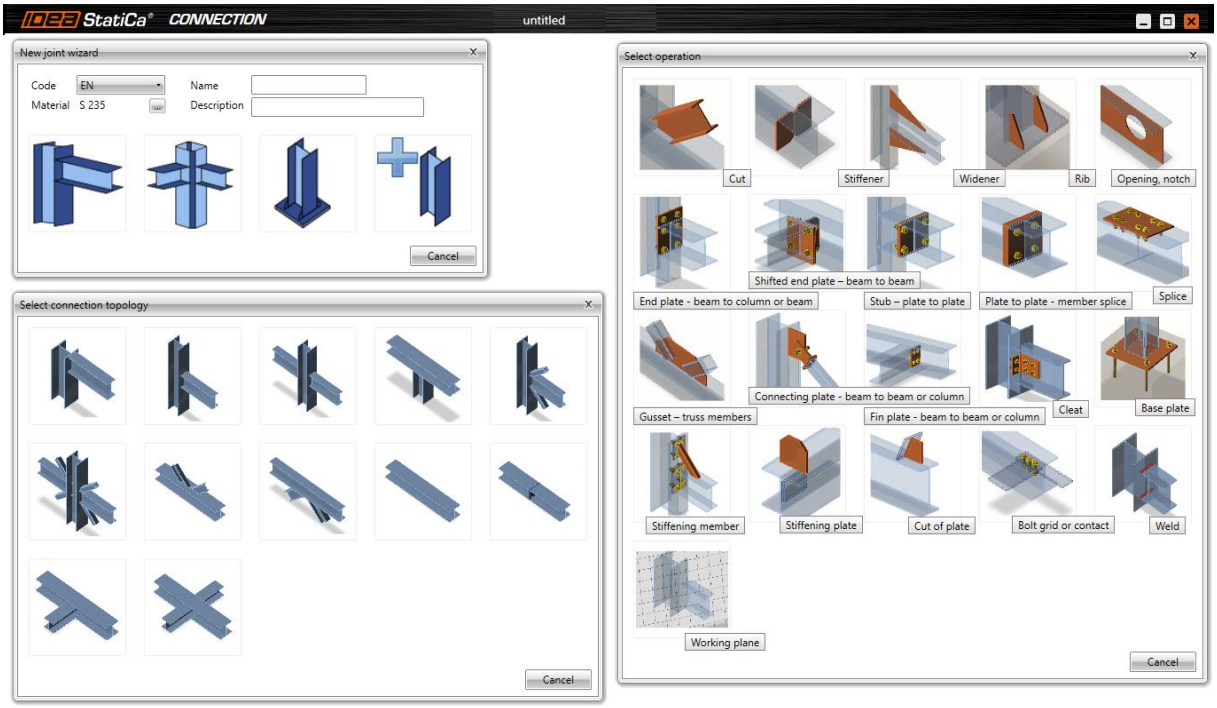

Figure 25. Initial windows in IDEA StatiCa.

The Component Based Finite Element Modeling (CBFEM) is based on the Component Method (CM) but enhanced by the use of Finite Element Method (FEM). The joint is divided into components in a similar way like in CM, and then the plates are modeled using shell elements and analysed by FEM assuming ideal elastic-plastic material. Bolts, welds, and concrete blocks are modeled as nonlinear springs. FE model is used for analysing the internal forces in each component and afterwards, each component is checked according to specific formulas. The CBFEM method allows a more detailed analysis of a connection, applied to any type of connection, beyond those typically covered by codes.

In the Connection Evaluation Module of IDEA StatiCa software, the joint is modeled with the composing members: column, beams, and braces; with forces acting on the members. The real configuration is obtained by using the so-called manufacturing operations that includes: cuts, offsets, holes, stiffeners, ribs end plates splices, angles gusset plates. Additionally, welds and bolts are

considered. Figure 25 shows some of the initial windows of the program as well as the complete set of manufacturing operations.

Internally, plates are modeled as shell elements with 4 node quadrangle and with 6 degrees of freedom in each node: 3 translations (ux, uy uz) and 3 rotations (ϕx, ϕy, ϕz). Materials are modeled with elasto-plastic behaviour, with a nominal yielding plateau, this is, the elastic behaviour is assumed before reaching the yielding strength. The failure criterion is based on Von Mises and the ultimate limit state is when the strain is 5% [see EN1993-1-5 app. C, C.8, note 1]. [23]

For FEM, the software specifies the mesh size, which is defined between minimum of 10 mm to maximum 50 mm. the default number of finite elements per cross section height is 8 and 16 for end plates. Meshes are independent of each other between flanges and webs, and end plates. The default values can only be modified in Code setup. The contact between plates is treated according to the penalty method, which is basically the application of a penalty stiffness added between the node and the opposite plate when penetration of a node into an opposite surface is detected. [23]

Bolts are considered in the CBFEM method as nonlinear springs with behaviour in a) tension, b) shear and c) bearing. The tension behaviour of bolts is described by 1) axial initial stiffness, 2) design resistance, 3) initialization of yielding and 4) deformation capacity. Plastic deformation in the threaded part of the bolt is assumed for the initialization of the yielding and deformation capacity. [23]

The force at beginning of yielding, is

$$F_{y,ini} = f_{y,b} \cdot A_t \tag{4}$$

Where $f_{y,b}$ is the yielding strength and A_t the tensile area of the bolt. To assure a positive value of plastic stiffness $F_{y,ini}$ is checked to be less than the design resistance, $F_{t,Rd}$. This is important for materials with low ratio of ultimate to yield strength. [23]

The deformation capacity of the bolt, δc, is taken as the elastic deformation of the bolt, δel, plus the plastic deformation of the threaded part only δpl.

$$\delta_c = \delta_{el} \cdot \delta_{pl} \tag{5}$$

$$\delta_{el} = F_{t,Rd} \cdot k_{ini} \tag{6}$$

$$\delta_{pl} = \varepsilon_{pl} \cdot l_t \tag{7}$$

Where k_{ini} is the initial deformation stiffness of the bolt in tension, ε_{pl} is the limit plastic strain (5%) and l_t, is the length of the threaded part.

The tensile force is transmitted to the plates by interpolation between the bolt shank and the nodes in the plate. For compression, the force is transmitted from the bolt shank to the plate in the bolt hole by interpolation links between the shank and hole edges nodes. Finally, the interaction between the axial and the shear forces is considered. The higher the tensile forces the less shear force is resisted by the bolt. [23]

Figure 26 shows the results that can be obtained using IDEA StatiCa. The figure shows the detailed model with the bolts, the mesh that is generated automatically, the equivalent stress with the deformed shape, and an example of equivalent stress in one of the plates that conforms the connection.

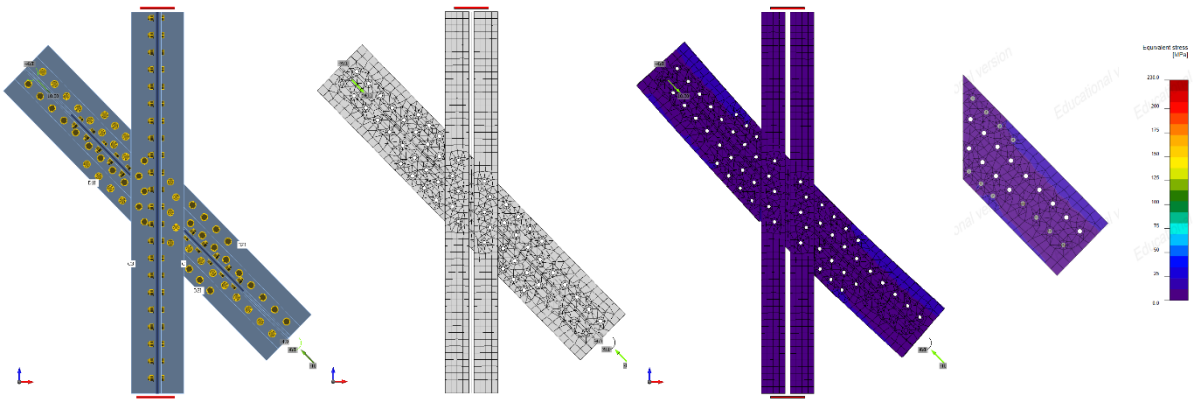

Figure 26. Types of results obtained with IDEA StatiCa. Model of connection, automatic generated mesh, equivalent stress with deformation, and stresses in each plate.

Another of the different results that can be obtained with the software is the shear force that is acting in each fastener, is it is verified in Figure 27. For the example shown, only axial force is applied to the elements so the resultant shear force is all in the same direction for all the fasteners. The force on the double angles is 10 KN and so is the sum of the shear forces of bolt in that section. The plate is loaded with other 10 KN, so the sum of the shear forces in the bolts for that plane is the total load of 20KN. It can be noted that the load is distributed regularly in the bolts. This regularity is lost when bending force is acting on the member, which is the real case in many structures, and to account for this is complicated without the correct tools.

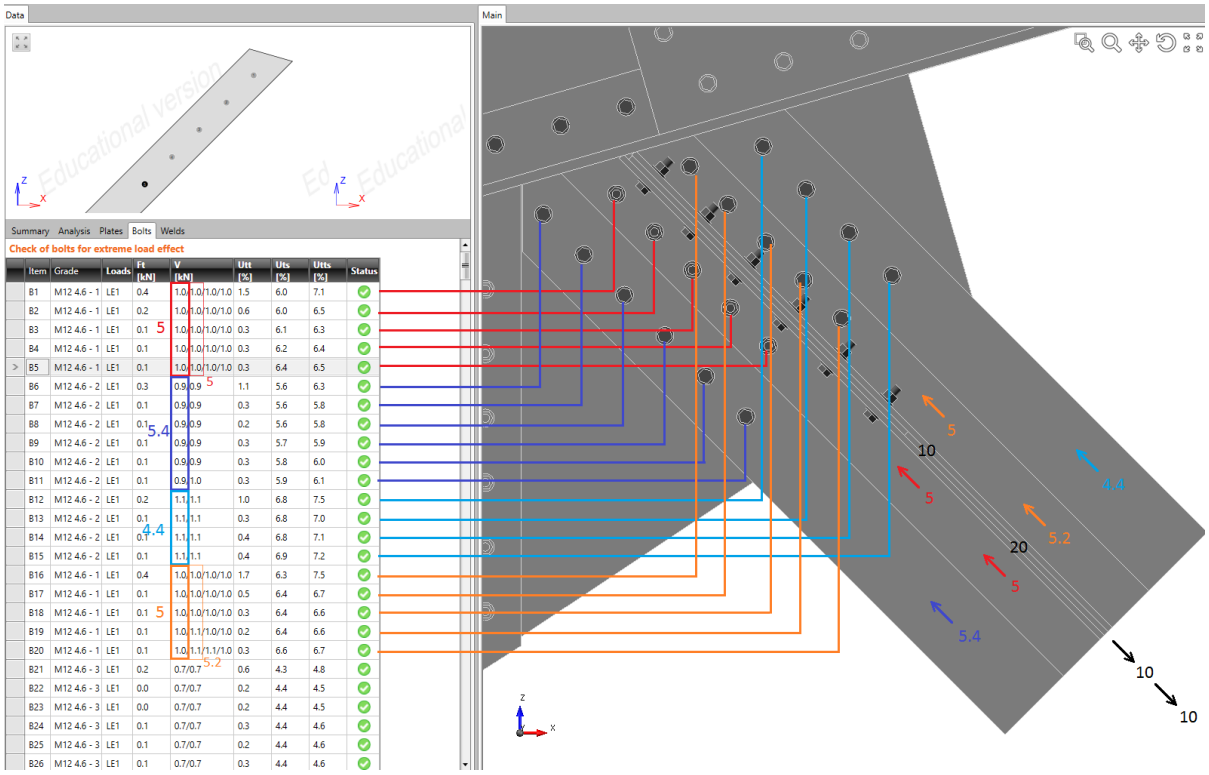

Figure 27. Verification of shear force in the bolts.

Among the software limitations is the fact that the stiffness analysis is made only in one member specified, while in the real connections of the bridge here analysed, diagonals members are typically formed by double angles and plates. There is a possibility to use a user defined section, and some trials where made using this to model the complete section as one member. However, as is later explained, it was decided to model separated elements and compute the stiffness for the whole section by adding the separated results.

Rivets were popular at the end of nineteenth and the beginning of the twentieth century, but its use was slowly replaced by the development of high strength bolts and welding. For modeling rivets in IDEA StatiCa, bolts were used instead. Besides the material specifications, the other important modification for the consideration of rivets is that the diameter of the rivet-bolt is equal to the hole in which it is placed.

4.3.1 Stiffness analysis.

A connection is made of different elements. To analyse each element, separate models must be created so that the stiffness is not influenced by other members but only by the node itself. For the stiffness analysis, all members except the analysed one are supported.

For the software to calculate rotational stiffness the element must be assigned with a bending moment and, accordingly, to calculate the axial stiffness an axial force must be assigned in the member.

The results are presented in both, a graph and a table as displayed in Figure 28. The table includes:

Item, name of the element analysed,

Comp., direction of analysis,

Loads, load pattern,

MEd, magnitude of the load applied

Mj,Rd, strength of the connection

Sj,ini, initial stiffness

Sjs, stiffness of the connection

φ, rotation at the load applied

φc, rotation at the strength

L, length of the member

Sj,R, lower limit to consider the connection as rigid

Sj,P Classification: rigid, semi-rigid or pinned

Class upper limit to consider the connection pinned

And the moment-rotation diagram, including the initial stiffness Sj,ini in light green, pinned limit in blue, and rigid limit in yellow.

The value of most interest in this work is the stiffness Sj. The limits Sj,R and Sj,P are calculated according to EN 1993 1-8 with equations (1) and (2), so they can be easily computed and used as a partial validation.

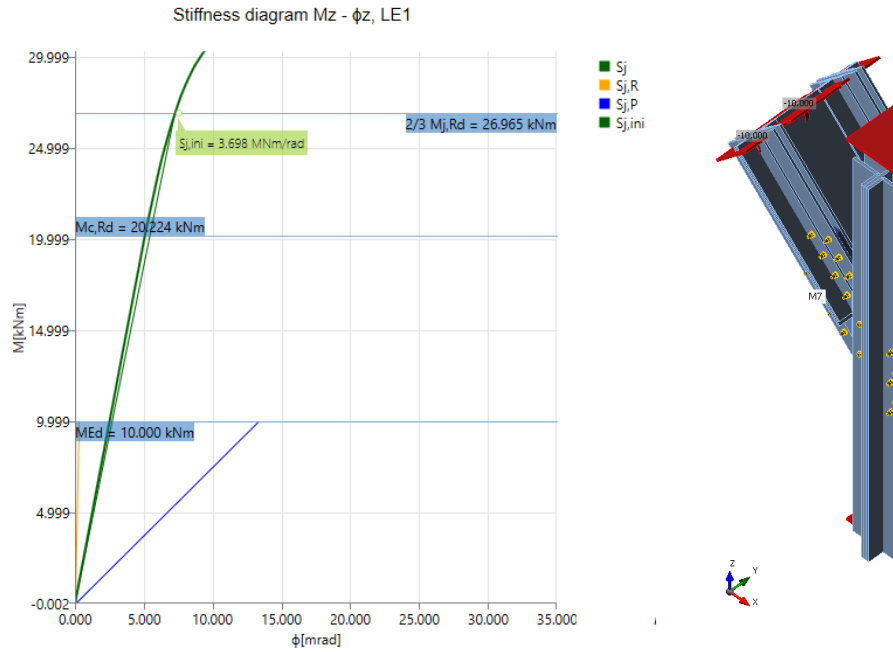

Summary | Rotational stiffness

Rotational stiffness of joint component

	Item	Comp.	Loads	MEd [kNm]	Mj,Rd [kNm]	Sj,ini [MNm/rad]	Sjs [MNm/rad]	Φ [mrad]	Φc [mrad]	L [m]	Sj,R [MNm/rad]	Sj,P [MNm/rad]	Class
>	M5	Mz	LE1	10.000	40.447	3.698	3.980	2.513	29.805	6.00	37.525	0.750	Semi-rigid

Figure 28. Example of the stiffness analysis output using IDEA StatiCa.

4.4 Properties of materials

In reserve for the results of the tests performed on the bridge, for the present analysis the material characteristics were determined for calculation purposes according to Appendix A of the SŽDC SR5. [24]. The properties used were those proposed for cast steel

Year of manufacture	Material	Allowable stresses σ_{adm} [MPa]	Guaranteed yield strength f_y [MPa]	Strength limit f_u [MPa]	γ_{M0}	γ_{M1}	γ_{M2}	Standard
until 1894	Wrought Iron (Svářkové železo)	130	210	340	1.1	1.2	1.3	
1895-1904	Wrought Iron (Svářkové železo)	130	210	340	1.1	1.2	1.3	Nařízení 97/1904
	Cast steel (plávková ocel)	140	230	360	1.1	1.2	1.3	

Similarly, the rivet strength was considered in accordance with the Appendix A of same ordinance [24].

Strength characteristics	Rivets		Precision Bolts	
	In constructions made of material with a yield strength			
	fy ≤ 300 MPa	fy > 300 MPa	fy ≤ 300 MPa	fy > 300 MPa
f_y [MPa]	200	245	300	
f_u [MPa]	310	440	500	

4.5 Loads

The parameter analysed for each individual connection is the stiffness, which is a property of the material and the geometry; and theoretically, it should not be affected by the load condition. As it will be further explained during the verification, the loads for each connection were reasonably low, to ensure that the behaviour of the material is within the elastic range.

4.6 Verification

The connections on this bridge, as is usual in riveted connections, are complex. They involve several plates with hundreds of rivets. Nevertheless, they are often symmetric, which allows making simplifications. To stablish the degree of simplification that can be achieved using the program, a special analysis was made on connection C-05, for which three models were prepared with different levels of detail, and the results compared. Another confirmation was performed to decide whether load the model with axial load and moment separately, obtaining rotational and axial stiffness separately or within the same model. Some interesting features were obtained from this analysis that help to understand the way the software operates, and also to familiarize with the interface and with the output presentation.

4.6.1 Level of detail

A first analysis was made to stablish the level of detailing in the models that is possible to make without affecting the results. The connection used was C-05.

Four levels of modeling where prepared [see Figure 29] with the following considerations:

a) Detailed, including every member as a separated element

b) Medium, using I and T sections.

c) Simplified, modeling only one half of the connection, considering its symmetry.

d) Unified, considering the user-defined section for the diagonal, having only one analysed member.

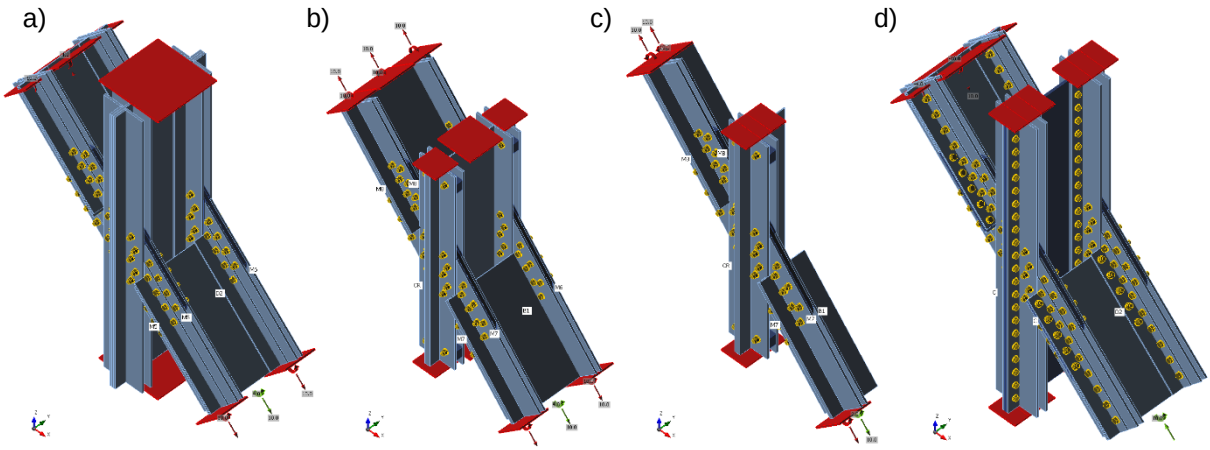

Figure 29. Models of connection C05 with different levels of detail

The results of the models are summarized in Table 1. For models ***a*** and ***b***, the total stiffness is obtained by adding the stiffness of the central element plus twice the stiffness of the lateral elements. For model ***c***, the total stiffness is twice the addition of central and lateral element. For model ***d***, the total stiffness is the element stiffness. The limit values Sj,R and Sj,P for the total section were computed using the moment of inertia of total element. Additionally, the percentage of the stiffness Sj with respect to the limits Sj,R and Sj,P is calculated.

It is possible to observe that for the first 3 models the total stiffness Sjs is around 27.2 MN·m/rad, which is 16.5 % of the range between pinned and rigid connection. For the last model, the result is significantly lower (18.3 MN·m/rad).

Table 1. Results of verification 1 for connection C-05.

	Roational stiffness											Axial Stiffness			
Model	**Item**	**Med**	**Mj,Rd**	**Sj,ini**	**Sjs**	**φ**	**φc**	**L**	**Sj,R**	**Sj,P**	**Class**		**N**	**Nj,Rd**	**d**	**St**
		KN·m	KN·m	MN·m/rad	MN·m/rad	m·rad	m·rad	m	MN·m/rad	MN·m/rad		%	KN	KN	mm	MN/m
C5a	D2	4	180	13.6	13.7	0.3	53.7	6	75.1	1.5	S-R	17	10	18.5	0	845
	M5	10	40	6.8	6.8	1.5	5.8	6	37.5	0.8	S-R	16	10	40.0	0	382
	Total				**27.4**				150.4	3.0		**17**				1609
C5b	B1	4	149	13.5	13.5	0.3	31.4	6	68.5	1.4	S-R	18	10	18.5	0	855
	M7	-10	-48	6.8	6.8	-1.5	-7.1	6	34.5	0.7	S-R	18	10	40.0	0	478
	Total				**27.1**				150.4	3.0		**16**				1811
C5c	B1	2	73	6.8	6.8	0.3	27.3	6	34.4	0.7	S-R	18	10	36.6	0	372
	M7	-10	-48	6.8	6.8	-1.5	-7.1	6	34.5	0.7	S-R	18	10	40.0	0	464
	Total				**27.1**				150.4	3.0		**16**				1672
C5d	D2	10	334	18.2	18.3	0.5	52.1	5	164.5	3.3	S-R	9	-10	-17.2	0	2197
	Total				**18.3**				164.9	3.3		**9**				2197

When defining the entire section using the general cross-section editor a warning appears stating that the cross section is not a single integral and 'the displayed results may be incorrect'. However, the Area and the moment of inertia in Y and Z are correct. This may have an influence in the calculation of the stiffness, and consequently in the results presented.

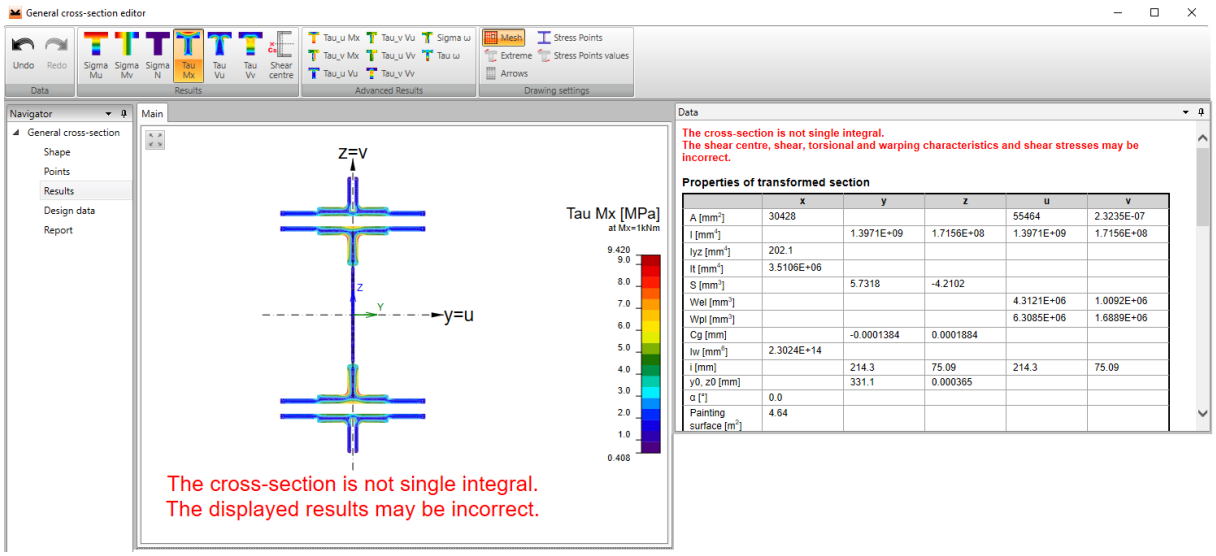

	x	y	z	u	v
A [mm²]	30428			55464	2.3235E-07
I [mm⁴]		1.3971E+09	1.7156E+08	1.3971E+09	1.7156E+08
Iyz [mm⁴]	202.1				
It [mm⁴]	3.5106E+06				
S [mm³]		5.7318	-4.2102		
Wel [mm³]				4.3121E+06	1.0092E+06
Wpl [mm³]				6.3085E+06	1.6889E+06
Cg [mm]		-0.0001384	0.0001884		
Iw [mm⁶]	2.3024E+14				
i [mm]		214.3	75.09	214.3	75.09
y0, z0 [mm]		331.1	0.000365		
α [°]	0.0				
Painting surface [m²]	4.64				

Figure 30. Message displayed when defining the cross section uusing the general cross-section editor.

Finally, from this analysis it can be concluded that it is correct to model half of the connection as it results in half the stiffness of the whole element, which helps to save computational time. Also, using the user-defined section for the whole element produces uncertain results; therefore, it is decided to model the rest of the connections with separated elements.

4.6.2 Axial and rotational stiffness

A second set of models were prepared aimed to determine if the axial and rotational stiffness should be obtained in the same model or separately. In the reality, the element is subjected to both type of actions at the same time, and therefore, it is reasonable that the analysis should be made considering both actions acting simultaneously. However, at this moment only the stiffness is being analysed, and should not be dependent of the loads applied.

The connections chosen for this analysis were again connection C-05, and connection C-07. For each connection, models with only a) axial force, b) only bending moment, and c) a combination of axial and bending moment were prepared. The results are summarized in Table 2 for connection C-05 and in Table 3 for connection C-07. The first three rows are for the results considering axial and rotational stiffness at the same time, the following three rows are for the axial stiffness only, and the last three rows are for the rotational stiffness only.

Table 2. Results of verification 2 for connection C-05

	Roational stiffness								Axial Stiffness				
Model	**Item**	**Med**	**Mj,Rd**	**Sjs**	**φ**	**L**	**Sj,R**	**Sj,P**	**Class**	**Item**	**N**	**Nj,Rd**	**d**	**St**
		KN·m	kN·m/ rad	MN·m/ rad	m·rad	m	MN·m/ rad	MN·m/ rad			KN	KN	mm	MN/m
C5_a	M5	10.0	39.6	**6.8**	1.5	6.00	37.5	0.75	Semi-rigid	M5	10.00	40.0	0.0	**382**
C5_b	D2	4.0	180.0	**13.8**	0.3	6.00	75.1	1.50	Semi-rigid	D2	10.00	18.5	0.0	**845**
C5_c	M6	-10.0	-39.6	**6.8**	-1.5	6.00	37.5	0.75	Semi-rigid	M6	-10.00	-40.0	0.0	**382**
C5a_a										M5	10.00	-110.0	-0.1	**423**
C5a_b										D2	10.00	-110.0	0.0	**873**
C5a_c										M6	-10.00	-110.0	-0.1	**423**
C5r_a	M5	10.0	40.4	**6.8**	2.5	6.00	37.5	0.75	Semi-rigid					
C5r_b	D2	10.0	113.6	**13.8**	1.3	6.00	75.1	1.50	Semi-rigid					
C5r_c	M6	-10.0	-40.4	**6.8**	-2.5	6.00	37.5	0.75	Semi-rigid					

Table 3. Results of verification 2 for connection C-07.

	Roational stiffness								Axial Stiffness				
Model	**Item**	**Med**	**Mj,Rd**	**Sjs**	**φ**	**L**	**Sj,R**	**Sj,P**	**Class**	**Item**	**N**	**Nj,Rd**	**d**	**St**
		KN·m	kN·m/ rad	MN·m/ rad	m·rad	m	MN·m/ rad	MN·m/ rad			KN	KN	mm	MN/m
C7_a	DE	10.0	27.8	**2.4**	4.1	6.00	11.0	0.20	Semi-rigid	DE	10.00	40.0	0.1	**173**
C7_b	DI	-10.0	-27.8	**2.4**	-4.1	6.00	11.0	0.20	Semi-rigid	DI	10.00	40.0	0.1	**173**
C7_c	D2I	10.0	16.7	**0.6**	16.9	6.00	2.9	0.10	Semi-rigid	D2I	10.00	30.6	0.1	**79**
C7a_a										DE	10.00	110.0	0.0	**308**
C7a_b										DI	10.00	110.0	0.0	**306**
C7a_c										D2I	10.00	110.0	0.1	**162**
C7r_a	DE	10.0	27.8	**2.4**	4.1	6.00	11.0	0.20	Semi-rigid					
C7r_b	DI	-10.0	-27.8	**2.4**	-4.1	6.00	11.0	0.20	Semi-rigid					
C7r_c	D2I	10.0	16.8	**0.6**	16.8	6.00	2.9	0.10	Semi-rigid					

As it was expected, the results for the rotational stiffness Sjs are identical no matter the presence of the axial force. This is explained considering that the position of the axial force is automatically placed by the software in the center of gravity of the member, thus, it does not affect the bending moment in the connection.

As for the axial stiffness St, the results are different in both scenarios, that is, they are affected in a certain way for the bending moment. It is clear that the axial strength is reduced when bending moment is considered, but for both connections even though they are different, the strength reported is 110 KN. This is probably an upper threshold used by the software when the material has entered the nonlinear state, and the deformations are significantly increasing, thus the calculation is stopped when the load applied is 1100% the prescribed load, which in both cases was 10 KN.

In the present study, the main focus is on the rotational stiffness. It is correct then to use the load conditions for when both axial and flexural moment are applied at the same time. In addition, to avoid problems with the non-linearity of the material, the loads applied are set to small values to ensure that the calculation is done in the elastic range. A load of 10% of the strength is assumed to provide good results.

4.7 Results

In this section, the results of the rotational stiffness obtained from the models of each connection are presented.

An indirect verification with the limit values of rigid and pinned connections Sj,R and Sj,P obtained from the software compared with those computed by means of equations (1) and (2) using the properties of the whole transversal sections. The tables include also the *percentage of rigidity* %, representing the position of the stiffness value between the two ranges. This percentage is obtained following two methods, the first one, *%rel* as a weighted average using the inertia of the members, and the second method, *%sect*, is using the stiffness and the limits calculated for the entire section. This serves also to check that the sections in the models are correct.

$$\%_{rel} = \frac{\sum_i \left[\frac{Sjs_i - Sj,P_i}{Sj,R_i - Sj,P_i} \cdot I_i\right]}{I_s} \tag{8}$$

$$\%_{sect} = \frac{Sjs_s - Sj,P_s}{Sj,R_s - Sj,P_s} \tag{9}$$

$$Sjs_s = \sum_i Sjs_i \cdot n_{el} \tag{10}$$

Where *Sjs* is the rotational stiffness, *Sj,P* is the pinned boundary, *Sj,R* is the rigid boundary, and *I* is de moment of inertia. The subscript *i* is for the properties of the elements (angles and plates), the subscript *s* is for the properties of the whole section, and n_{el} is the number of elements in the section, for instance the sections of the crossbeam are formed by two sets of double angles or two plates and one vertical plate, therefore, $n_{el} = 2$ for the angles and plates, and $n_{el} = 1$ for the vertical plate.

4.7.1 Connections in the truss

The connections in the truss include typically a vertical, a horizontal and a diagonal member. Vertical and horizontal elements are composed of relatively large plates and its connections are reasonable to consider rigid. Thus, the analysis is concentrated in the diagonals.

Table 4 summarize the values obtained for every model. It includes the bending moment used in the analysis Med, the resistant bending moment Mj,Rd, the rotational stiffness Sjs, the stiffness for the whole section Sjs total, the tension or compression N used for the analysis of axial stiffness, the axial capacity Nj,Rd, the Axial stiffness per element and the stiffness of the whole section, St,total.

Table 4. Results for stiffness in connections in truss.

Connection	Item	L	Med	Mj,Rd	Sjs	Sjs total	N	Nj,Rd	St	St.total
		m	KN·m	KN·m	MN·m/ rad	MN·m/ rad	KN	KN	MN/m	MN/m
C2_1	D1_AE	6.1	2.0	12.1	1.6		-10.0	-22.6	529.4	
C2_1	D1_PE	6.1	2.0	8.1	17.2	75.3	-10.0	-40.0	846.0	5501.4
C2_2	D2_AE	3.9	2.0	12.3	1.9		-10.0	-22.9	623.8	
C2_2	D2_PE	3.9	2.0	9.0	26.0	111.8	-10.0	-40.0	897.6	6085.7
C3	DE	6.1	1.2	12.0	1.7		2.2	4.9	407.5	
C3	DPE	6.1	0.5	8.1	18.6	81.0	4.0	16.0	754.0	4645.8
C4	DAE	4.9	-1.2	-12.0	1.9		2.0	4.5	426.7	
C4	DPE	4.9	-0.5	-5.6	16.0	71.5	2.0	8.0	830.7	5029.4
C5	D2E	5.5	4.0	39.6	6.9		-10.0	-40.0	441.9	
C5	D2	5.5	10.0	176.4	13.8	27.5	-10.0	-18.1	966.7	1850.6
C6	DE	6.1	-2.0	-13.4	1.6		2.5	6.3	307.1	
C6	DPE	6.1	-0.5	-3.7	10.1	47.1	4.0	16.0	531.8	3355.8
C7_1	DE	6.8	3.0	27.3	2.4		4.0	16.0	195.5	
C7_1	DI	6.8	-3.0	-27.3	2.4	9.7	4.0	16.0	194.6	782.1
C7_2	D2I	3.3	1.5	16.5	0.6	1.2	4.0	12.3	110.3	220.5
C8	D2	3.6	1.2	12.0	0.7	1.5	2.0	4.5	112.8	225.7

Table 5 include the percentage of rigidity computed according to equations (8) and (9). It can be verified that the two ways of calculating the percentage follow to a similar result. Also, the connections of the diagonals are around 30% rigid. This percentage is reduced in the connection C-05 of the diagonal and vertical element, and the connections C-07 and C-08, where the sections of diagonals are smaller.

Table 5. Verification of stiffness parameters for the elements in the truss.

Connection	Item	Sjs	Sjs total	Sj,R	25·E·Ib/ Lb	Sj,P	0.5·E·Ib/ Lb		25·E·Ib/ Lb	0.5·E·Ib/ Lb	
		MN·m/ rad	MN·m/ rad	MN·m/ rad	MN·m/ rad	MN·m	MN·m	$\%_{Rel}$	MN·m	MN·m	$\%_{Sect}$
C2_1	D1_AE	1.6		2.7	3.2	0.1	0.1				
C2_1	D1_PE	17.2	75.3	46.9	46.9	0.9	0.9	37%	200.3	4.0	36%
C2_2	D2_AE	1.9		4.3	4.9	0.1	0.1				
C2_2	D2_PE	26.0	111.8	101.0	101.0	2.0	2.0	25%	423.9	8.5	25%
C3	DE	1.7		2.7	3.2	0.1	0.1				
C3	DPE	18.6	81.0	46.9	46.9	0.9	0.9	40%	200.3	4.0	39%
C4	DAE	1.9		3.4	3.9	0.1	0.1				
C4	DPE	16.0	71.5	41.9	41.9	0.8	0.8	38%	183.4	3.7	38%
C5	D2E	6.9		41.2	3.5	0.8	0.1				
C5	D2	13.8	27.5	82.3	37.7	1.6	0.8	15%	41.2	0.8	15%
C6	DE	1.6		2.7	2.8	0.1	0.1				
C6	DPE	10.1	47.1	23.5	23.5	0.5	0.5	44%	105.2	2.1	44%
C7_1	DE	2.4		9.7	9.9	0.2	0.2				
C7_1	DI	2.4	9.7	9.7	0.0	0.2	0.0	21%	39.6	0.8	23%
C7_2	D2I	0.6	1.2	5.3	5.2	0.1	0.1	10%	10.4	0.2	10%
C8	D2	0.7	1.5	4.6	4.7	0.1	0.1	15%	9.5	0.2	14%

The final stiffness is shown in Figure 31 for each connection. The stiffness of diagonal 1 is slightly bigger in the connection C-03 than in connection C-02, (81.03 and 75.2 MN·m/rad, respectively) which is not expected because the plate in connection C-02 looks stiffer. This is not the case of diagonal 2 in connection C-02 which is stiffer than that of the diagonal in connection C-04, (with values of 111.8 and 81.03 MN·m/rad). Diagonal 4 in connection C-06 shows a bigger reduction in stiffness compared to that of connection C-03. The reduction is more evident in connections C-07 and C-08 with extremely low stiffness values, similar to the results observed previously.

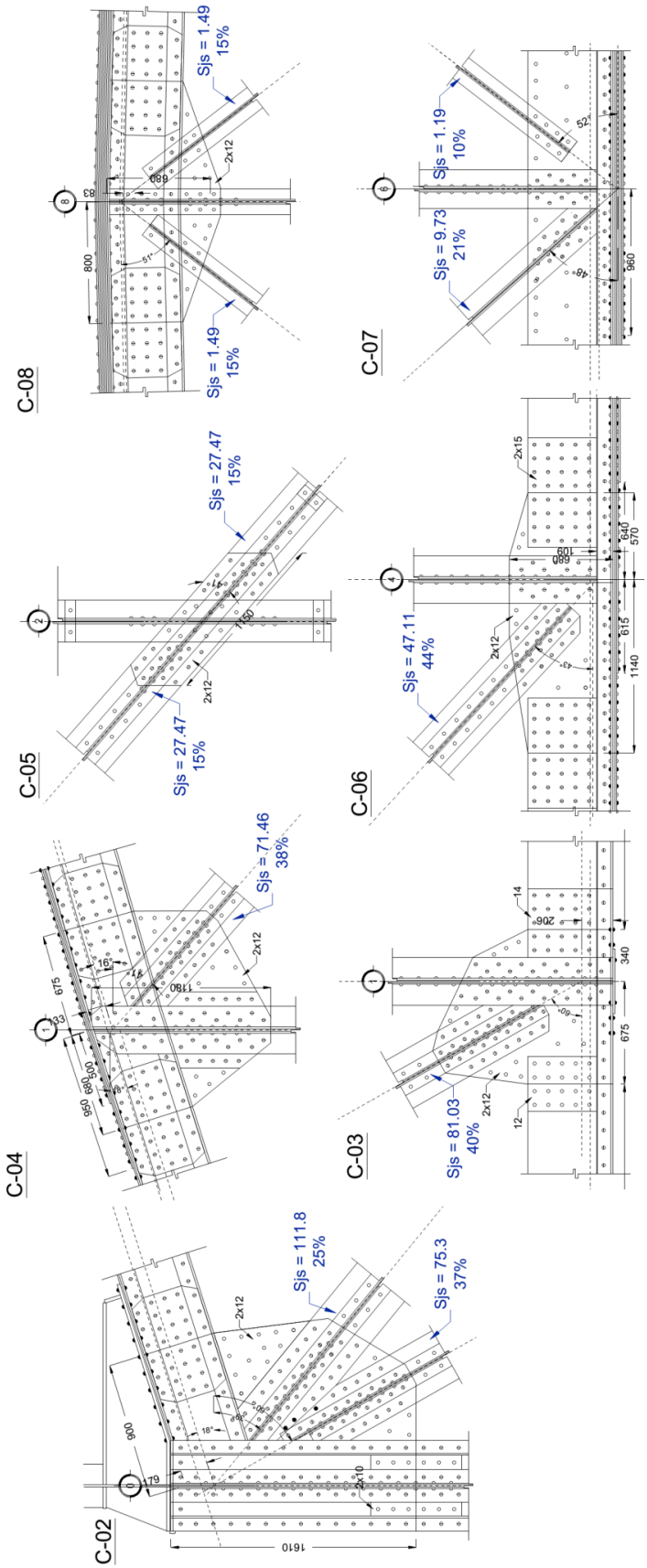

Figure 31. Results of stiffness in truss. All values are in MN·m/rad

The graph in Figure 32 shows the relation between the value of the stiffness Sj and the inertia of the member I_s, as well as with the number of rivets in the connection n_r. There is almost a linear relation with each of these two parameters. However, thinking about the design process of the structure, the elements were dimensioned according to the force they were to resist, and thus the connections were designed to resist those forces. In any case, the stiffness of the connection is proportional to both parameters.

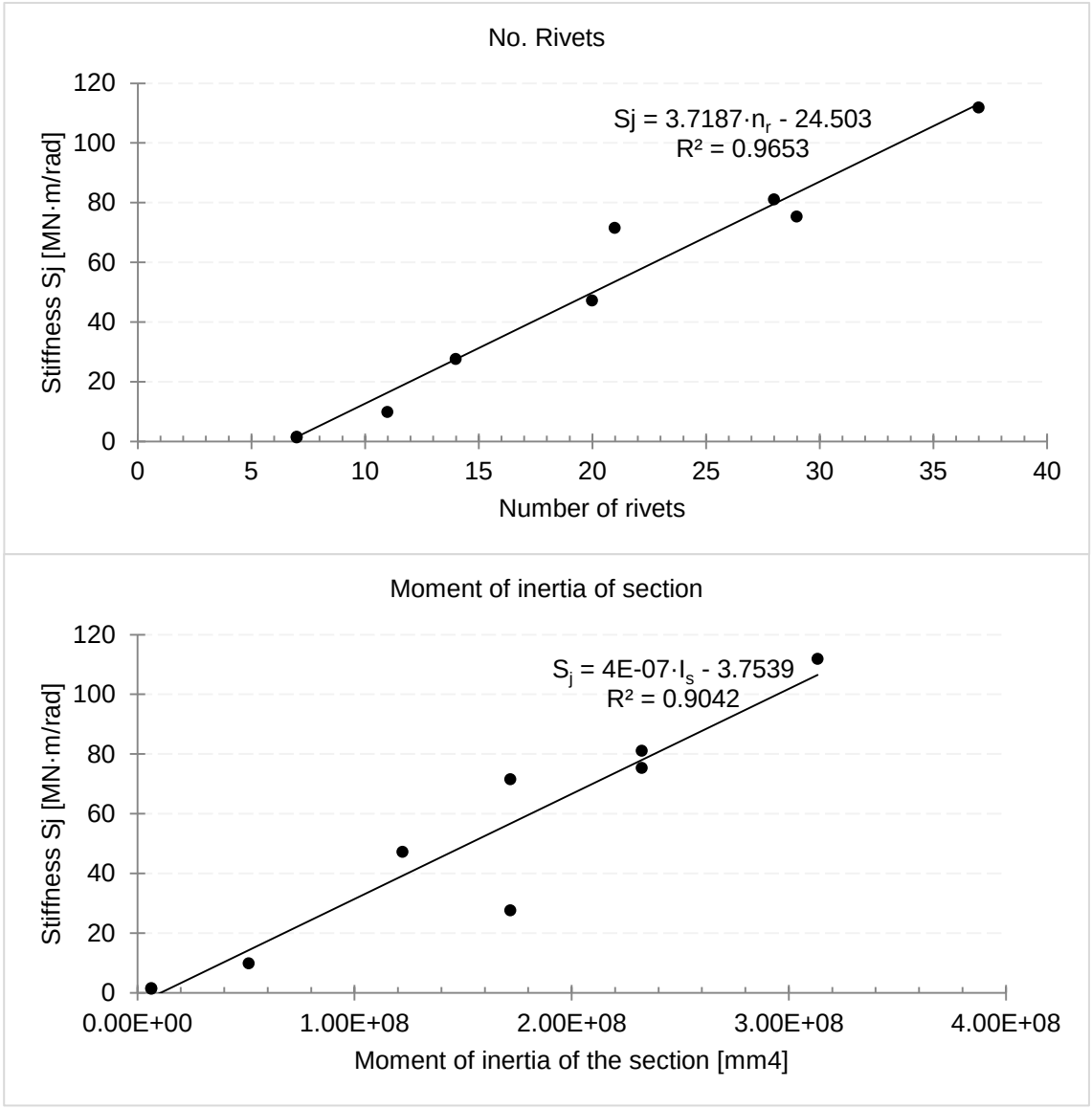

Figure 32. Relation between the stiffness and A. number of rivets (top). B. moment of inertia of the section (bottom).

With the information from the report prepared by SUDOP, an

Figure 33 shows again the relation of number of rivets and the stiffness, but with the values of the connections from Tábor – Písek bridge [ref. [18]]. Connections on the Tábor – Píske Bridge have smaller values of stiffness that does not follow the linear relation observed in the steel railway bridge.

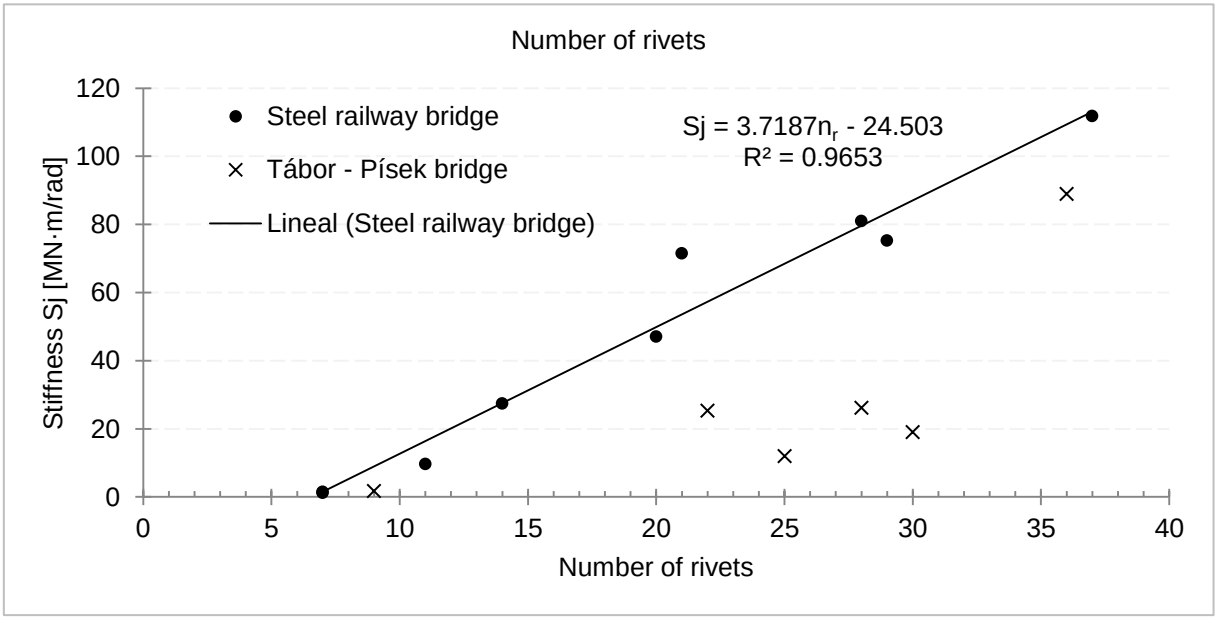

Figure 33. Comparison of relation stiffness - number of rivets, with the values from ref. [18].

Figure 35 shows again the moment of inertia of the section and the stiffness. It includes the moment of inertia of the elements composing the section, as well as the values from ref [18]. The linear relation is maintained for the analysis of the elements individually, probably because the general stiffness was calculated according to the individual stiffness. For the examples in ref [18], the values do not fall in the linear relation.

There is little information about the cross section of the elements in the joints on ref. [18] so the values are only a few. However, the inertia can be obtained from the parameters Sj,P y Sj,R if the length is correctly estimated. This procedure was done to obtain the graph for the complete set of data shown in Figure 34. Here, it is possible to observe a different linear relation between the moment of inertia of the section and the stiffness, for both set of data. Perhaps the difference is in the assumptions taken to model the connections and that is not accounted here, but the fact that a linear relation can be obtained is true.

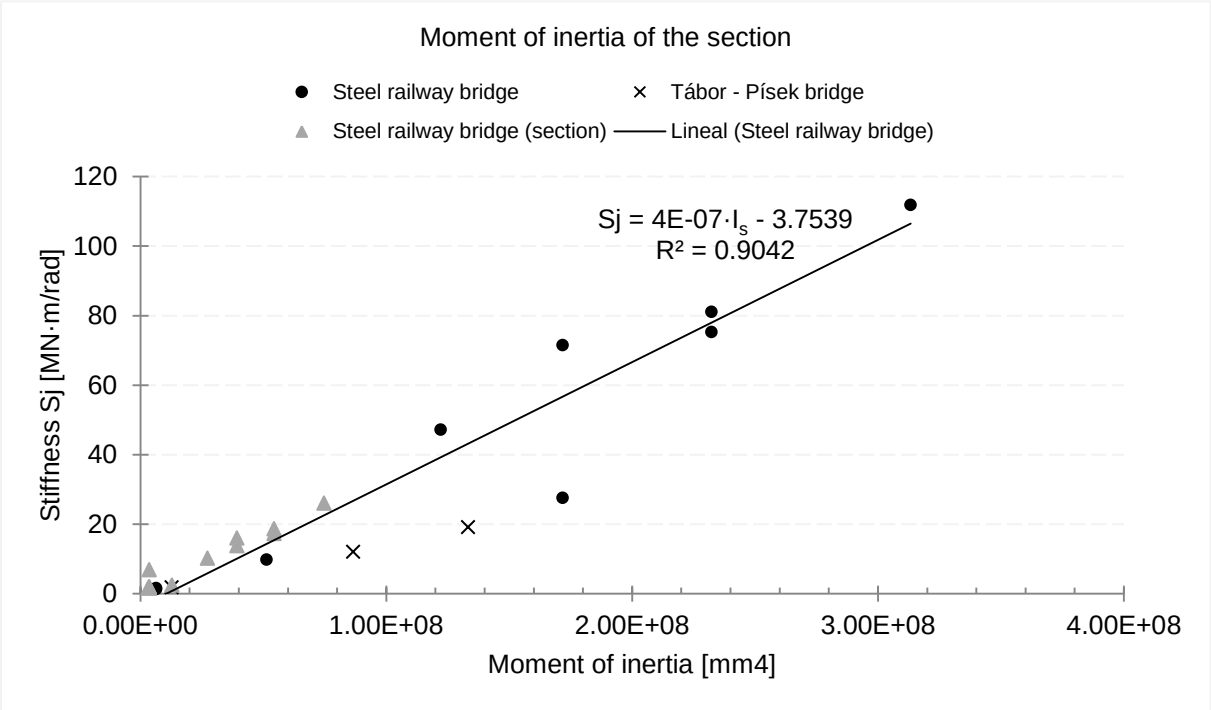

Figure 35. Relation Moment of inertia - stiffness of the joint.

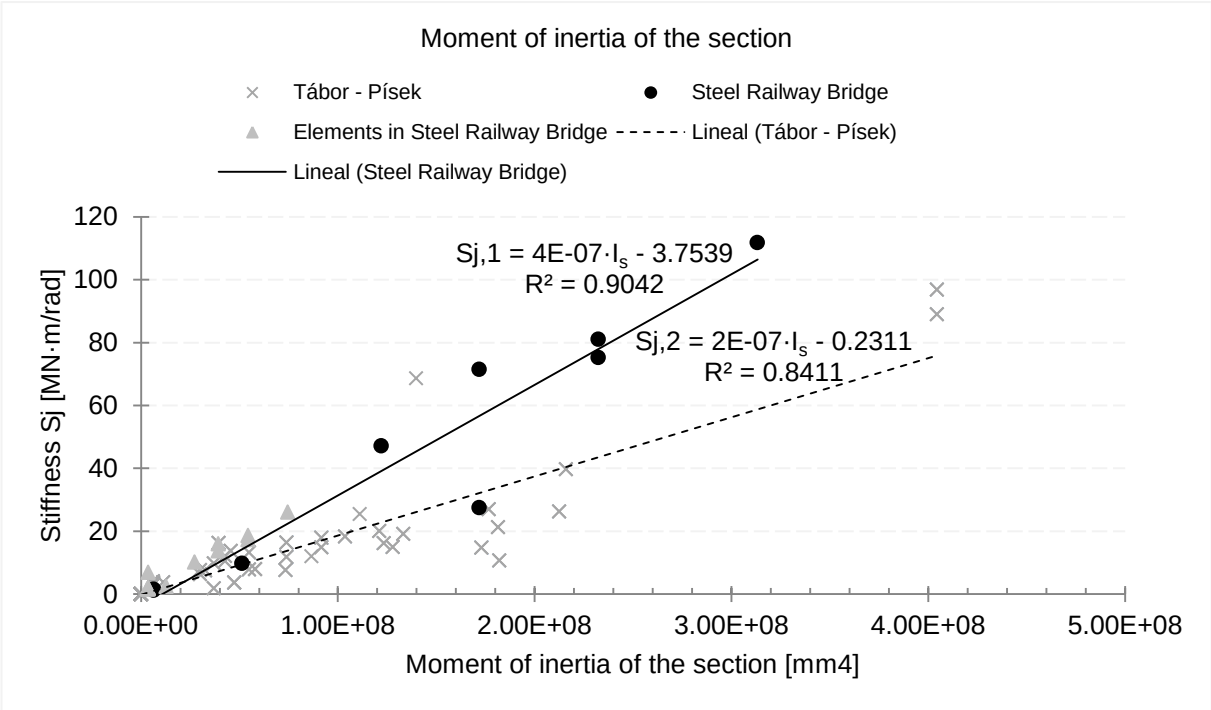

Figure 34. Relation Moment of inertia - stiffness of the joint, with calculated inertia

4.7.2 Connections in the deck.

Table 6 concentrates the results for those connections located in the deck. Table 7 summarize the analysis of the percentage of rigidity and the verification using equations (8) and (9).

Models labelled as '_M2' analyse the rotational stiffness in the weak direction of the element Figure 36]. Here the influence of the connecting plate can be observed in the difference of stiffness in for example inferior and superior plates (elements G_PI and G_PS respectively). For connection C-09, the stiffness of the upper plate is 46% greater than the inferior plate. In the case of C-10, the increment is even bigger: 88%. This influence is barely noticeable in the angles, in both connections the increment of stiffness between inferior and superior angles is 3% (look for the elements G_AI and G_AS).

Model labelled as C9_M2_8 was run with the length of 8.3 m, and no change in the stiffness for each element was observed (Compare the values Sjs for G_AI, G_PI and G_PV). The change in the value of the total stiffness is because for the later neither the superior angles nor the superior plate were analysed, and the total stiffness was calculated considering superior elements having the same stiffness as the inferior, which is not correct as seen from the previous paragraph. The impact of the length in this analysis is only in the percentage of rigidity, which indeed is inversely proportional to the length (eq. 1 and 2). For this, in Table 7 can be observed that model C9_Hor has a percentage of rigidity of barely 4% while in the model considering 8.3 m the percentage is increased to 42%.

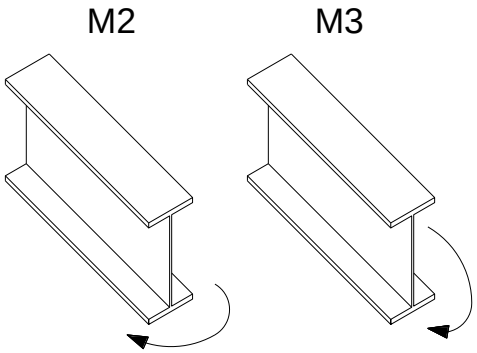

Figure 36. Directions of analysis.

Table 6. Results for connections in the deck.

Connection	Item	L	Med	Mj,Rd	Sjs	Sjs total	N	Nj,Rd	St	St.total
		m	KN·m	KN·m	MN·m/ rad	MN·m/ rad	KN	KN	MN/m	MN/m
C9_M3	G_AI	8.3	-2.0	-35.0	5.3		10.0	14.6	1264.0	
C9_M3	G_PI	8.3	-2.0	-22.7	1.6		10.0	1.9	930.3	
C9_M3	G_PV	8.3	2.0	20.0	342.3	356.1	-10.0	-40.0	1649.8	6038.4
C9_M2	G_AI	1.3	2.0	41.9	9.3		10.0	26.0	1252.7	
C9_M2	G_PI	1.3	2.0	31.1	32.0		10.0	40.0	941.9	
C9_M2	G_AS	1.3	2.0	44.1	9.1		10.0	27.4	1252.9	
C9_M2	G_PS	1.3	2.0	31.1	21.8		10.0	40.0	890.6	
C9_M2	G_PV	1.3	2.0	17.6	0.1	72.2	10.0	0.4	1622.9	5960.9
C9_M2_8	G_AI	8.3	2.0	41.9	9.3		10.0	26.0	1252.7	
C9_M2_8	G_PI	8.3	2.0	31.1	32.0		10.0	40.0	941.9	
C9_M2_8	G_PV	8.3	2.0	17.6	0.1	82.6	10.0	0.4	1622.9	6012.0
C10	DH1	5.9	2.0	35.1	2.3	4.6	10.0	23.3	124.1	248.3
C10_M2	G_AS	1.3	2.0	44.1	9.1		10.0	27.4	1252.5	
C10_M2	G_PS	1.3	2.0	31.1	21.8		10.0	1.9	930.3	
C10_M2	G_AI	1.3	2.0	41.9	9.4		10.0	26.0	1255.3	
C10_M2	G_PI	1.3	2.0	31.1	41.2		10.0	1.9	930.3	
C10_M2	G_PV	1.3	0.5	17.6	0.1	81.6	-10.0	0.4	1631.1	5999.4
C11_M3	B1_AI	3.3	-2.0	-11.0	1.1		-10.0	-14.1	505.8	
C11_M3	B1	3.3	2.0	7.9	73.3	75.6	-10.0	-40.0	749.0	1760.7
C11_M2	B1_AI	3.3	0.1	14.9	0.8		-10.0	-27.8	323.3	
C11_M2	B1	3.3	0.1	8.6	0.0	1.5	-10.0	-0.6	747.2	1393.8

Table 7. Verification of stiffness parameters for the elements in the deck.

Connection	Item	Sjs	Sjs total	Sj,R	25·E·Ib/ Lb	Sj,P	0.5·E·Ib/ Lb		25·E·Ib/ Lb	0.5·E·Ib/ Lb	
		MN·m/ rad	MN·m/ rad	MN·m/ rad	MN·m/ rad	MN·m	MN·m	$\%_{Rel}$	MN·m	MN·m	$\%_{Sect}$
C9_M3	G_AI	5.3		3.8	3.8	0.1	0.1				
C9_M3	G_PI	1.6		0.4	0.4	0.0	0.0				
C9_M3	G_PV	342.3	356.1	748.8	748.8	15.0	15.0	6%	6011.6	120.2	4%
C9_M2	G_AI	9.3		56.6	57.2	1.1	1.1				
C9_M2	G_PI	32.0		560.0	560.0	11.2	11.2				
C9_M2	G_AS	9.1		56.6	57.2	1.1	1.1				
C9_M2	G_PS	21.8		560.0	560.0	11.2	11.2				
C9_M2	G_PV	0.1	72.2	0.8	0.8	0.0	0.0	4%	1235.2	24.7	4%
C9_M2_8	G_AI	9.3		8.9	9.0	0.2	0.2				
C9_M2_8	G_PI	32.0		87.7	87.7	1.8	1.8				
C9_M2_8	G_PV	0.1	82.6	0.1	0.1	0.0	0.0	42%	193.5	3.9	42%
C10	DH1	2.3	4.6	9.6	9.6	0.2	0.2	23%	19.2	0.4	23%
C10_M2	G_AS	9.1		56.6	57.2	1.1	1.1				
C10_M2	G_PS	21.8		560.0	560.0	11.2	11.2				
C10_M2	G_AI	9.4		56.6	57.2	1.1	1.1				
C10_M2	G_PI	41.2		560.0	560.0	11.2	11.2				
C10_M2	G_PV	0.1	81.6	0.8	0.8	0.0	0.0	5%	1235.2	24.7	5%
C11_M3	B1_AI	1.1		2.3	2.4	0.0	0.0				
C11_M3	B1	73.3	75.6	440.9	440.9	8.8	8.8	5%	1258.1	25.2	4%
C11_M2	B1_AI	0.8		5.3	5.4	0.1	0.1				
C11_M2	B1	0.0	1.5	0.1	0.1	0.0	0.0	13%	11.0	0.2	12%

Figure 37 represents graphically the stiffness values presented in Table 6. Here it is easier to see how the bigger plate and the diagonals contribute to increase the stiffness in the weak direction of the cross beam in connections C-09 to C-10, around 13% of increment. Also, it can be observed how the vertical rotational stiffness is much bigger than horizontal rotational stiffness.

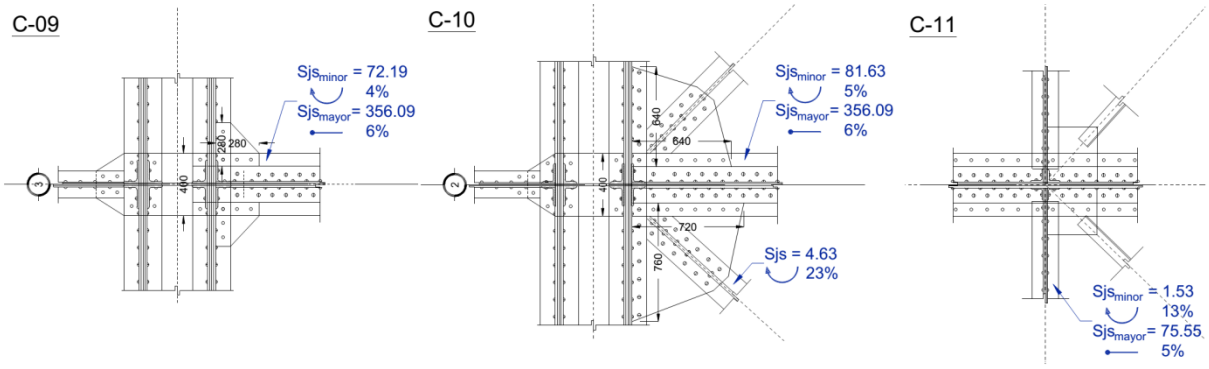

Figure 37. Stiffness in connections in the deck. All values in MN·m/rad.

5. PARAMETRIC ANALYSIS

5.1 General model.

The general model has been prepared by Filip Kramoliš from the Department of Steel and Timber Structures of the Faculty of Civil Engineering in Prague as part of his final thesis [25]. The software used to build the 3D model is CSI Bridge and includes the geometry of one entire section of the bridge.

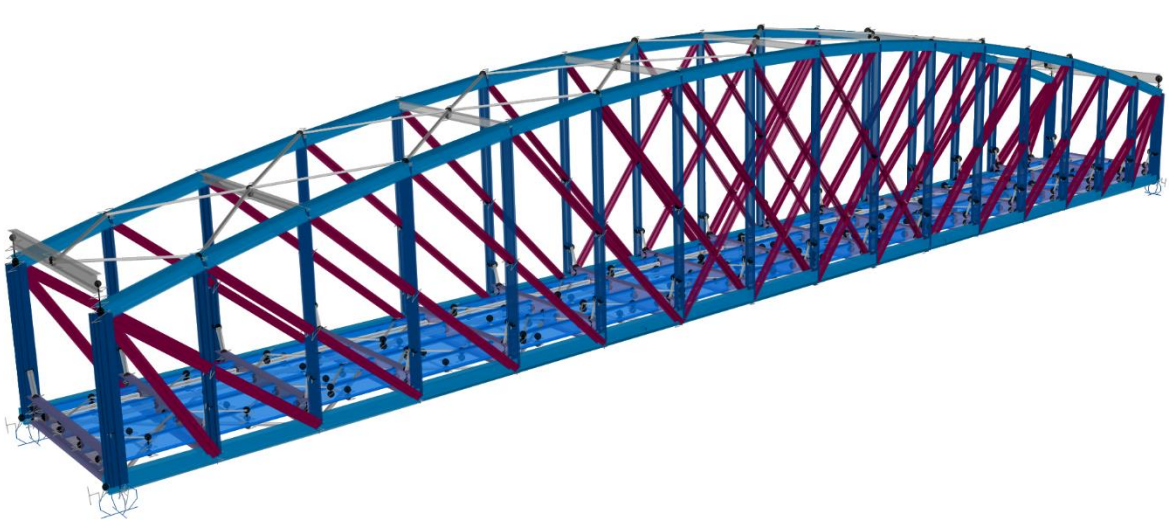

Figure 38. General view of the 3D model.

In the model created, all the cross sections are user-defined sections according to the real geometry of the structure. Some representative examples of sections are shown in Figure 39. Note that diagonals have a web smaller than the gap between the angles; this is to account for the strip plates that join the two sections of the element. Also, two sections of vertical elements were created, the first one for the part of the connection in which the web is a continuous plate (in the connections), and the second, with a smaller web to account for the crossing strip plates. The different elements are connected using links with a specified stiffness, this is done so the real position of the member is considered, aimed for taking into account the effects due to the eccentricities in the connections. Figure 41 shows a detail of the line model, the extrusion of the elements and the real connection. Note here the crossing plates that in the model are represented by a continuous plate.

The model is simply supported in four points, restraining only vertical displacement. In four supports, a spring is assigned in the perpendicular direction of the bridge, and only in one end, additional spring is assigned to the direction of the bridge. Members like the bracing in the upper chords and the small bracing in the deck have release in both ends. In the principal members, the releases were modified to account for the stiffness, as it is later specified.

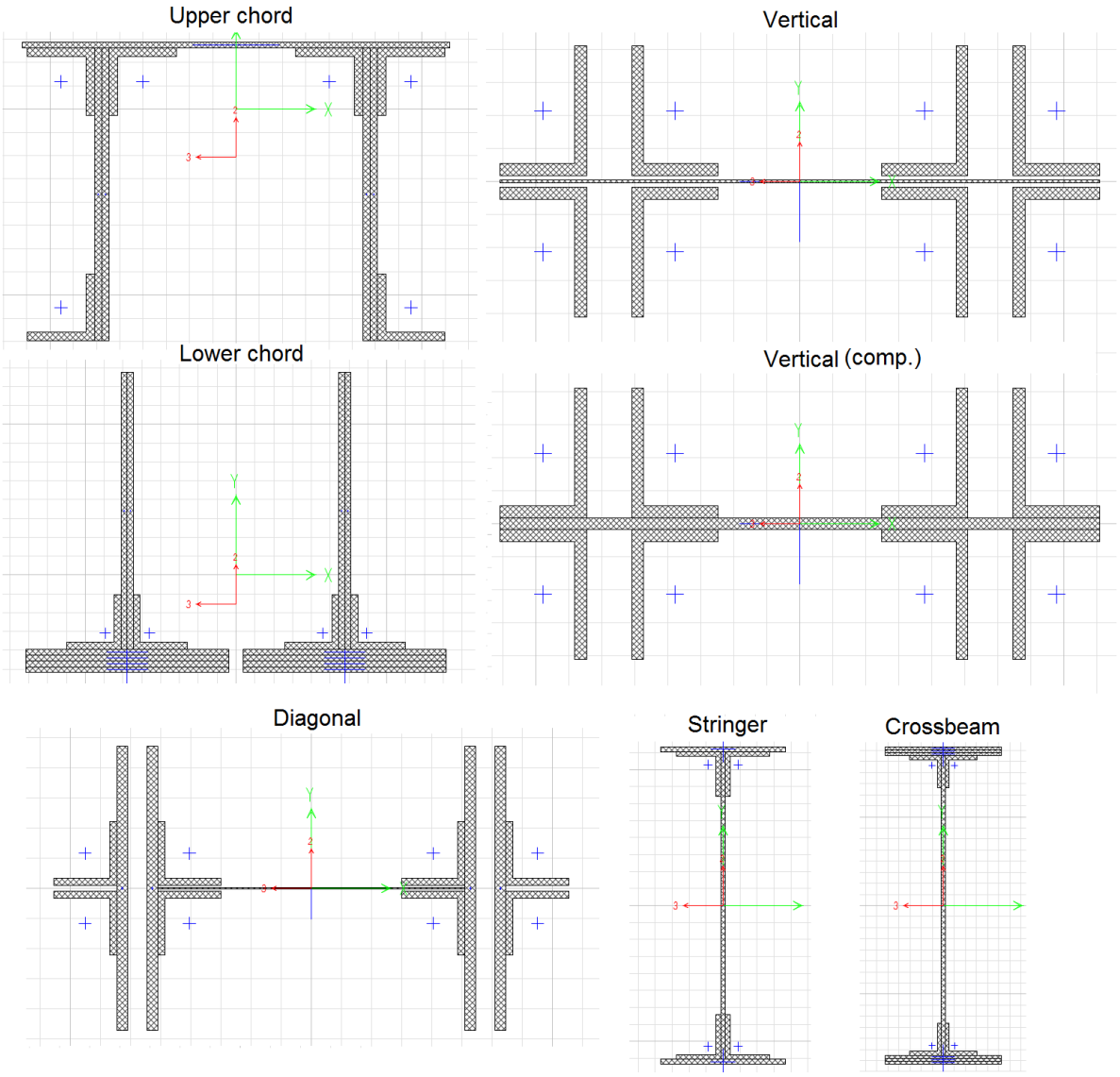

Figure 39. Cross sections definition for the general model.

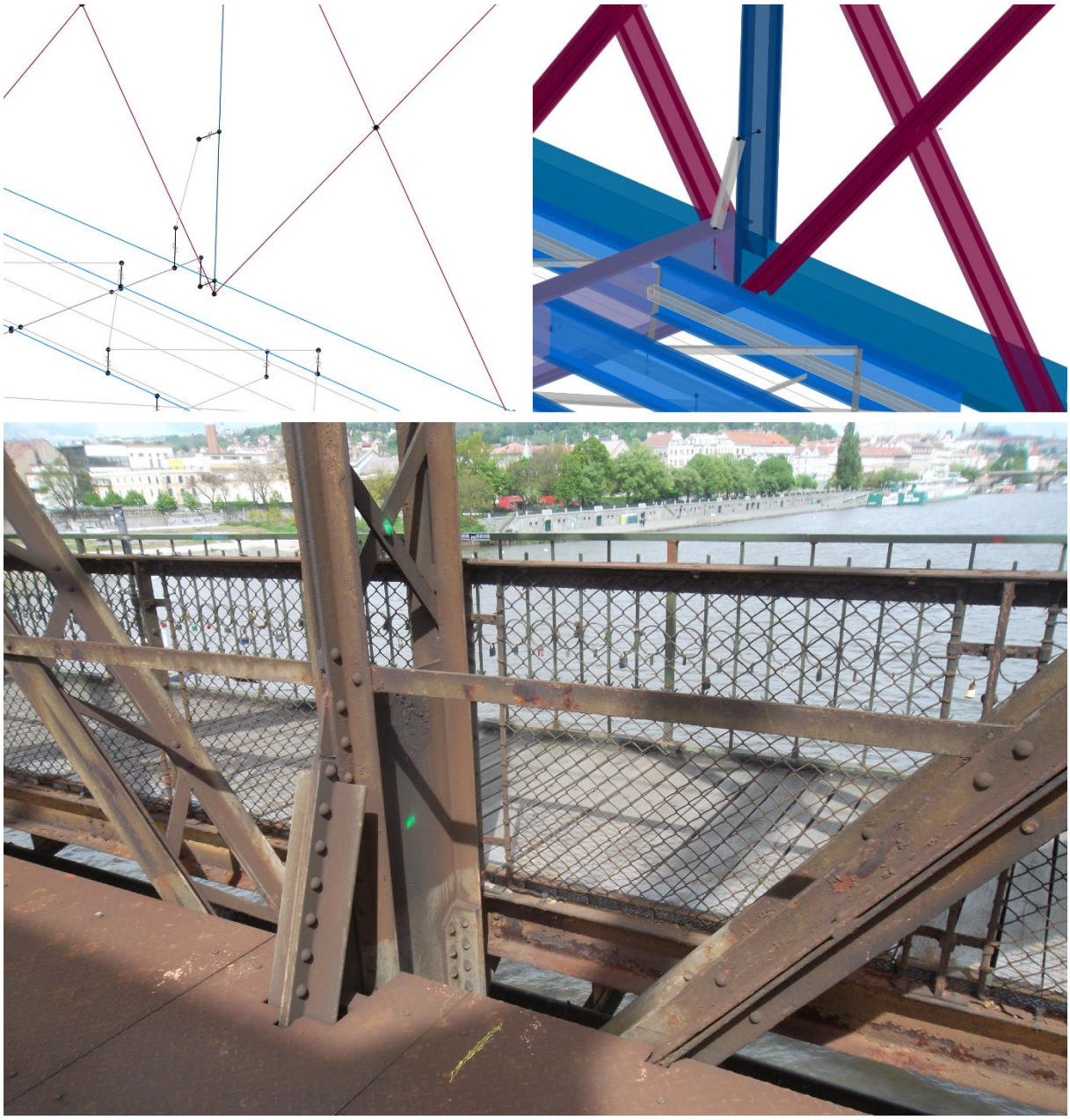

Figure 41. Detail of the line model, extruded view and the real structure.

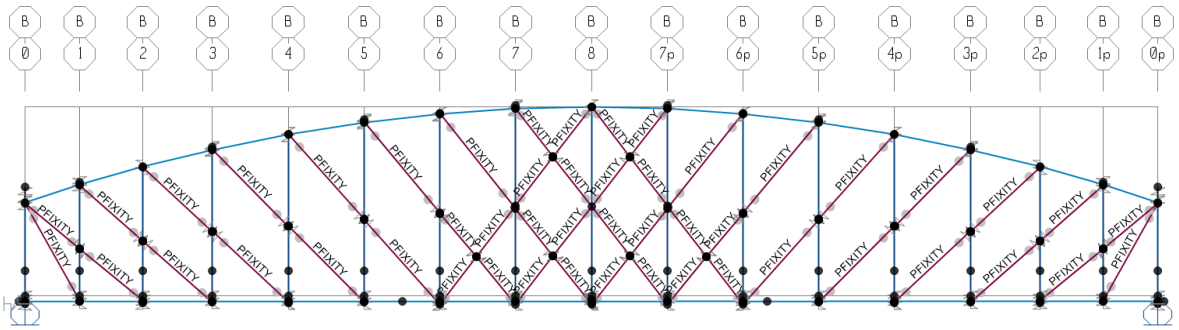

Figure 40. Analytical model.

CSI Bridge is a software developed by Computers and Structures, Inc. focused on the modelling, analysis, design, and optimization of bridges. The environment of the software contains tools to create an object-based model which is converted into a finite element model for the analysis. In this program, the elastic linear behaviour of the materials is considered, as well as the deformations due to bending moment, axial load, shear and torsion in the computation of the total response of the structure. [26]

The results from this model are compared using the stress S11, which is computed as

$$S11 = \frac{P}{a} - x2\frac{M3}{i33} - x3\frac{M2}{i22} \tag{11}$$

Where *P* is the axial force, *a* is the cross-sectional area, *M3* and *M2* are the bending moments in both directions, *i33* and *i22* are the section moments of inertia. *X2* and *X3* are the coordinates of the point in which the stress is calculated. For sections created in the section-designer tool, the points are assumed in the four corners of the rectangular bounding box of the section [See Figure 42]. The stress is also calculated at the centroid of the section (point 0), which is the stress due to axial force only. Tensile stresses are positive and compressive stresses are negative. [26]

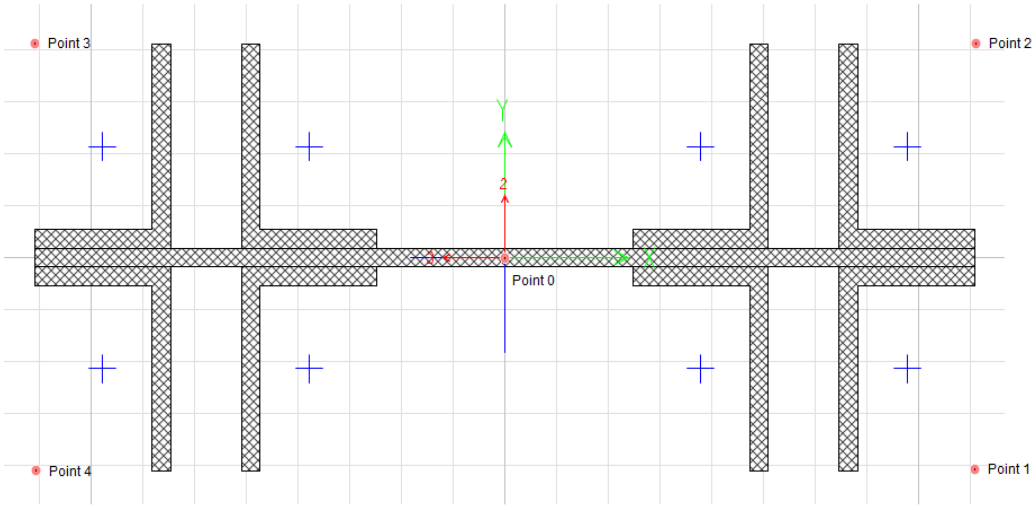

Figure 42. Points used for the calculation of the stresses in CSI Bridge.

It is important to notice that the cross sections on the bridge analysed are composed of different plates an angles, and they were built up in the section designer subprogram. As explained in the previous paragraph, the stress reported are in the four corners of the rectangle that bounds the cross section, so they do not reflect the real stresses on the elements of the bridge, which may be overstressed in theory but not necessarily in reality. Thus, the use of the stresses for the comparison is not meant to express the capacity of the member, but to compare the different models. Furthermore, the stresses are distributed among the different elements as they approach the connections, where the higher

stresses are presented. This can be avoided by using the end offsets option included in the program, but it is not used in this analysis. In other words, the stresses compared are those with maximum values but they are normally overestimating the real stress in the elements.

5.2 Loads

The analysis is made for static loads only. Two load cases are considered: dead load, including the self-weight; and the live load, for which the train model used was LM7 and whose characteristics are presented in Figure 44.

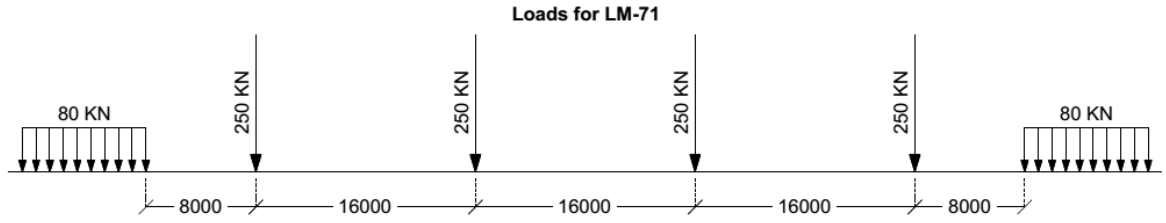

Figure 44. Load characteristics for train LM71.

The load was applied only in one track of the two that are held by the bridge. This is the most common condition and serves to this analysis.

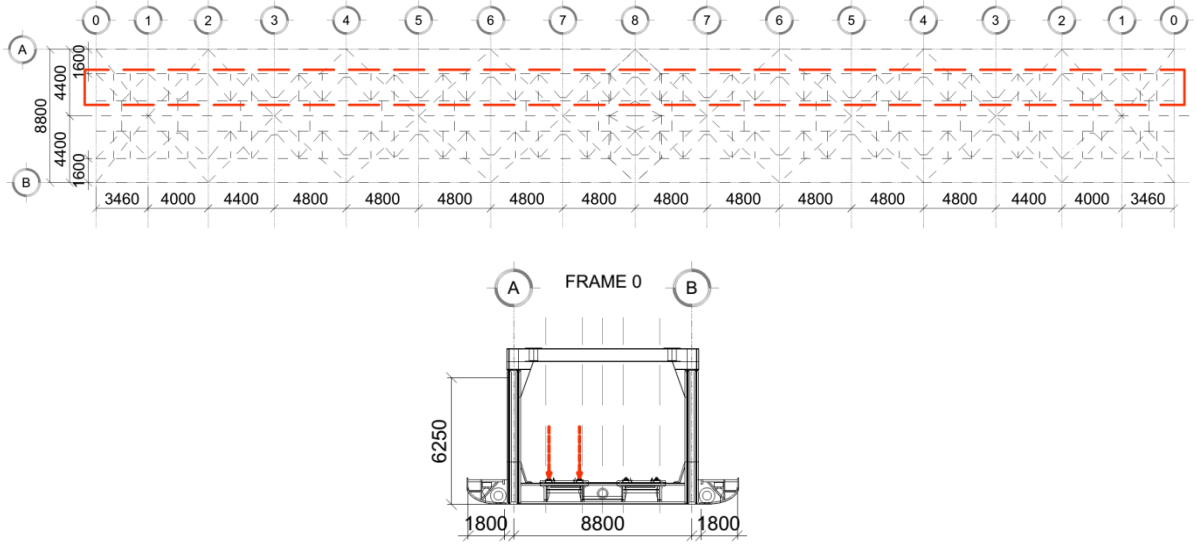

Figure 43. Loaded track.

For the live load, three positions of the load were used.

LL-50 Live load centered at frame 8, midspan.,

LL-33 Live load centered at frame 6, approximately at one third of the span length

LL-25 Live load centered at frame 4, approximately at one quarter of the span length.

- Load combinations.

Four load combinations were used in the general model to make the comparison of the results. These combinations do not include any factor.

Dead Dead load

UIC_50 1.0 (Dead load + LL-50)

UIC_33 1.0 (Dead load + LL-33)

UIC_25 1.0 (Dead load + LL-25)

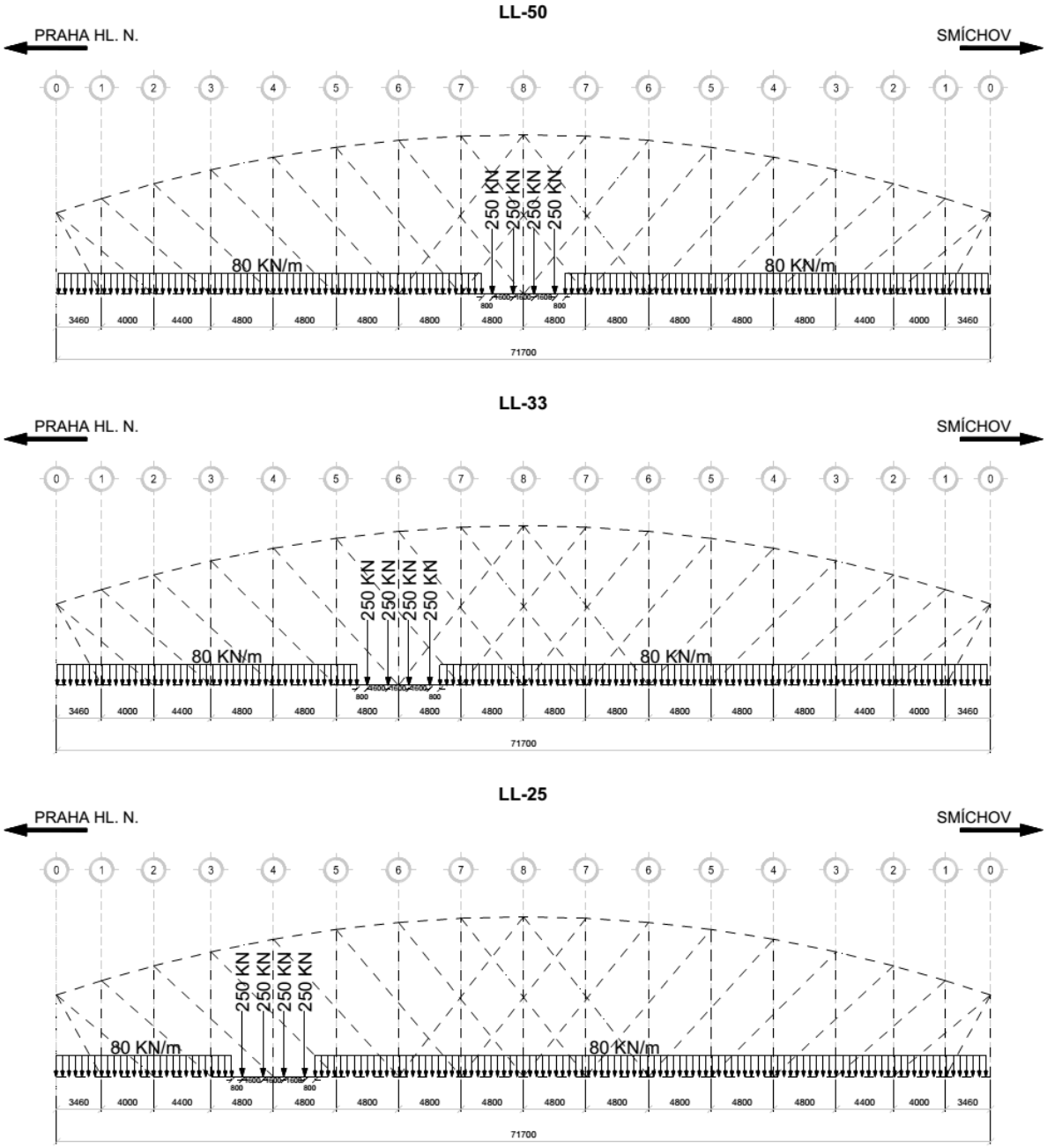

Figure 45. Position of loads for live load combinations.

5.3 Parametric study

The values of stiffness obtained were for both, connections in the truss of diagonals with chords and verticals, and for connections of cross beam and stringer in the deck. Based on this, four families of models were prepared:

- D – to investigate the impact of the connections of diagonals
- C – to investigate the impact of the connections among diagonals
- B – to investigate the impact of the connections of the cross beam
- S – to investigate the impact of the connections of the stringer.

The first two families are related with the behaviour of the truss, while the last two are in relation with the deck analysis.

For the parametric study, each family was analysed with the assumption of the fully rigid connection and with the pinned connection. In the case of the crossbeam and the stringer, the analysis of the two directions is important so another pair of models were prepared restraining the connection in one direction maintaining the stiffness for the other direction [see Figure 46]. In this analysis, rotational stiffness in the plane perpendicular of the truss is not accounted. In total, 12 models where prepared according to the following matrix.

No.	Model	Member to analyse	Stiffness value	
			M2	M3
0	A	Diagonals	S_J	1
		Crossbeam and stringer	S_J	S_J
1	D0	Diagonal	0	1
2	D1	Diagonal	1	1
3	C0	Crossings in diagonals	0	1
4	C1	Crossings in diagonals	1	1
5	B0	Cross Beam	0	0
6	B1	Cross Beam	1	1
7	BM20	Cross Beam	0	S_J
8	BM30	Cross Beam	S_J	0
9	S0	Stringer	0	0
10	S1	Stringer	1	1
11	SM20	Stringer	0	S_J
12	SM30	Stringer	S_J	0

M2: Minor axis of the section

M3: Major axis of the section

Sj: The theoretical value of stiffness, obtained in section 4.

1: Rigid behaviour, (the value was left unchecked)

0: Pinned behaviour (a value of zero is assigned to the release)

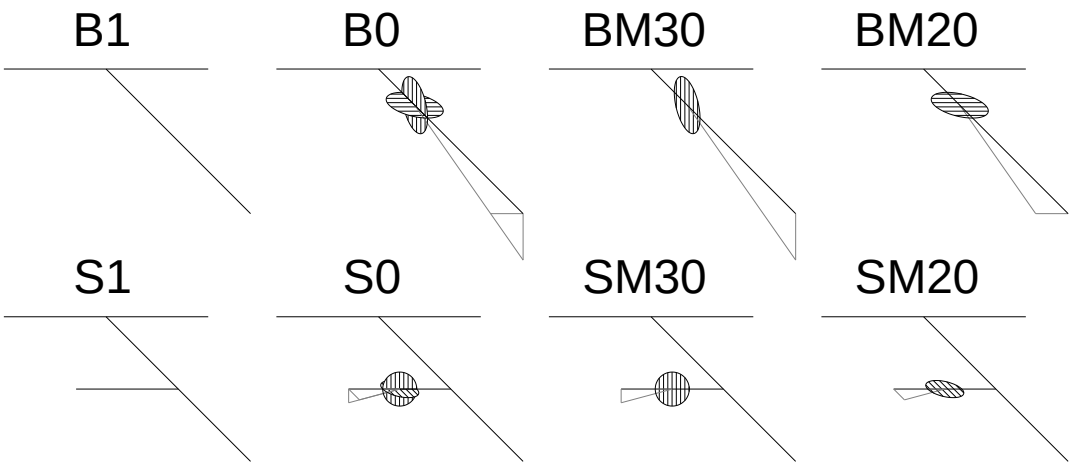

Figure 46. Directions of analysis in the parametric study.

In CSI Bridge, the end conditions of the elements are assigned to the frames with the releases. [Figure 47]. The values of the stiffness were directly introduced on the corresponding boxes.

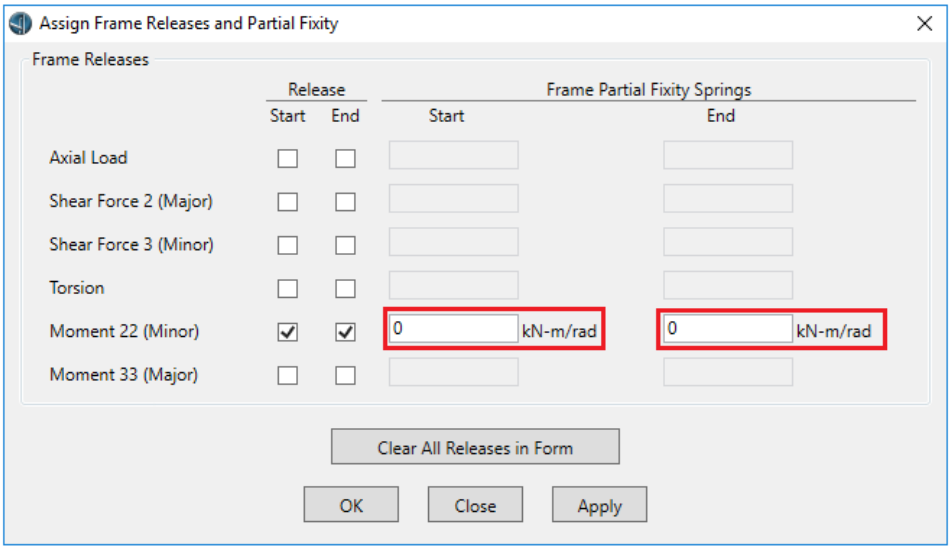

Figure 47. Releases window for assign end properties in CSI Bridge.

5.4 Results for model A

Model A is the model taken as a reference for the parametric analysis. In this model the stiffness obtained in section 4.7 were assigned as releases in the corresponding elements. The results presented in this section include the vertical displacements, the stresses in the truss, and the stresses in the deck. The truss for which the results are reported is the one on the side of the loaded lane (A axis). The stresses on the deck are those on the crossbeams and in the stringer.

5.4.1 Vertical displacement

Figure 48 shows the deformation shape in the crossbeams for dead load (DEAD) only and for the train located at midspan (UIC_50). The first load case produces a uniform deformation of the beam with a maximum value of 11.67 mm, located at the midspan crossbeam (point obj. 1 in Frame 8). The live load produces an asymmetrical deformation as depicted for the second load case (UIC_50), with a maximum absolute deflection of 37 mm measured in the same point as for the dead load case (point obj. 1 in Frame 8). This represents a relative deflection of 25.4 mm for the live load, 218% of the initial displacement. The asymmetrical deformation for the UIC_50 load case produces a distortion in the frame of 1.8e-5 (1.44 mm/8800 mm).

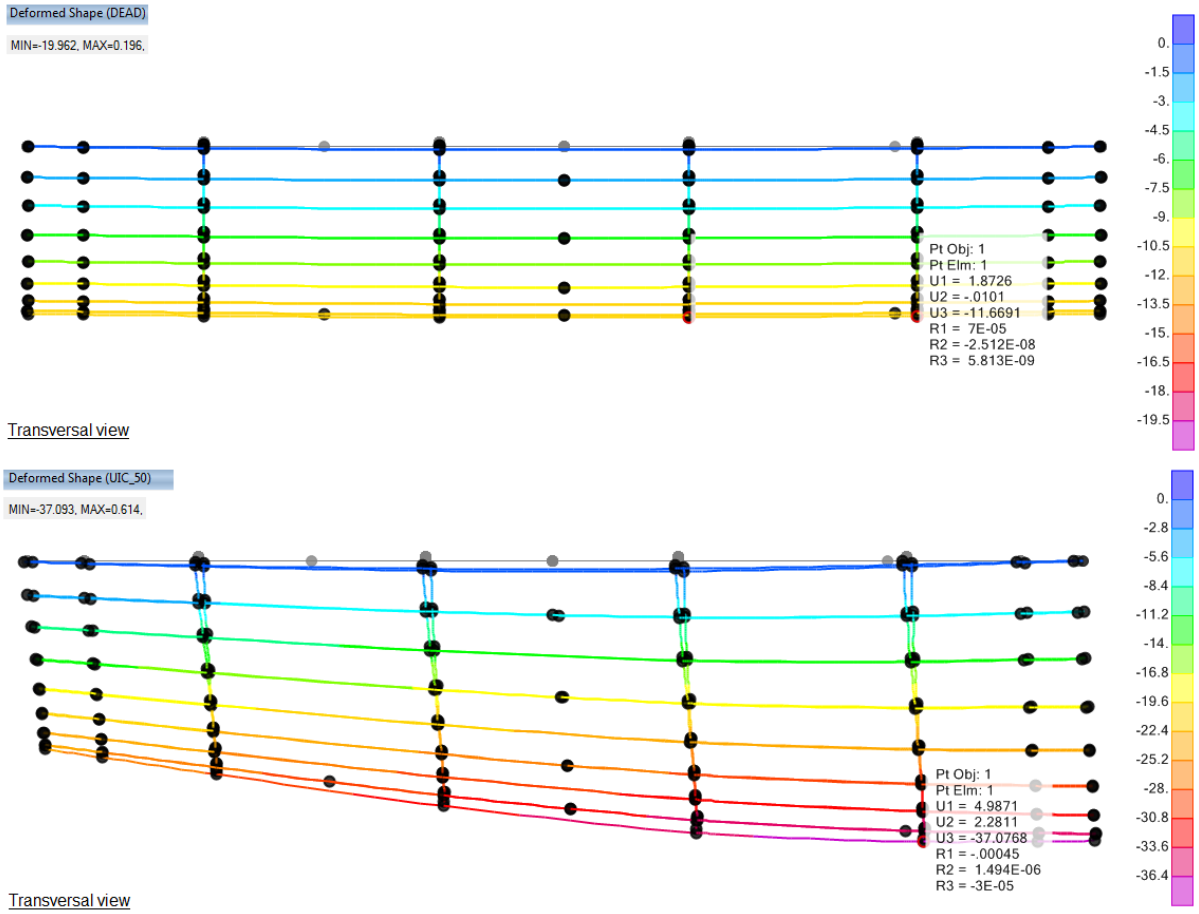

Figure 48. Vertical displacements in the deck in model A, for Dead and UIC_50 load cases. Values in mm

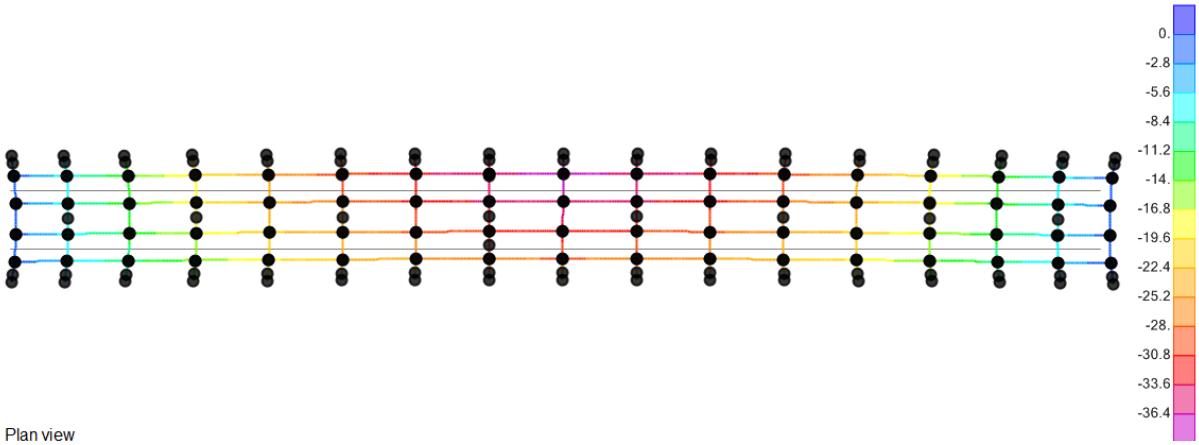

Figure 49. Displacement in the deck, model A (Plan view). Values in mm

The deformation contours in a plan view for the UIC_50 load case is shown in Figure 49, where it is clear that the maximum displacements are concentrated in the central frames. This figure also shows the typical behaviour of steel decks, where the cross beams are deformed not only in the vertical (major) axis as normal beams, but there is also a small deformation in the weak (minor) axis which is greater in the frames closer to the supports, and is reduced in the midspan.

5.4.2 Stresses in the truss

The maximum stress contours in the truss are shown for two load conditions DEAD and UIC_50 in Figure 50. The general behaviour of a truss can be observed, where the upper chord is in compression and the lower chord is in tension. Vertical elements are in high compression in the frames closer to the supports, and the stress is gradually decreasing in the central frames, where there are even members in tension. On the contrary, diagonals are normally in tension in the frames closer to the supports, which are decreasing in value towards the center. The stress values of two points are also shown, as representative values for the maximum and minimum. The maximum stress is located in diagonal D2 close to the frame 0, where the maximum tension force is also presented. The minimum stress, associated with the maximum compression force, is located in the vertical element of frame 0 as well.

Table 8 shows the exact values of the stresses in the points where they are maximum and minimum, for each of the four load cases. The effect of the live load increases the stresses over 300% for both, the maximum and minimum stress. The table reports also the stresses in the point 0 (axial stress) and its percentage with respect to the maximum stress. It can be noted that the axial part of the stress is 73 % of the maximum stress, in other words, the participation of the stresses due to bending moment is 27 % of the maximum stress. For the case of minimum stress, the participation of the bending moment in the total stress is 38 %.

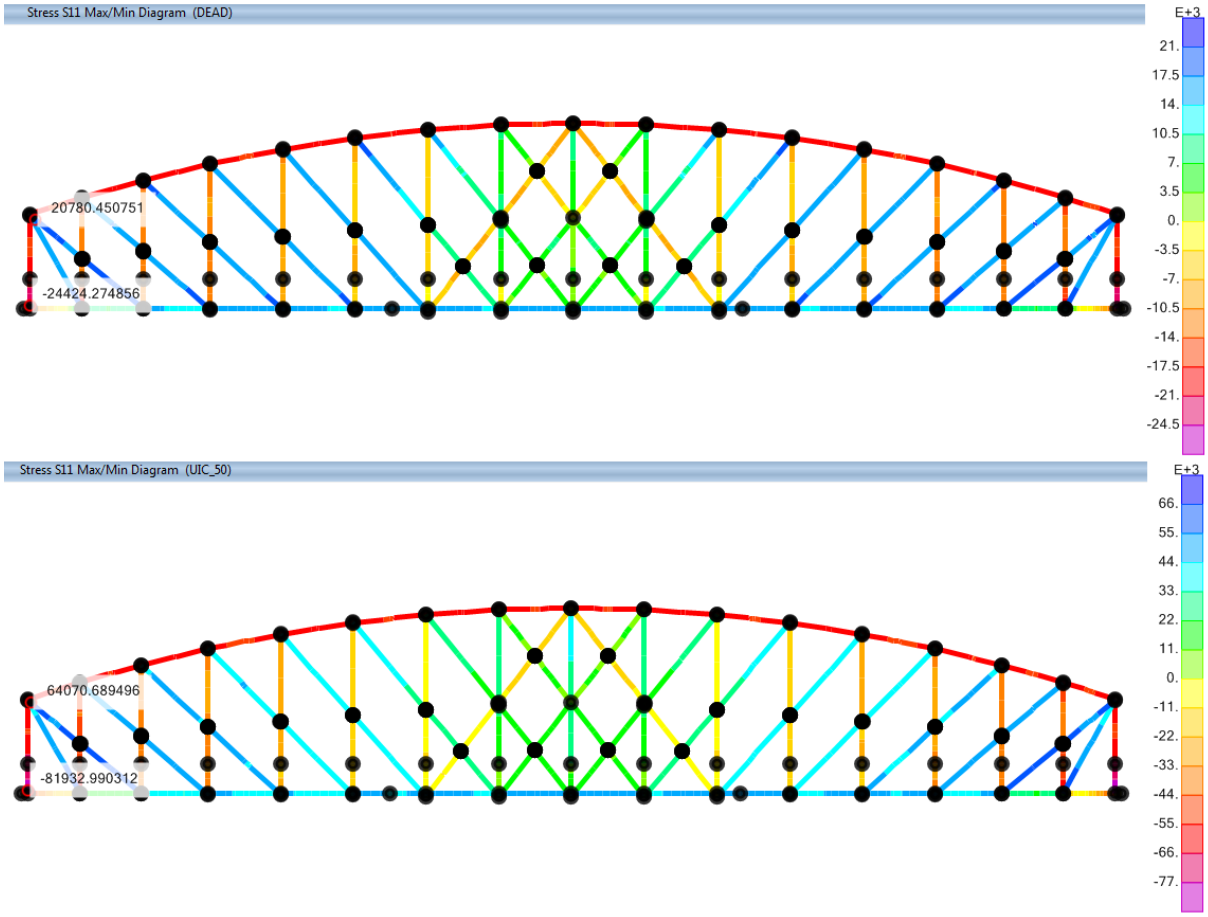

Figure 50. Maximum and minimum stress diagram of model A [kPa].

Table 8. Maximum and minimum stress in the truss for model A

Load Case	S0	SMax	S0/ SMax	SMax/ SMax,dead	S0	SMin	S0/ SMin	SMin/ SMin,dead
	kPa	kPa	%	%	kPa	kPa	%	%
DEAD	15,758	21,578	73%	100%	-15,399	-25,136	61%	100%
UIC_50	51,041	65,798	78%	305%	-50,779	-83,497	61%	332%
UIC_33	51,853	67,147	77%	311%	-51,105	-83,081	62%	331%
UIC_25	52,841	68,348	77%	317%	-51,844	-84,093	62%	335%

5.4.3 Stresses in the deck

Figure 51 shows schematically the distribution of the maximum stresses in the cross beam for the 4 load cases. For the case of the dead load, the maximum stresses are bigger in the ends and decrease towards the center; this behaviour is related with the component of the moment on the minor axis of the cross beam, which is normally weak, and therefore, the stresses are increased. For the live load cases, the most relevant change in the behaviour is the increase of stress in the loaded area. For load case UIC_50, the stresses in the central crossbeams are increased, and the location of the maximum is displaced to the upper crossbeams for UIC_30, and UIC_25 load cases.

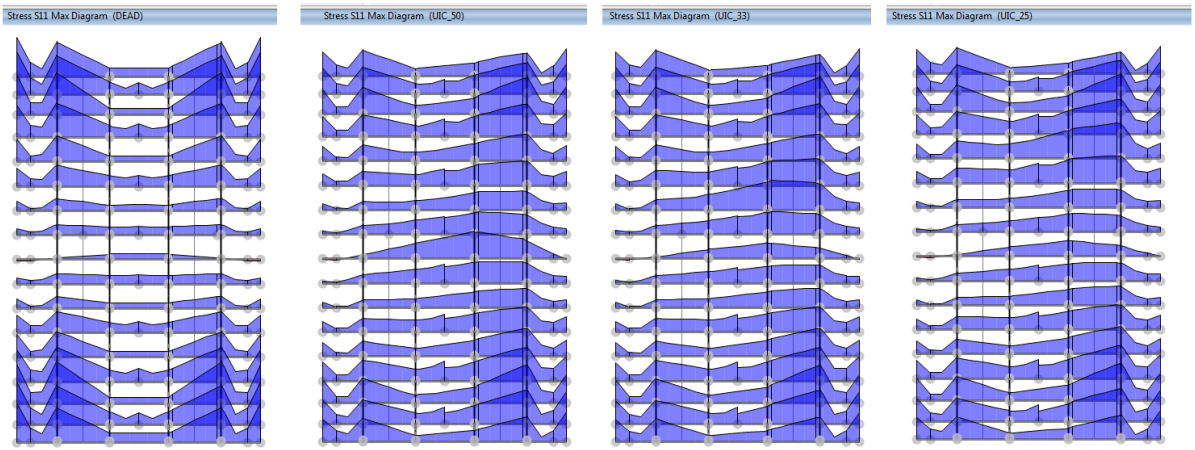

Figure 51. Maximum stresses in the crossbeams.

Figure 52 shows the maximum stress in the crossbeams right below the loaded track. For the dead load case, the participation of the axial stress is practically zero, that is, the stress is influenced almost totally for the bending stresses. Also, the maximum stress is present not in the supports but in frame number 2, this is due to the interaction between the M2 and M3 stresses as it is shown in the following calculation. Note that the axial stress is 2%, the M3 (major) is 8% and the minor stress M2 is 90% of the stress.

$$S11 = \frac{P}{a} - x2\frac{M3}{i33} - x3\frac{M2}{i22} = \frac{20.6}{0.045} - 0.54\frac{26.801}{9.5e-03} + 0.2\frac{27.53}{3.06e-04} \\ = 457 + 1522 + 18005 = 19985\ \text{kPa} \tag{12}$$

In the lower diagram, it is shown the significant increasing of stress for the live load. A small variation in the maximum for fames 6 and 4 is presented for UIC_33 and UIC_25 load cases.

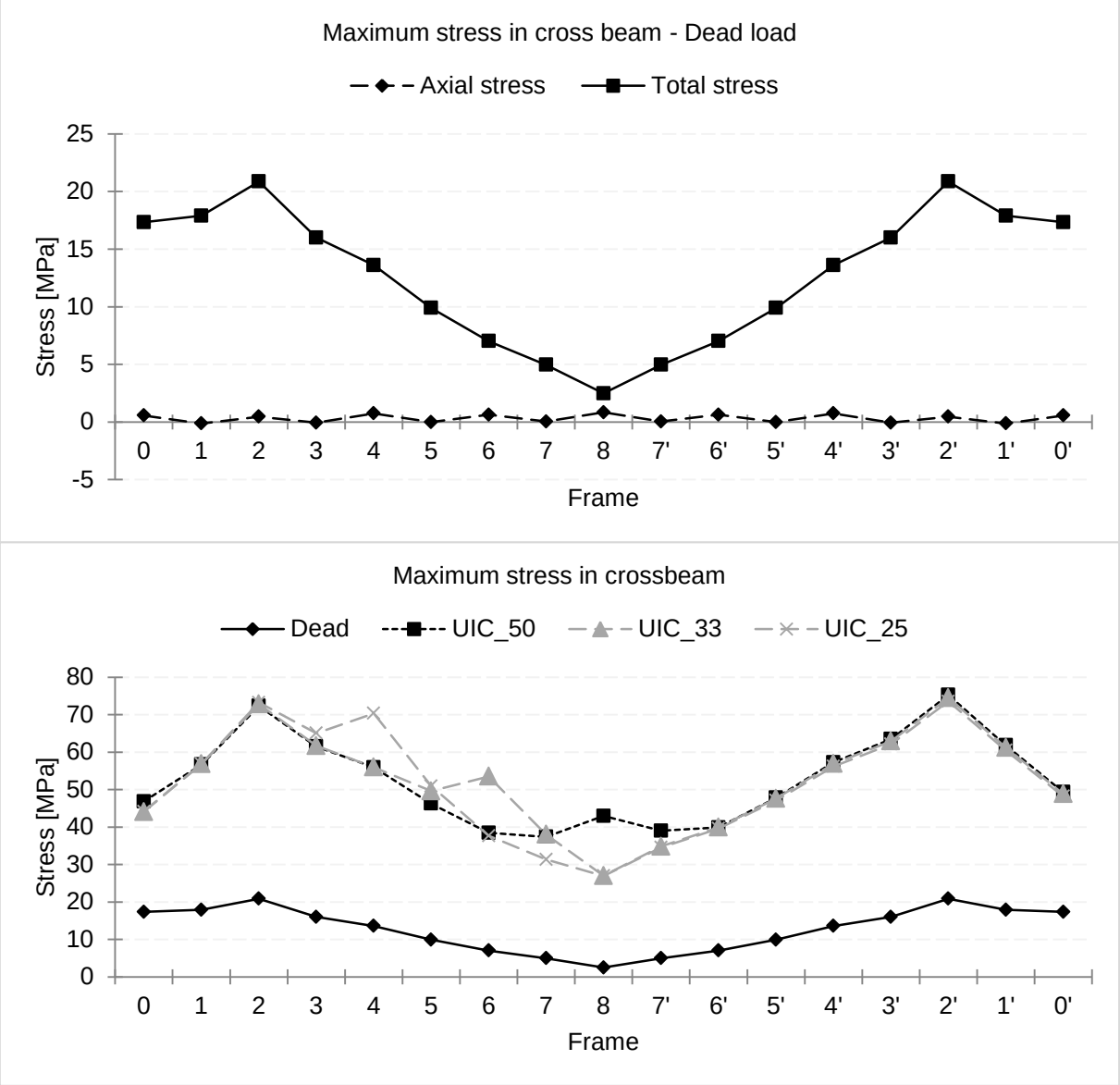

Figure 52. Maximum stress in crossbeams.

In the case of the stringer, the results are presented in Figure 53. The participation of the axial stress is higher, composing around 80% of the total stress. The axial force is increasing towards the midspan, with also an increasing participation of bending moments.

The effect of the live load only increments the value of the stress, showing the peaks for when the load is acting in the section.

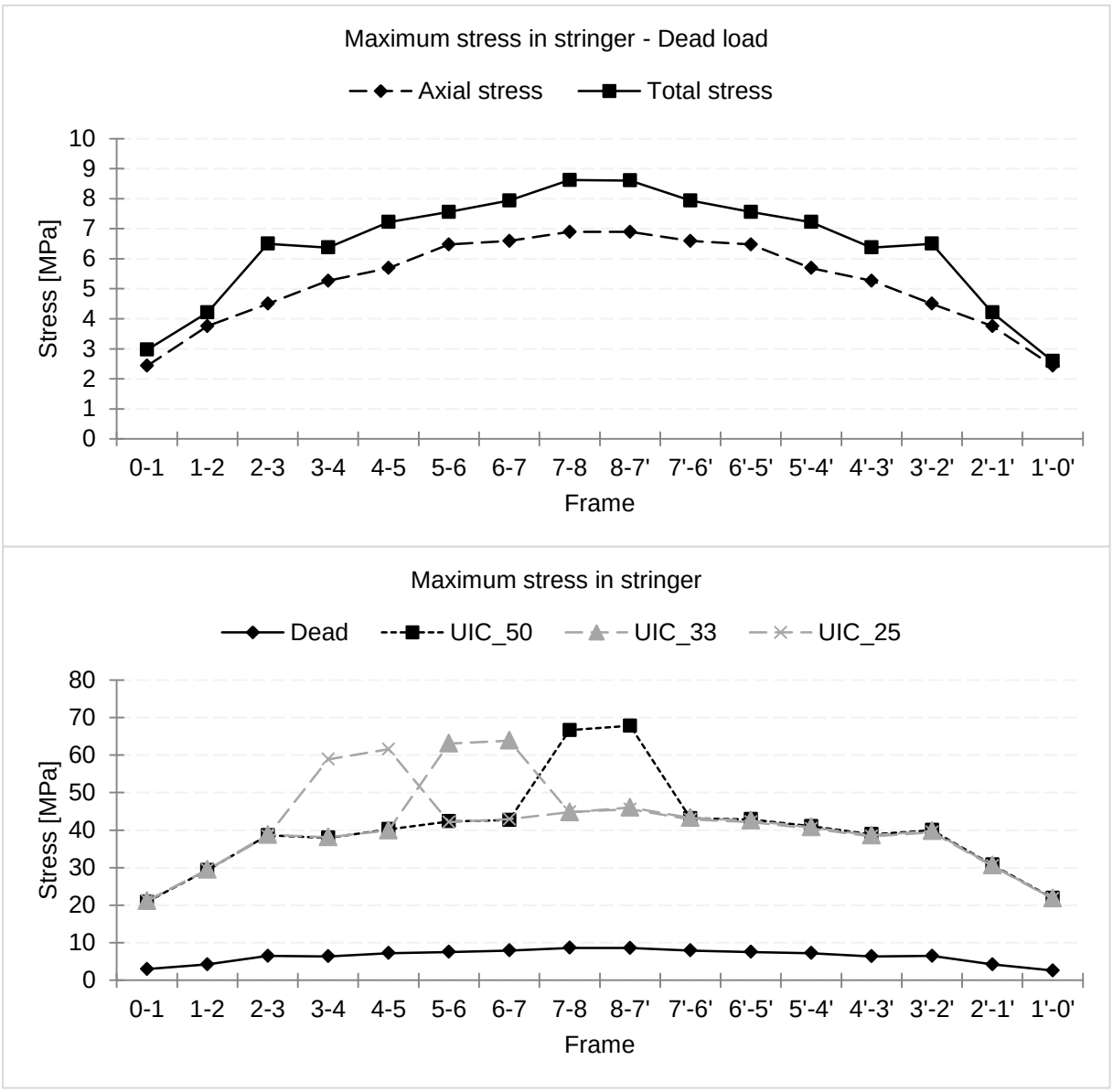

Figure 53. Maximum stresses in the stringers.

5.5 Results from the parametric analysis

The following section summarizes the results of the 12 models specified in section 2.7 for the parametric analysis together with the results from model A, taken as a reference. In this section, more than the values, the percentage with respect to the results in the base model is used to determine the degree in which each parameter influences in the results. For this, normalization with respect to the results of model A is made, so that the results are certain percentage of the reference model. The percentage of error is used as well, defined as the difference between the value observed and the corresponding value in the reference model, divided by the value on the reference model.

5.5.1 Vertical displacement.

Figure 54 presents the vertical displacements in the truss at the midspan (frame 8). The upper diagram is for dead load only, and the lower one is under the three live loads considered in this analysis. Both diagrams present a similar pattern; the only change is in the scale that, similar to the results from model A, is increased 200% for the live load.

It can be noted in Figure 55 that the models B present the largest error with respect to the reference

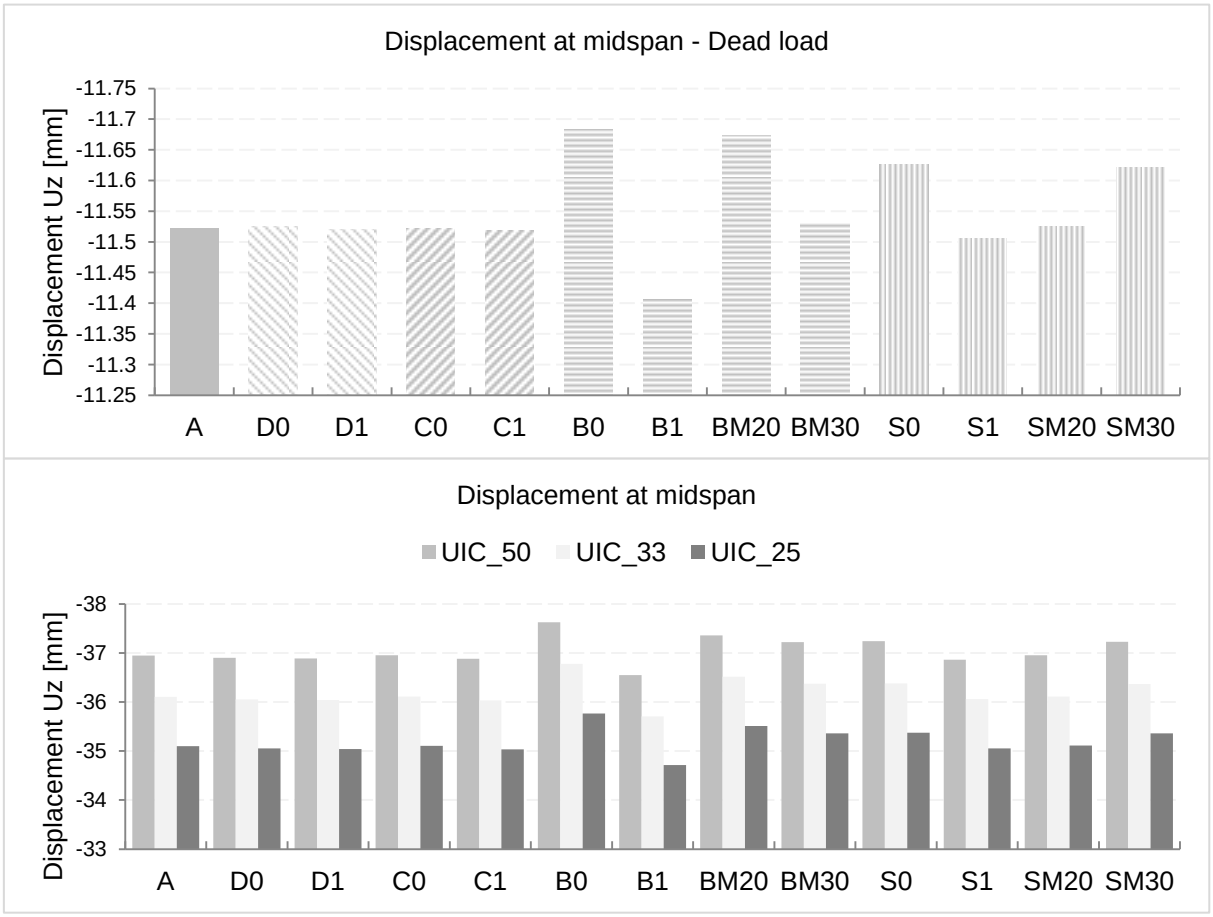

Figure 54. Vertical displacements at midspan in lower chord of the truss.

model A, that is, the deflection in the truss is sensitive to the consideration in the connections of the crossbeam. However, this represents only a difference of 3%. Similarly, but in a lower scale, the connections in the stringer influences also in the results.

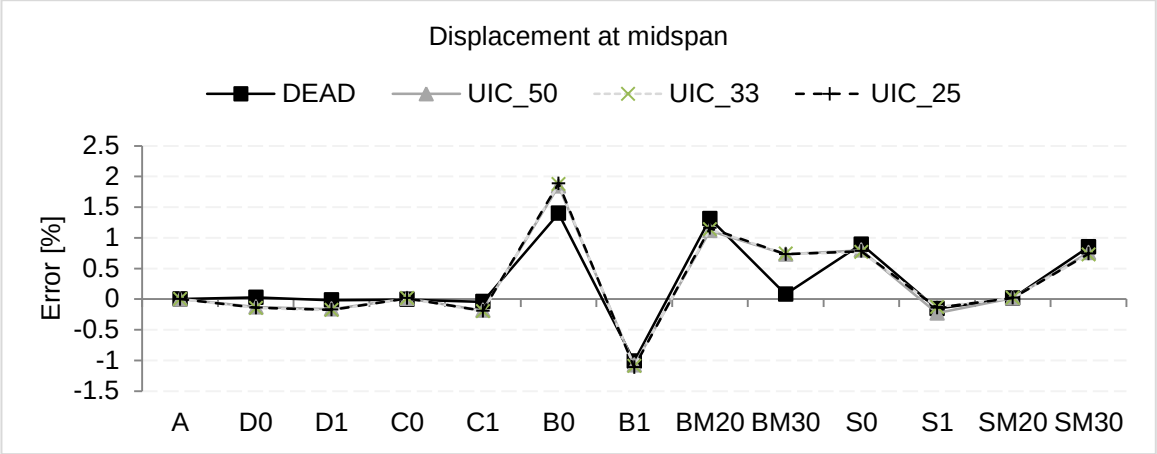

Figure 55. Error in the displacement at midspan.

Prevoius results were only for the displacements in the midspan. Figure 56 presents the error for the displacements in the length of the truss, for live load UIC_50. The error is bigger closer to the supports because the value of displacement has a smaller value. The same behaviour can be observed where the models with higher error ar those where the connection of the cross beams was modified (models B). The pinned connection and the pinned in the minor axis (B0 and BM20) overestimate the

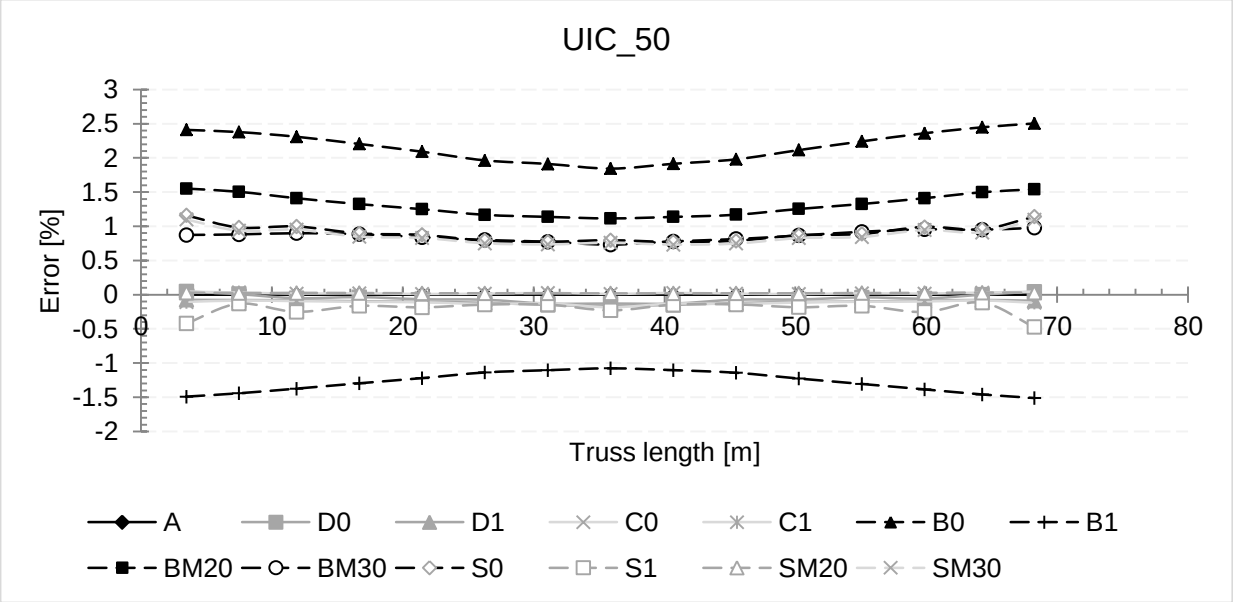

Figure 56. Error in displacements for live load.

displacements for 2 ans 1.5%. Considering the rigid connection in the crossbeams underestimates the displacements.

Figure 57 presents not the error but the difference between the vertical displacements of each model and the model A, in other words, the result for model A are in the horizontal axis. The results are presented in the length of the truss, for the dead load case (DEAD) and with live load at midspan (UIC_50). Here is easier to visualize the bigger difference in the displacements for models B and models S. It can be also noted that for the dead load, models B0 and BM20 produce similar results, but not in the live load, where the pinned condition in the crossbeam produces larger displacements.

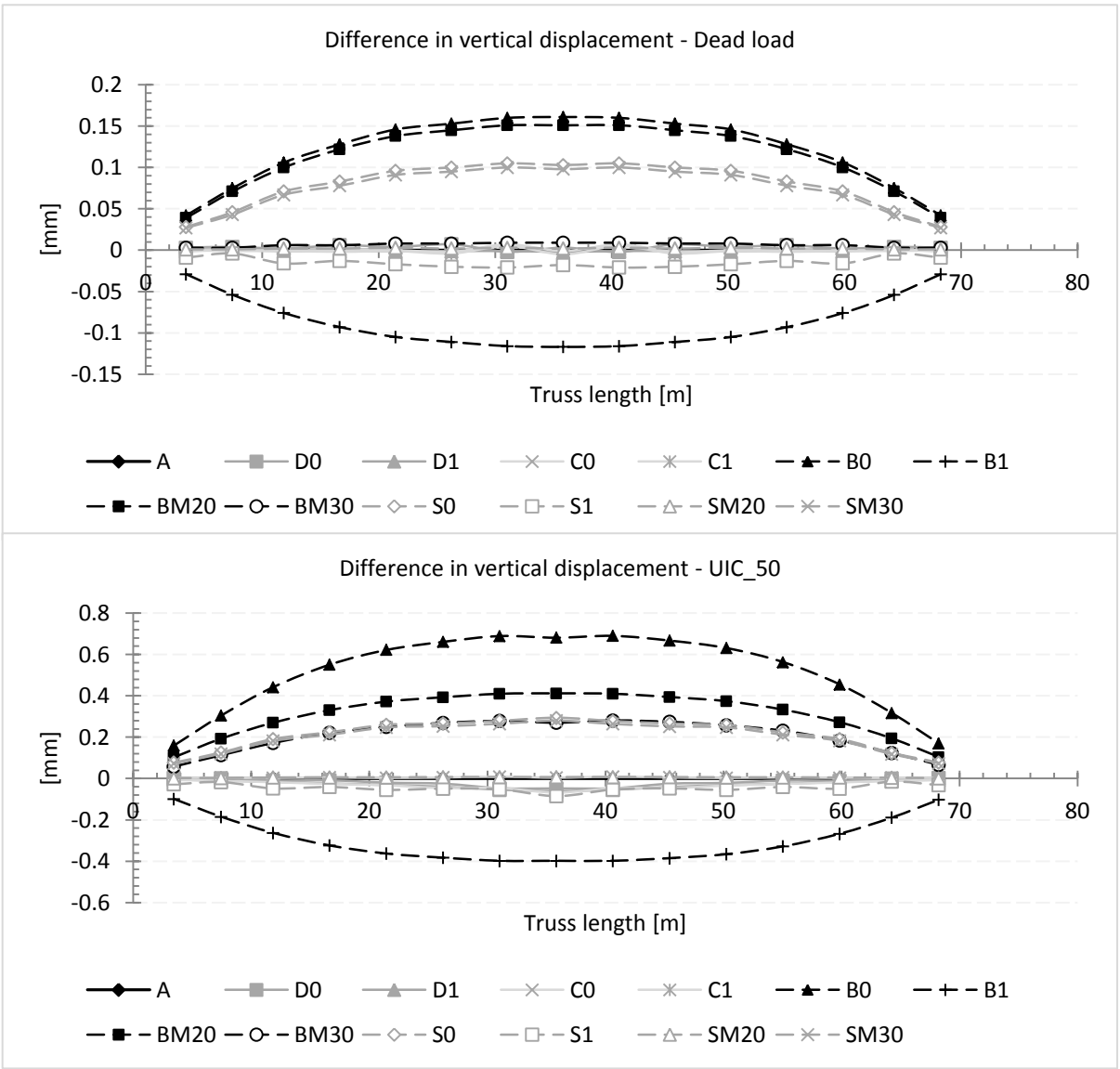

Figure 57. Displacements in the length of the truss.

The other two displacements graphs for the live load at 33% and 25% of the span, are similar to the response for load at 50% of the span, except for the models S, where the position of the load is reflected in the response, as depicted in Figure 58.

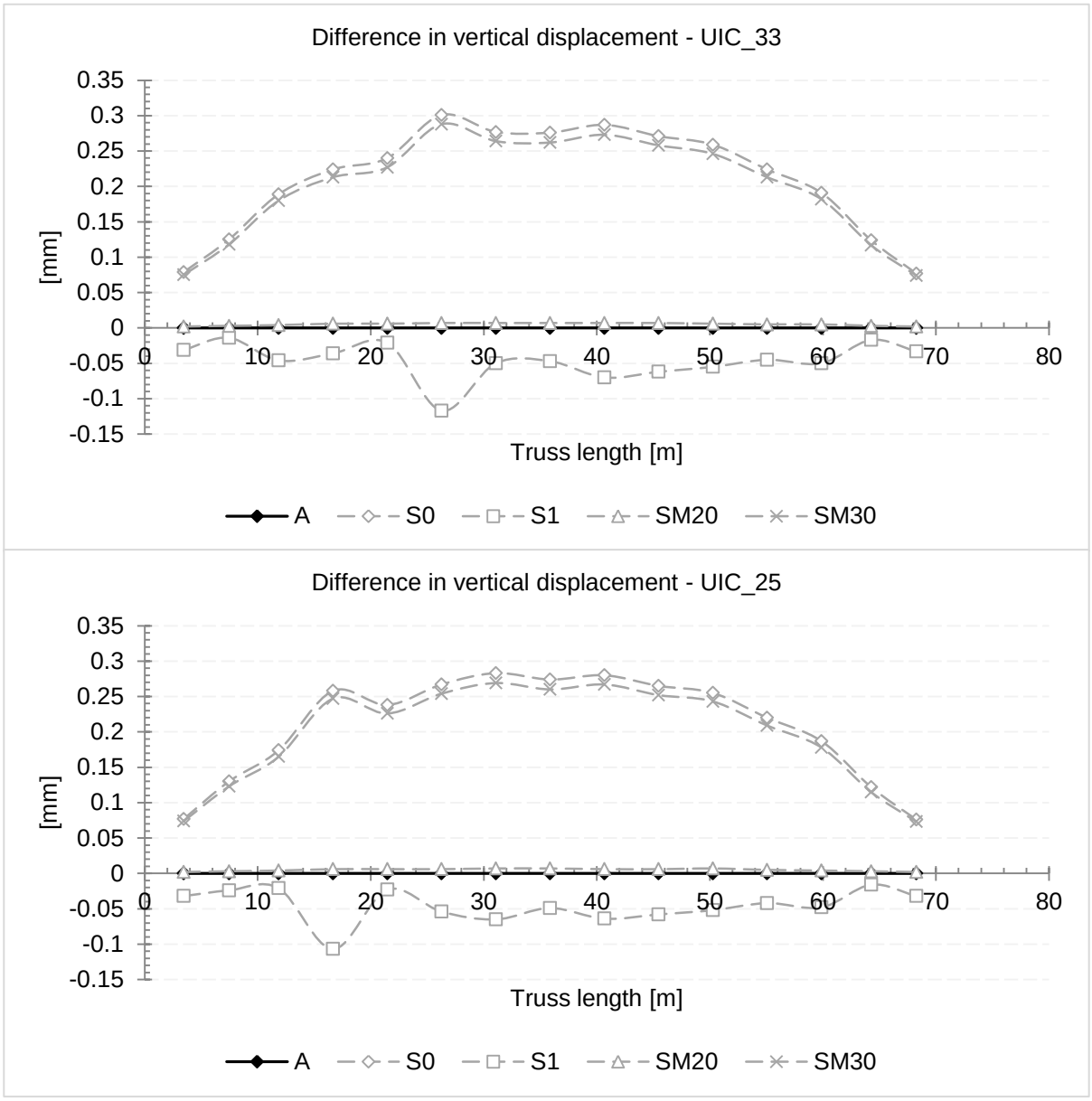

Figure 58. Difference between models S and models A, for load cases UIC_33 and UIC_25

5.5.2 Stresses in the truss.

Figure 59 shows the values of maximum stresses in the elements are summarized and 'normalized' according to the values for the model A. All the values were obtained for the same point, which was maximum in model A.

For the maximum stress, the parameter that influences the most in the result is the connection on the diagonals, as depicted for models D0 and D1. Model D0, the pinned connection, underestimate the stress in the elements around 20%, while the rigid connection in diagonals overestimates the stresses around 7%. This pattern is followed by the other models but with lower magnitude. In general, as it is expected, the pinned models result in a lower boundary and the rigid models an upper boundary for the stresses.

For the minimum stress, the parameter that influences the most in the results is the connections in the cross beam. It can be also noted the similarity of models B0 and BM30.

Finally, the connection of the stringer has no impact in the stresses of the truss.

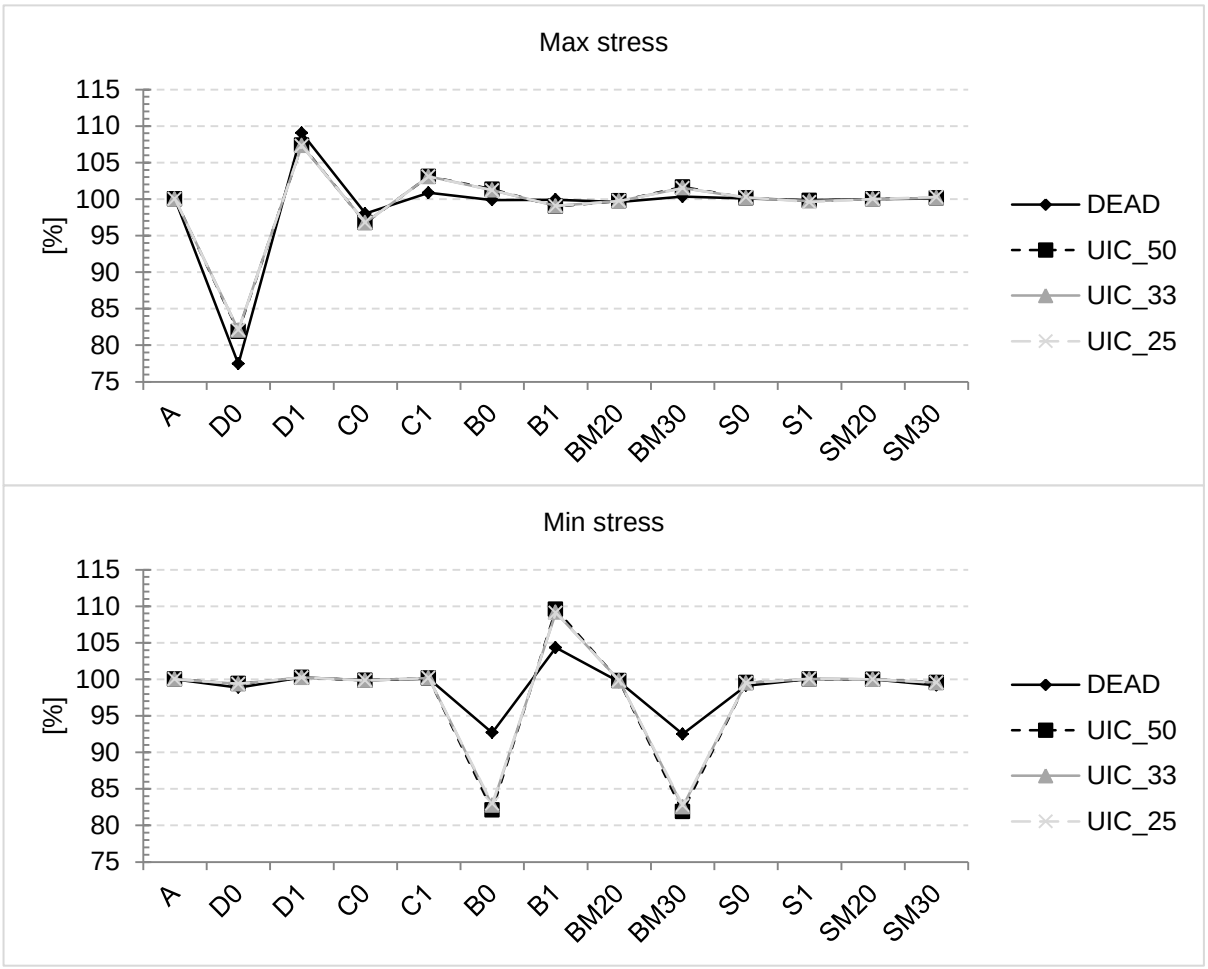

Figure 59. Maximum and minimum stresses in all the models.

5.5.3 Stresses in the deck.

Figure 60 presents the percentage of error for the maximum and minimum stress in all the crossbeams, in the same point as the one presented for model A. It can be noted that the error in the stress remains almost constant for the crossbeams, increasing only for the crossbeams close to the supports, and is practically zero for the crossbeam in frame 8. In the live load case (UIC_50), the error is gradually reduced from its maximum value close to the ends to practically zero at midspan crossbeam.

The models with more influence in the results are B (cross beam) and S (Stringer). Models B0 and BM20, present an increment of 30% in the stress of almost all the frames, model B1 underestimates the stresses around 20%. Model BM30 is more accurate for the stresses with an average error of 1.6%.

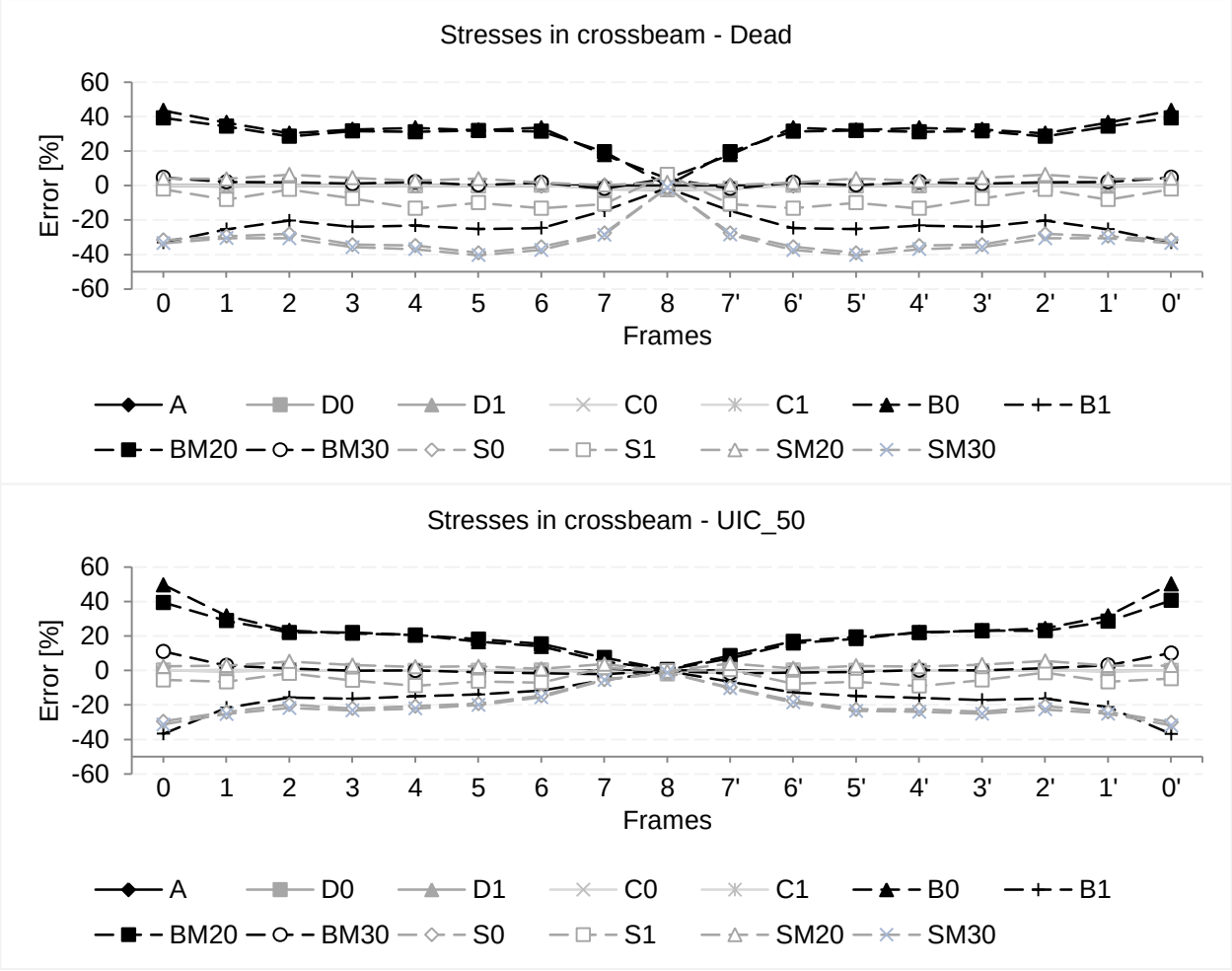

Figure 60. Error in the stresses on cross beams.

The stringer connection also underestimates the stresses in the crossbeam, models S0 and SM30 gives the less stresses, around 32%. Model S1 underestimates the stresses for 8%, and model SM20 has minimal error (3% average).

For the stresses in the stringers, Figure 61 presents the error calculated for the maximum stress under the dead load. Here it is really evident that the consideration of the connections in the stringers is what influences the most in the stresses. The greatest effect is in models S0 and SM30, where the connection on the stringer was considered as pinned. This increases the stresses nearly 150% on the elements closer to the supports and is rapidly reduce in the frame 2.

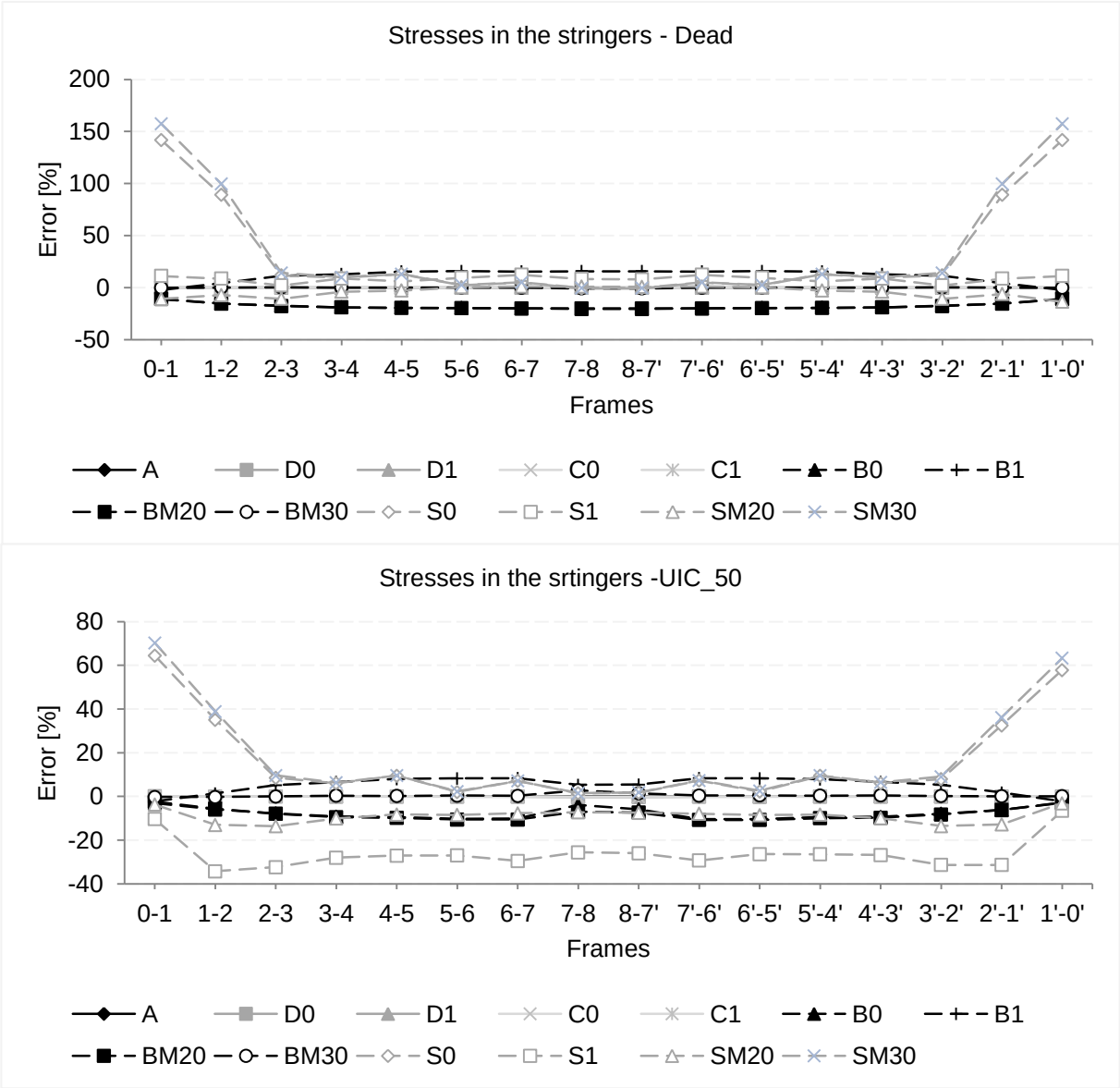

Figure 61. Error in the stresses on the stringers.

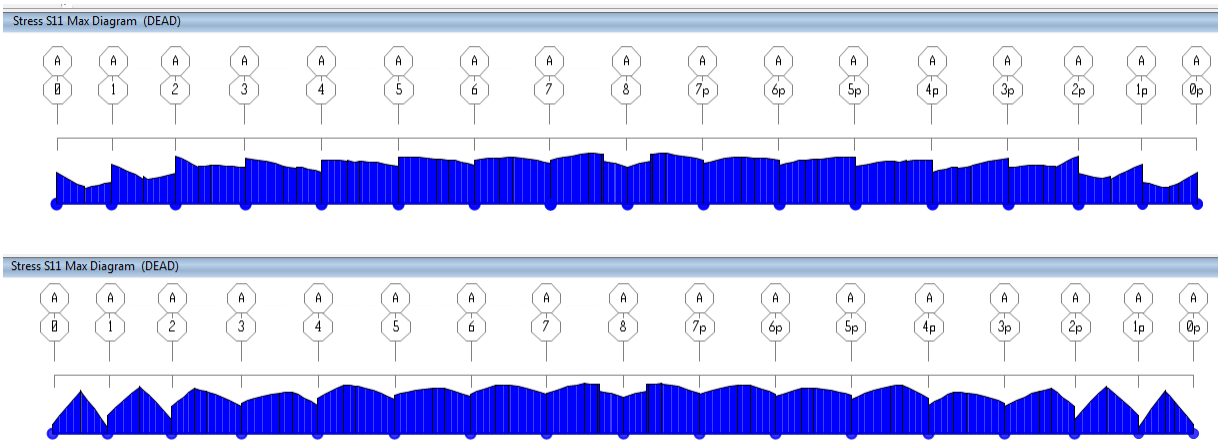

Figure 62. Maximum stresses in stinger for model A (top) and S0 (bottom).

This behaviour is better observed in Figure 62, where the maximum stresses are plotted for model A and model S0. The axial stress is increasing towards the center, as seen in Figure 53. In model S0, the stringer is a simply supported beam where the stress at midspan is maximum. In the adjacent elements, this effect is diminished for the axial stress that starts increasing, with similar values as the reference model, which is the behaviour observed in Figure 61.

The response for live load cases has some changes with respect to the dead load. The effect in the stringers close to the supports is 60% bigger than the reference model. Here is also noticeable that the model S1, the rigid connection, underestimates the stresses around 26 %.

The stresses in the stringer are also affected by the connection in the crossbeam, as noted from Figure 63. The pinned consideration on the crossbeams underestimates the stresses in the stringers around 17%, while the rigid consideration overestimates the stresses around 11%.

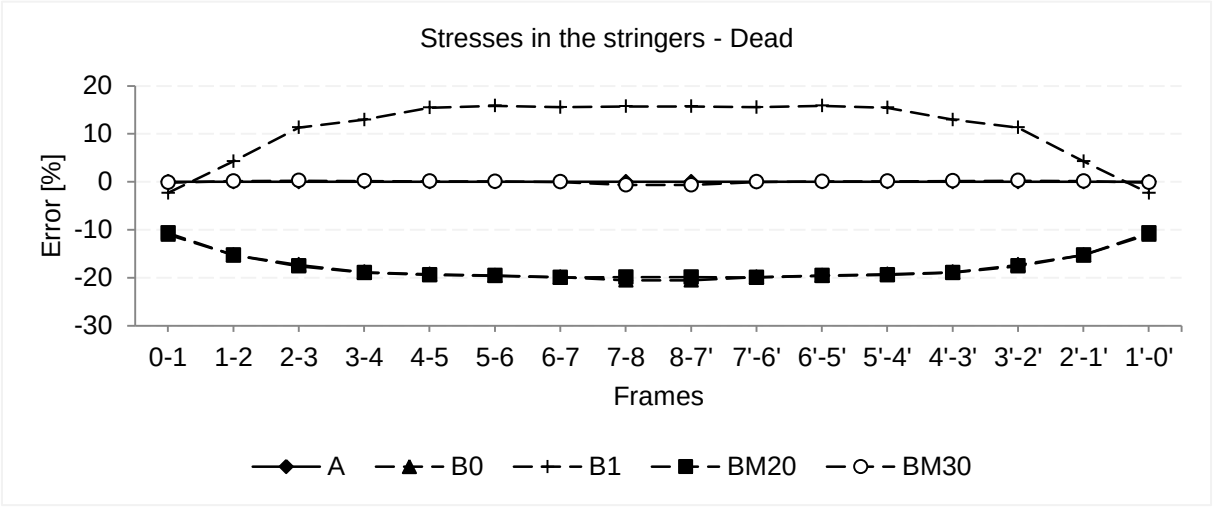

Figure 63. Stresses in stringer for different conditions on connections of crossbeams.

6. CONCLUSIONS

In this work analysis of connections of a steel bridge was done to investigate how the different considerations and in different elements influences in the general behaviour of the bridge. For this, the bridge used as real case is the steel railway bridge over the Vltavla River near Vysehrad, built on riveted steel truss. Connections were modelled in IDEA StatiCa software, and the results for each element are presented in section 3.3 and 3.2. The results are focused to characterize the behaviour in two sections: the truss on the loaded side, and the deck.

For the analysis of the connections, a linear relation between the moment of inertia of the element and the value of stiffness was obtained. Also, this relation can be observed in the number of rivets that are in the connection plates. This relationship, however, is more related with the strength required for the connection than for the contribution of each rivet to the rotational stiffness of the element. The analysis of more connections with different configurations needs to be done in order to define a simplified approximation of the stiffness of joints.

From the connections analysed in the truss, the value of stiffness obtained was between 15 and 40% of the boundaries between rigid and pinned connections. For the stringer and the crossbeam, the stiffness was between 5 and 15%.

The parametric analysis was performed modifying the connections conditions of the different elements.

For the vertical displacement in the truss, the biggest impact is with the connections of the crossbeam and, in a lower magnitude, the conditions in the stringer. The rigid condition resulted in displacements 1.5 to 2% bigger, while the pinned condition resulted in 1.5% of smaller displacements. The condition that adjusts the best to the results from the analysis of the joins is in the crossbeam when M3 = 0, and for the stringer when M2 = 0. The condition of the connections in the diagonals has negligible impact in the vertical displacements.

The stresses in the truss however, are highly influenced by the condition on the diagonals and in the case of minimum stress, by the condition of the crossbeam. The pinned assumption in diagonals underestimates the stresses by 20%, while the rigid assumption overestimates them by 7%. For the crossbeams, the minimum stresses located in vertical elements close to the supports, are overestimated 10% with the rigid assumption and underestimated around 15% in the pinned cases.

In the deck, the stresses in the crossbeams are highly influenced by their connections and with lower impact for the connections in the stringers. The composition of this stresses on the crossbeam is practically due to bending forces, (the axial stress is merely 3% of the total stress). The pinned

assumption in the crossbeams reduces the stresses around 20% while the rigid assumption increases these values to more than 30% for dead load case.

For the stringers, the stresses are highly affected by their connection conditions. The pinned connection increases the stresses more than 100%, but these elements are usually small and their connections are closer to the pinned assumption, for which the error is less than 50% in the stringers close to the supports. Also, the stresses in the stringers are influenced by the connections on the crossbeam, increased more than 10% if the connection in the crossbeam is rigid, and decreased more than 15% if the connection in the crossbeam is pinned.

Finally, it is shown that the connection condition with most impact in the general behaviour of the bridge is the crossbeam, affecting not only the deck but also the stresses in the truss.

REFERENCES

[1] Institute for Steel Development & growth, "Chapter 27 - Trusses," 2011. [Online]. Available: http://www.steel-insdag.org/TeachingMaterial/chapter27.pdf. [Accessed 28 06 2017].

[2] Institute for Steel Development & growth., "Chapter 43 - Steel bridges - I," 2011. [Online]. Available: http://www.steel-insdag.org/TeachingMaterial/chapter43.pdf. [Accessed 28 06 2017].

[3] B. K. e. al, "Assessment of Existing Steel Structures: Recommendations for Estimatiion of Remaining Fatigue Life.," JRC Scientific and Technical Reports, Luxemburg, 2008.

[4] J. W. F. J. H. A. S. Geoffrey L. Kulak, Guide to Design Criteria for Bolted and Riveted Joints, Chicago: AISC, 2001.

[5] I. Lyse, "Advantages of welding in continuous structures," *Welding Journal,* no. Paper 1186, 1935.

[6] R. T. L. B. E. S. C. W. R. G.P. foricera, "Sesimic performance of riveted connections," *Journal of constructional steel research,* no. 58, pp. 779-799, 2002.

[7] C. a. D. N. Person, "Collapse of the Quebec Bridge," *J.Perform.Constr.Facil.,* vol. 1, no. 20, pp. 84-91, 2006.

[8] C. y. a. K. Jackson, "The relative rigidity of welded and riveted connections," *Can J Res,* vol. 1, no. 11, pp. 62-134, 1934.

[9] H. B. A. B. M. M. M.E. Kartal, "Effects of Semi-rigid Connections on Structural Responses," *Electronic Journal of Structural Engineering,* no. 10, pp. 22-35, 2010.

[10] T. D. R. M. K. C. Boulent M. Imam, "Numerical modelling of riveted railway bridge connections for fatigue evaluation.," *Engineering Structures.,* no. 29, pp. 3071 - 3081, 2007.

[11] R. K. M. Al-Emrani, "FE analysis of stringer-to-floor-beam connections in riveted ralway bridges," *Journal of constructional steel research.,* no. 59, pp. 803-818, 2003.

[12] J. J. a. J. G. J. Vican, "Determination of Fatigue Category and nNumerical Analysis of the Stringer to Crossbeam Connection of Riveted Steel Railway Bridges.," *Procedia Engineering,* no. 40, pp. 177-182, 2012.

[13] T. D. R. Boulent M. Imam, "Fatigue evaluation of riveted railways bridges through global and local analysis.," *Journal of Constructional steel research. ,* no. 66, pp. 1411-1421, 2010.

[14] E. M. L. a. W. F. Chen, "Steel Frame Analysis with Flexible Joints.," *J. Construct, Steel Research,* no. 8, pp. 161-202, 1987.

[15] CEN, Eurocode 3 - "design of steel structures" part.1-8: Design of joints., Brussels, 2005.

[16] F. C. T. gomes, "The EC3 Classification of joints and alternative proposals.," *Eurosteel,* no. 19-20, pp. 987-996, 2002.

[17] K. W. J. J. C. M. J. F. Bemonceau, "Application of Eurocode 3 to steel connecions with four bolts per horizontal row.," in *SDSS Rio 2010 Stability and Ductility of Steel Structures.*, Rio de Janeiro, BRazil., 2010.

[18] F. Kutina, "C.5.1 - Analyza tuhost sticniku," SUDOP PRAHA a.s., Praha, 2015.

[19] T. Kovárník, "Železniční doprava v USA a v ČR," [Online]. Available: http://lide.gymcheb.cz/~tokovar/vos/svetovahistorie.html. [Accessed 29 Jun 2017].

[20] Správa železniční dopravní cesty, "History of our Railway in a Nutshell," [Online]. Available: http://www.szdc.cz/en/o-nas/zeleznice-cr.html. [Accessed 29 June 2017].

[21] "Pražský svět," 5 02 2012. [Online]. Available: http://homolinka2.blog.cz/1202/vysehradsky-most. [Accessed 3 05 2017].

[22] "ZelPage," Jiří Průša, 20 10 2007. [Online]. Available: http://www.zelpage.cz/clanky/historie-vyhybny-praha-vysehrad?lang=cs. [Accessed 03 05 2017].

[23] IDEA StatiCa Connection, "IDEA StatiCa - Theoretical background," 06 2017. [Online]. Available: https://www.ideastatica.com/resource/#02_Steel/Theoretical_background/IDEA_Connection_Theoretical_Manual_EN_ver_8_1.pdf%3FTocPath%3DSteel%7C_____8. [Accessed 21 06 2017].

[24] Správa železniční dopravní cesty, Metodický Pokyn Pro Určování Zatížitelnosti Železničních Mostních Objektů, Praha: SŽDC, 2015.

[25] F. Kramoliš, Fatigue assessment of the railway, Prague: Czech Technical University in Prague, 2017.

[26] Computers and Structures, Inc., CSI Analysis Reference Manual, California, USA, 2016.

ANNEX A – DETAILS OF CONNECTIONS.

The following drawings are the details of connections, the sections used for the analysis and the dimensions of plates that were used in the building of the models of the joints. All the dimensions are in mm, and the stiffness is in MN·m/rad.

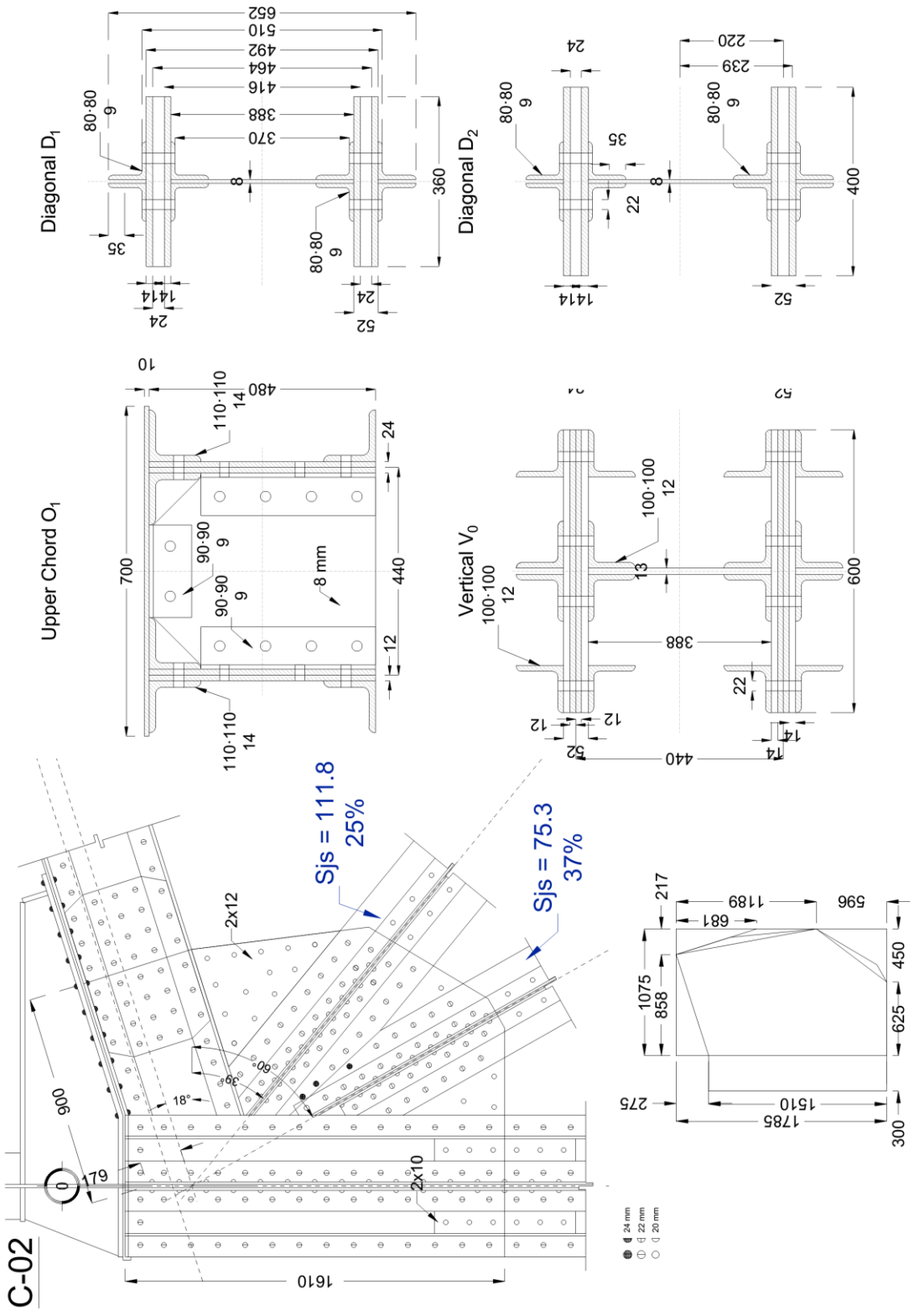
Diagonal D1
Diagonal D2
Upper Chord O1
Vertical V0
C-02
Sjs = 111.8
25%
Sjs = 75.3
37%
2x12
2x10
8 mm
1610
900
179
18°
39°
60°
24 mm
22 mm
20 mm

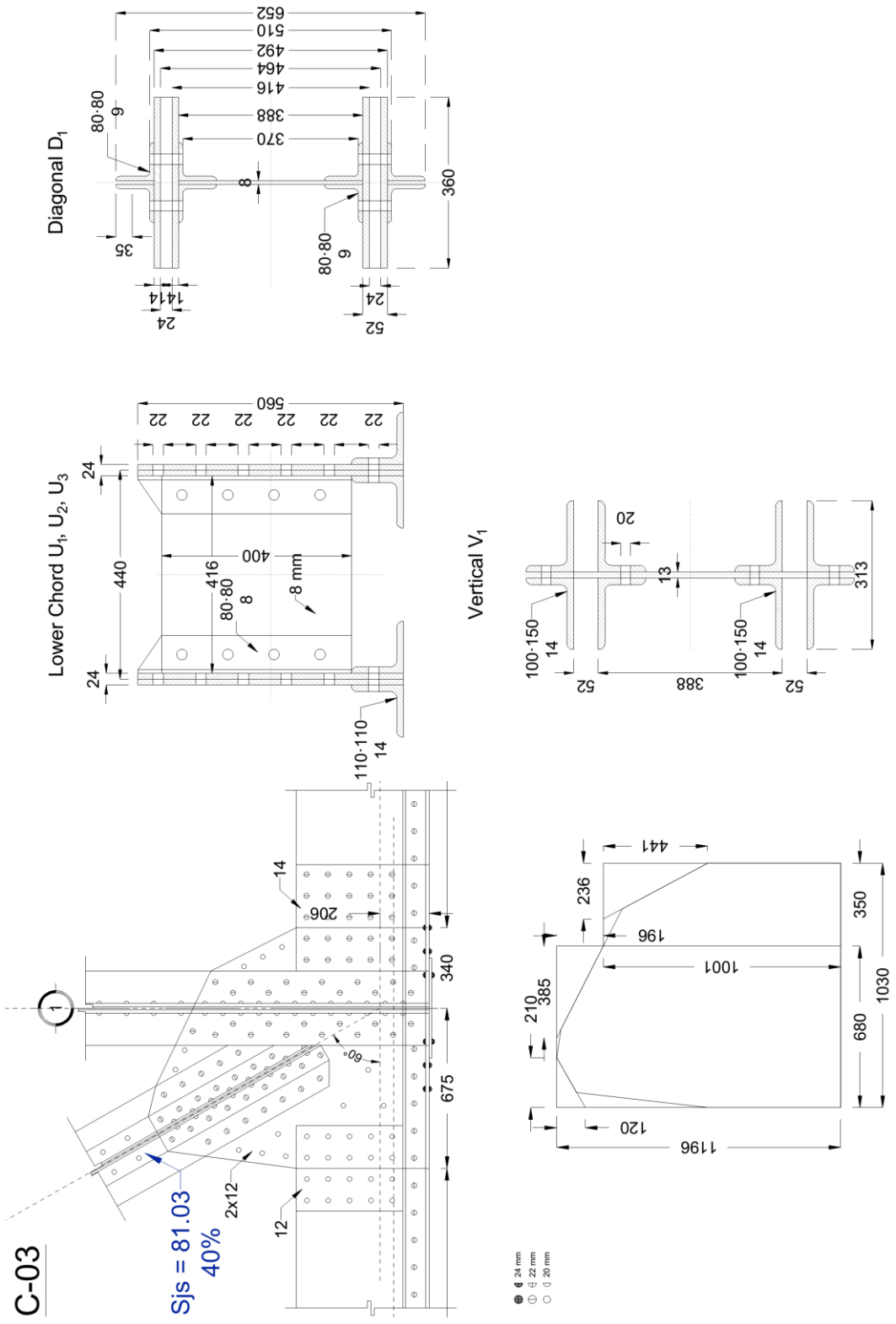
Diagonal D1
652
510
492
464
416
388
370
80·80
6
8
360
35
24
14
14
24
52
Lower Chord U1, U2, U3
560
22
22
22
22
22
22
24
440
24
400
416
80·80
8
8 mm
110·110
14
Vertical V1
20
13
313
100·150
14
52
388
52
C-03
Sjs = 81.03
40%
2x12
12
14
206
340
675
60°
441
236
196
1001
350
210
385
680
1030
120
1196
24 mm
22 mm
20 mm

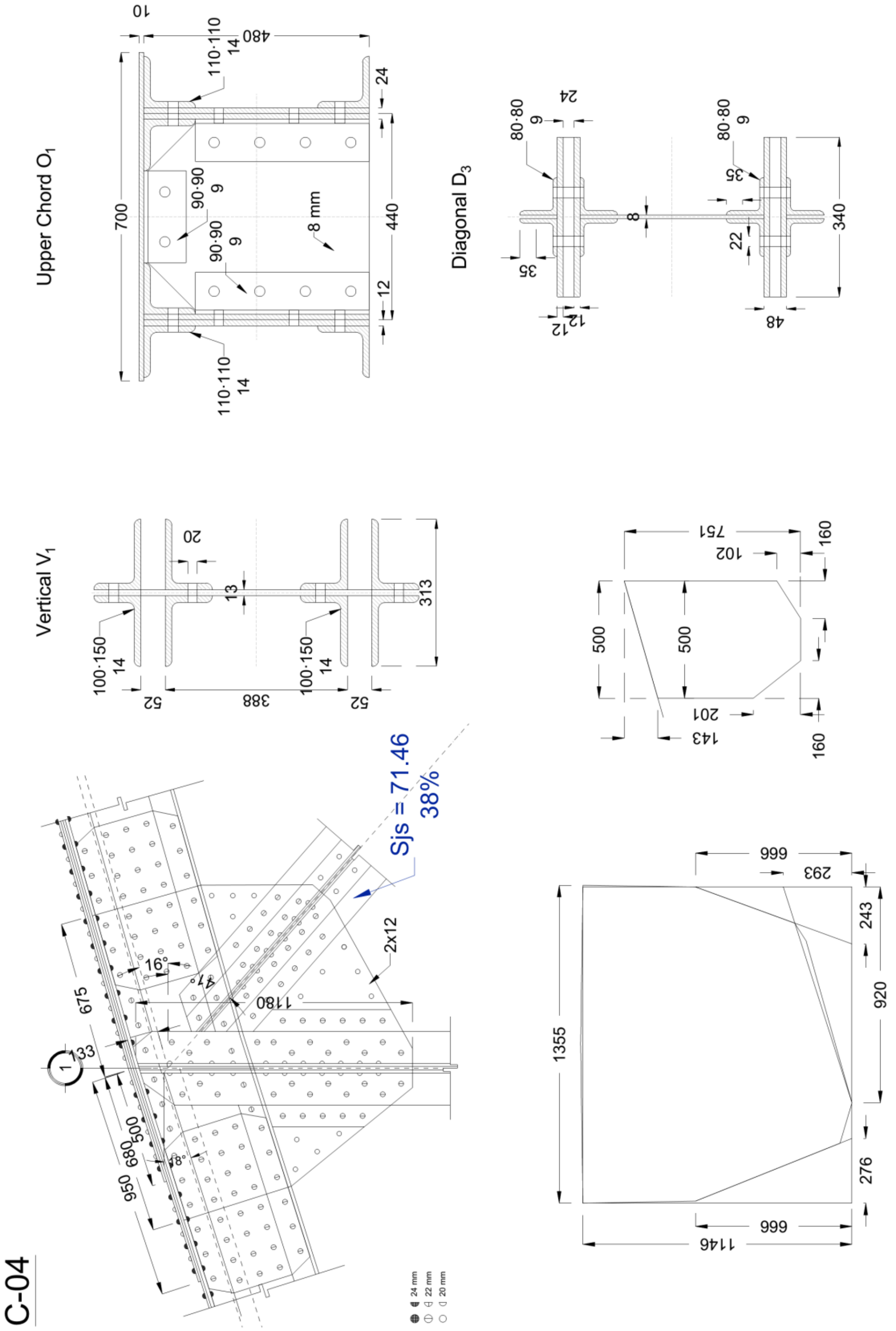
C-04
Upper Chord O1
Diagonal D3
Vertical V1
Sjs = 71.46
38%
2x12
24 mm
22 mm
20 mm

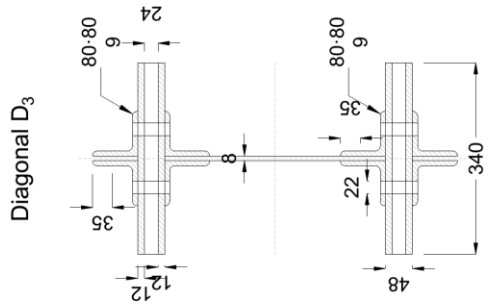
Diagonal D3
80·80
6
24
8
35
22
340
12
12
48

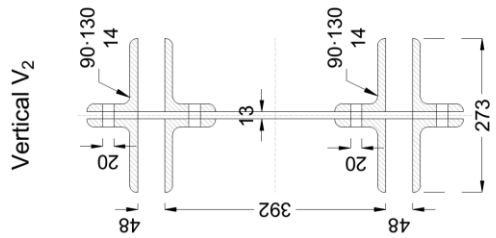
Vertical V2
90·130
14
13
20
273
392
48

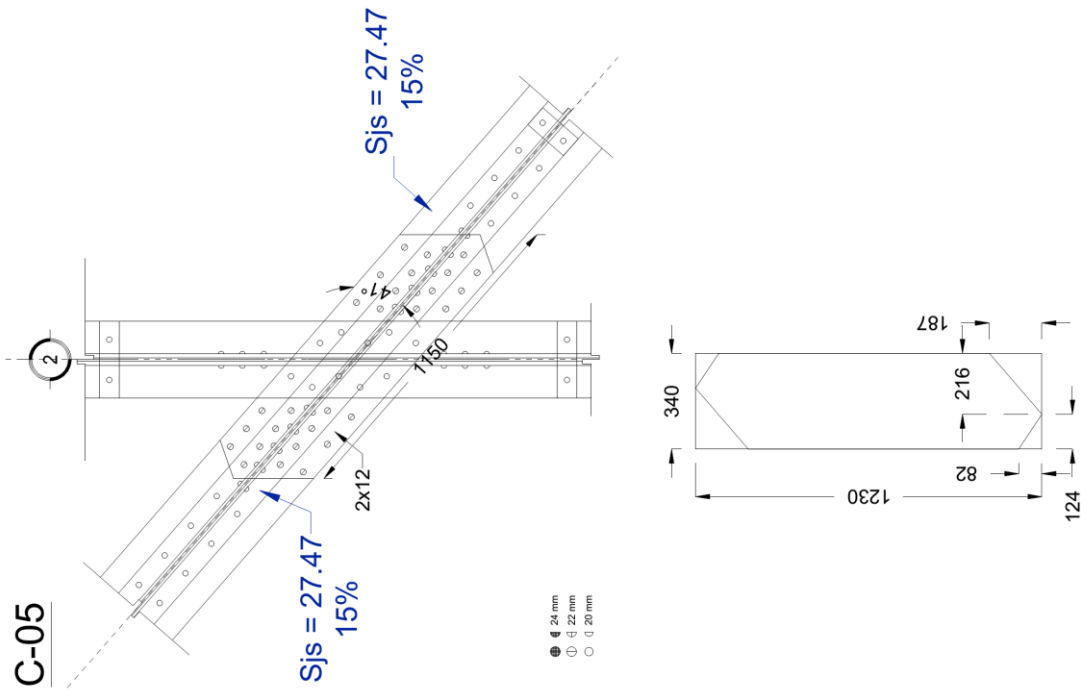
Sjs = 27.47
15%
47°
1150
2x12
Sjs = 27.47
15%
C-05
24 mm
22 mm
20 mm
187
216
340
82
1230
124

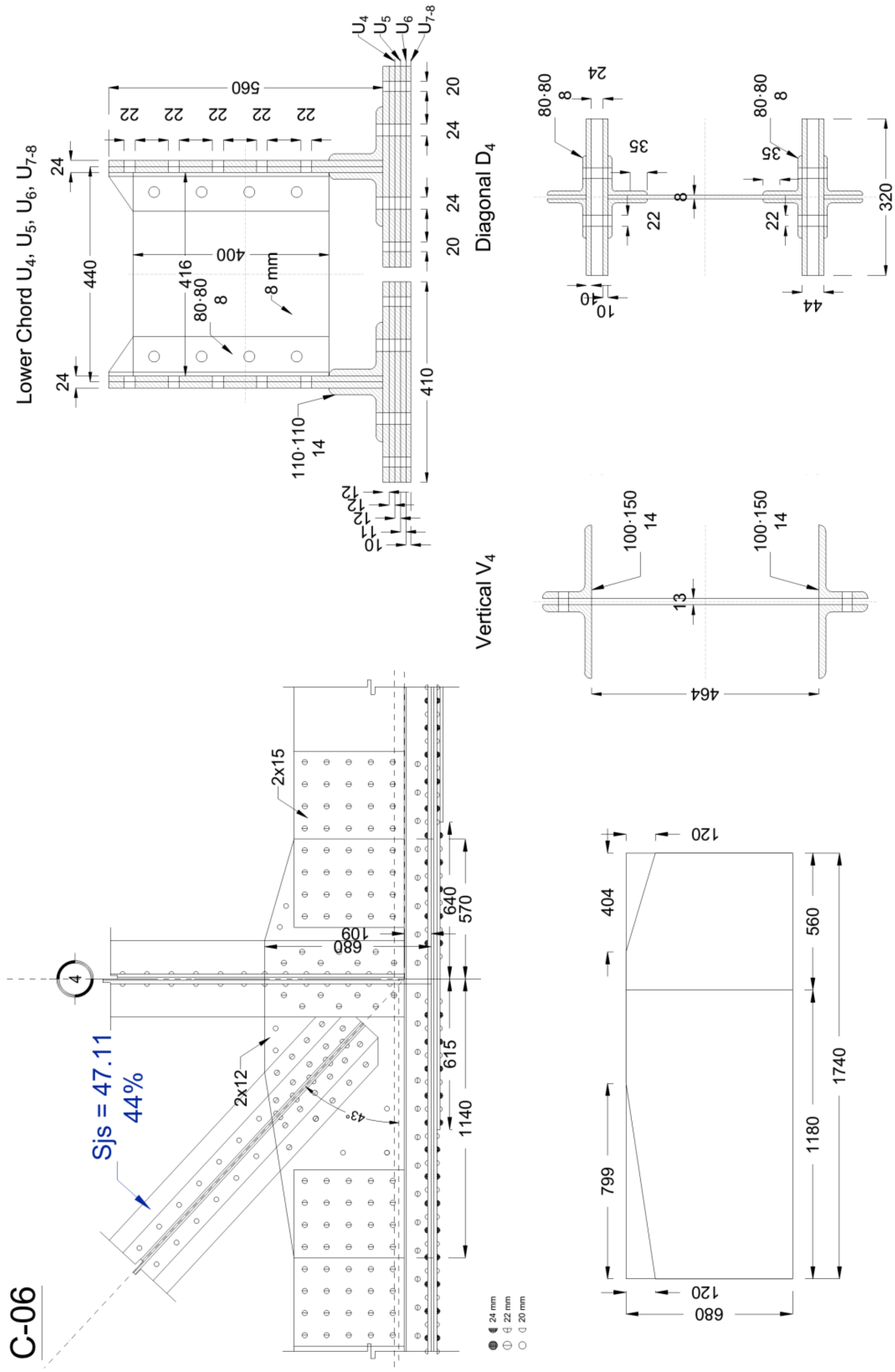
C-06
Lower Chord U4, U5, U6, U7-8
Diagonal D4
Vertical V4
Sjs = 47.11
44%
2x15
2x12

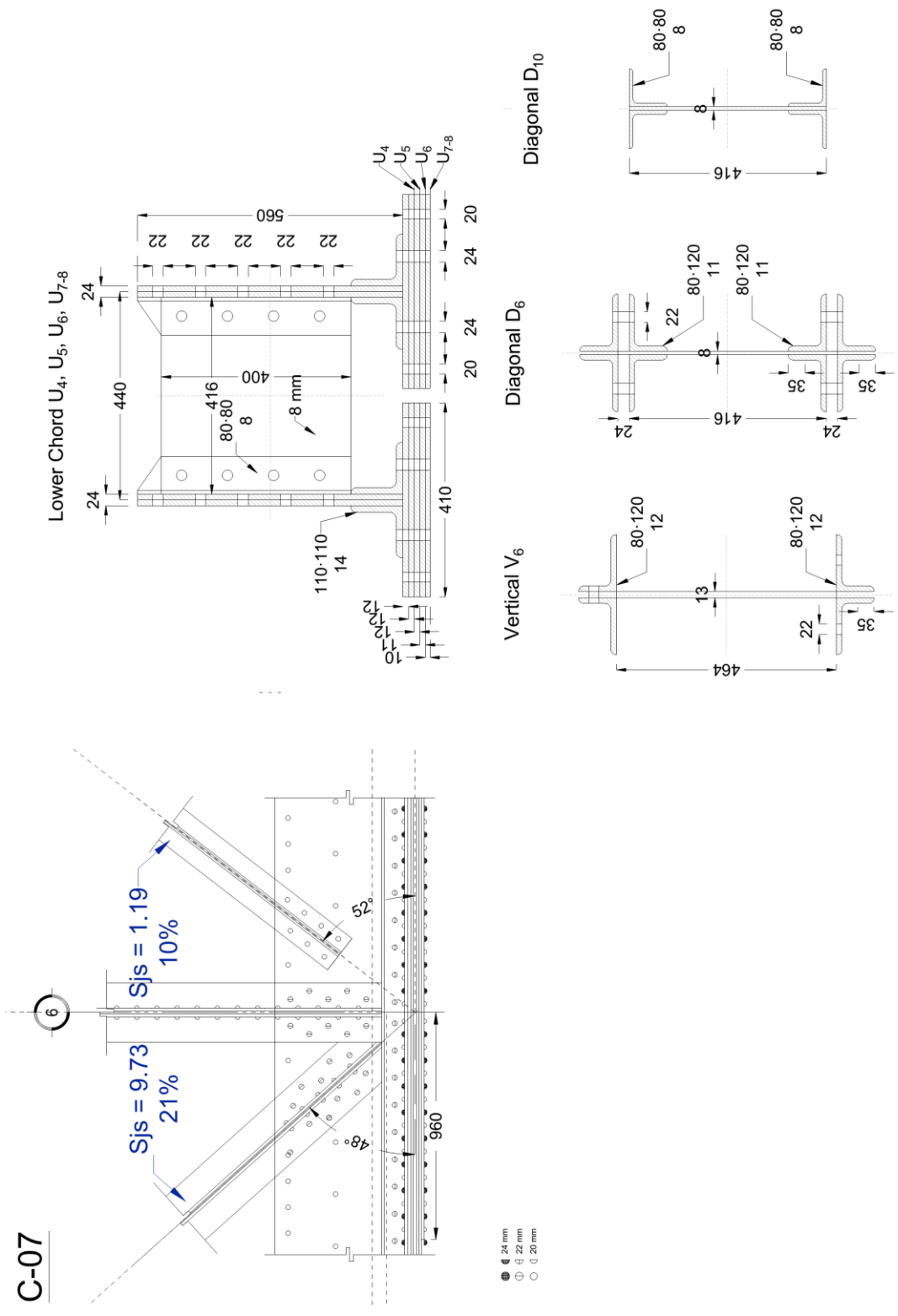
C-07
Sjs = 1.19
10%
Sjs = 9.73
21%
52°
48°
960
Lower Chord U4, U5, U6, U7-8
Diagonal D10
Diagonal D6
Vertical V6
U4
U5
U6
U7-8
560
22
400
416
440
410
80·80
8
8 mm
110·110
14
80·120
11
12
13
464
24 mm
22 mm
20 mm

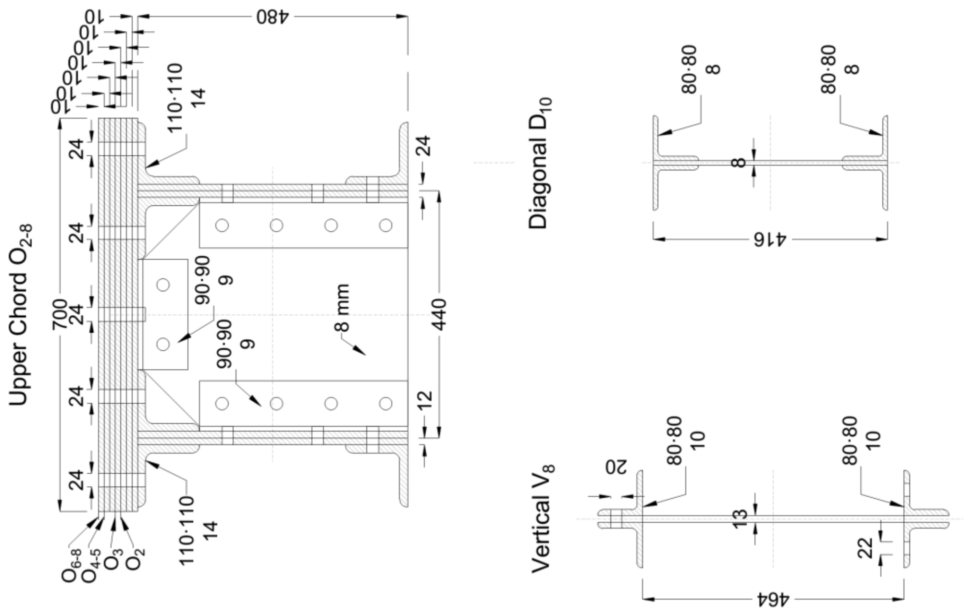
Upper Chord $O_{2\text{-}8}$
Diagonal D_{10}
Vertical V_8

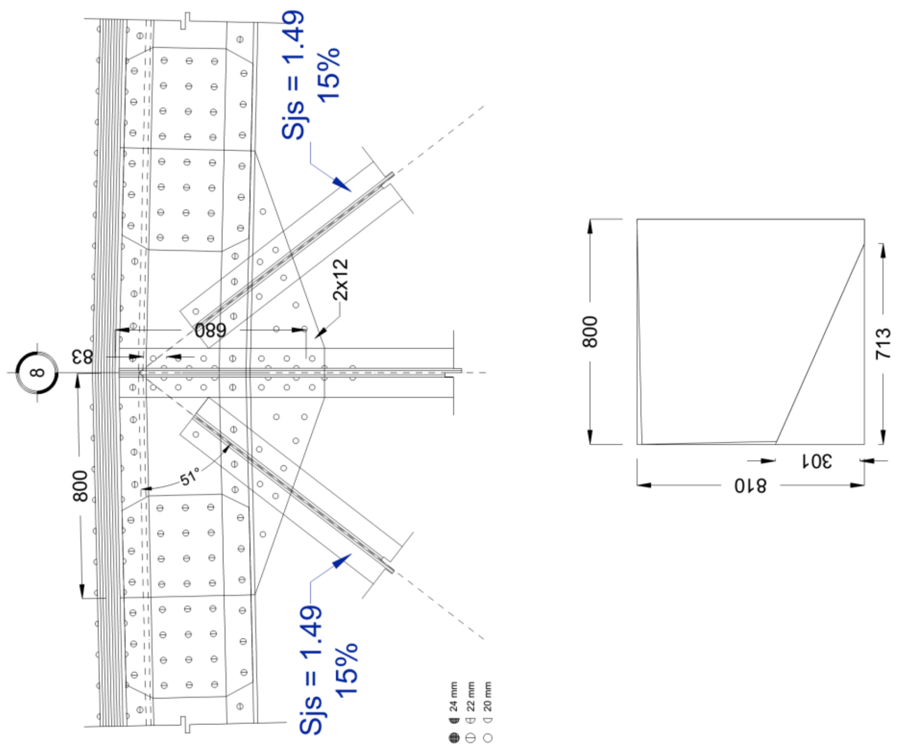
Sjs = 1.49
15%
Sjs = 1.49
15%

C-08

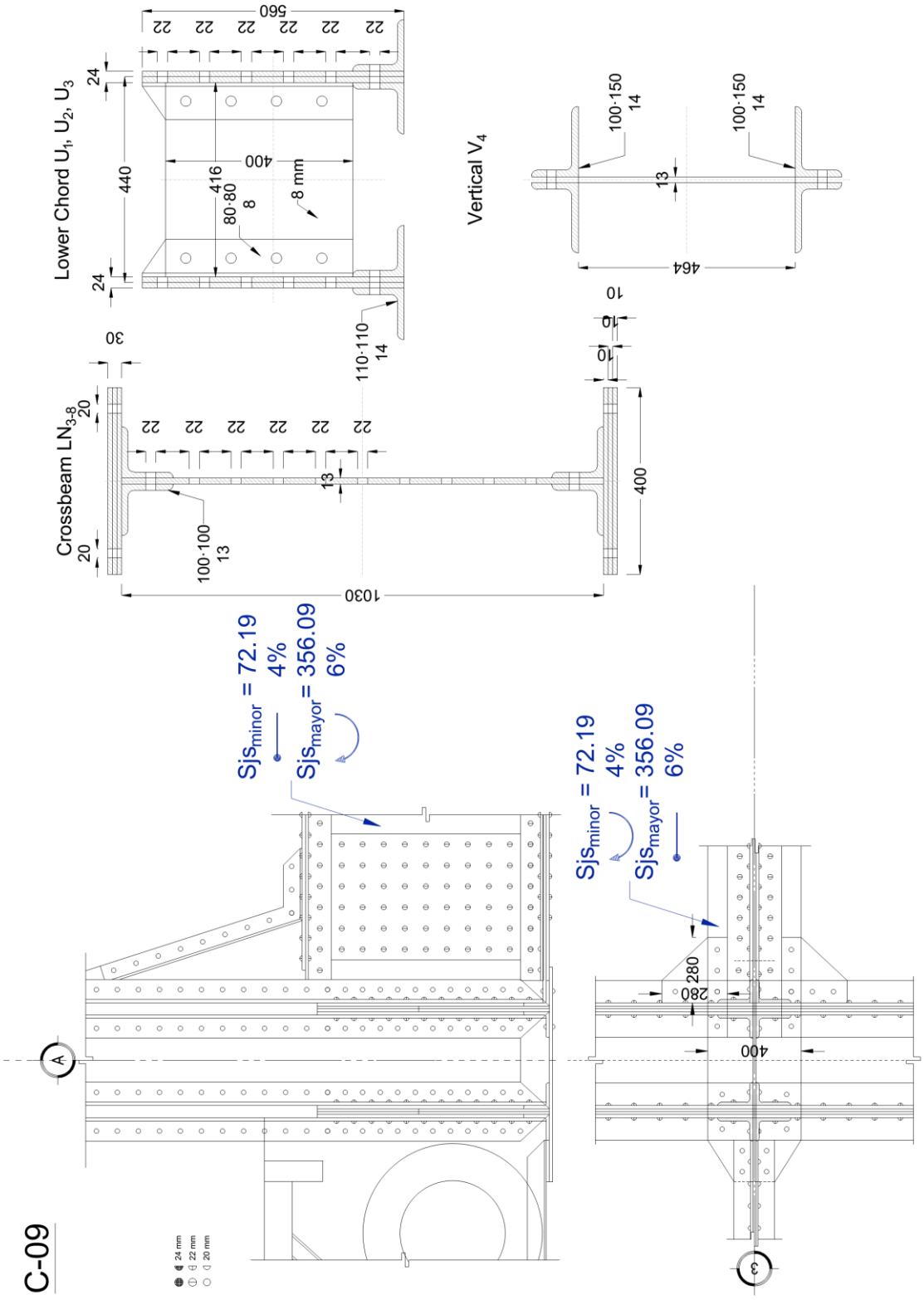
Lower Chord U_1, U_2, U_3
Vertical V_4
Crossbeam LN_{3-8}
560
440
400
416
80·80
8
8 mm
24
110·110
14
100·150
14
464
13
30
20
100·100
1030
Sjs_{minor} = 72.19
4%
Sjs_{mayor} = 356.09
6%
280
C-09

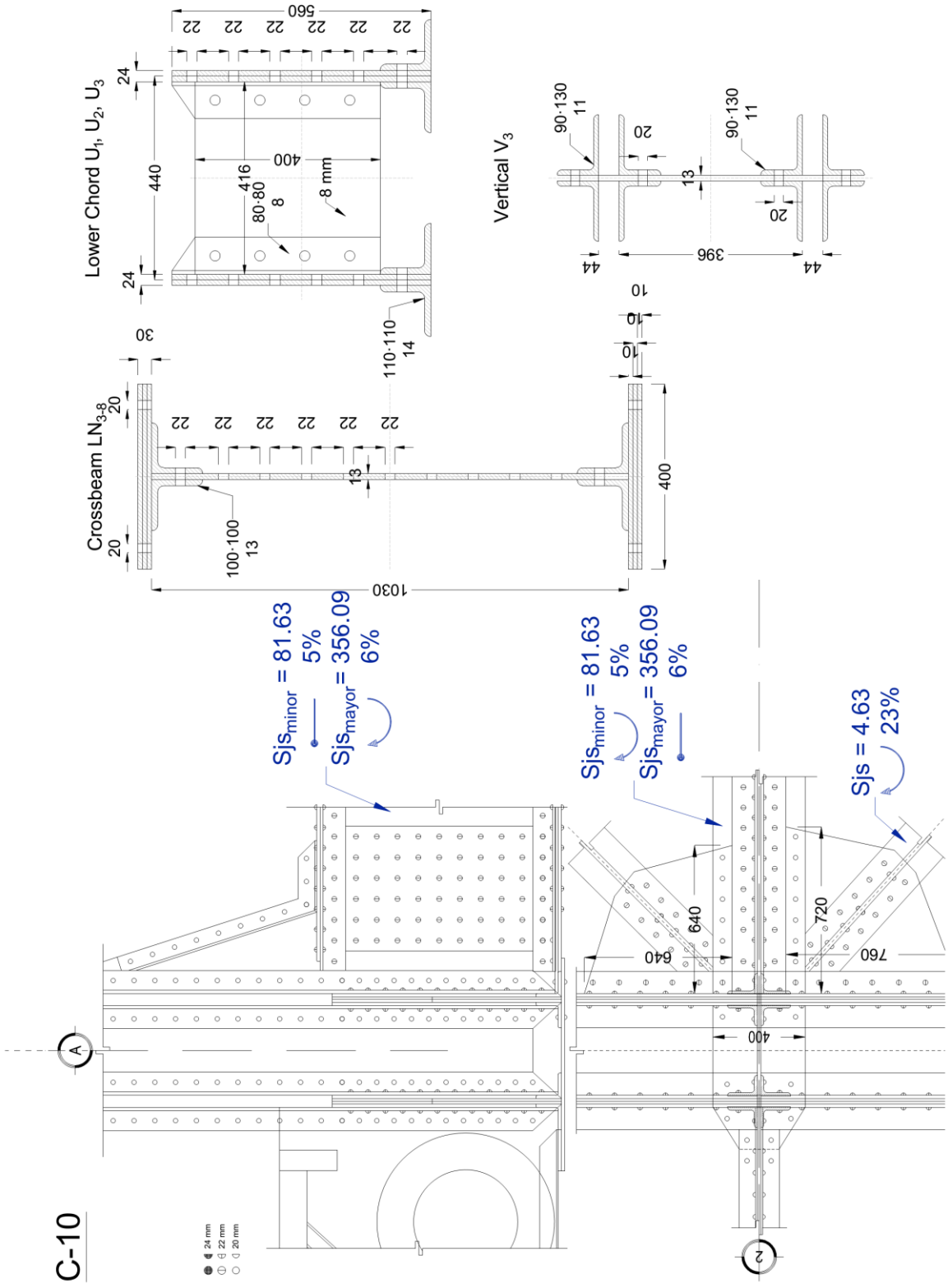
Lower Chord U_1, U_2, U_3
Vertical V_3
Crossbeam LN_{3-8}
Sjs_{minor} = 81.63 5%
Sjs_{mayor} = 356.09 6%
Sjs_{minor} = 81.63 5%
Sjs_{mayor} = 356.09 6%
Sjs = 4.63 23%
C-10

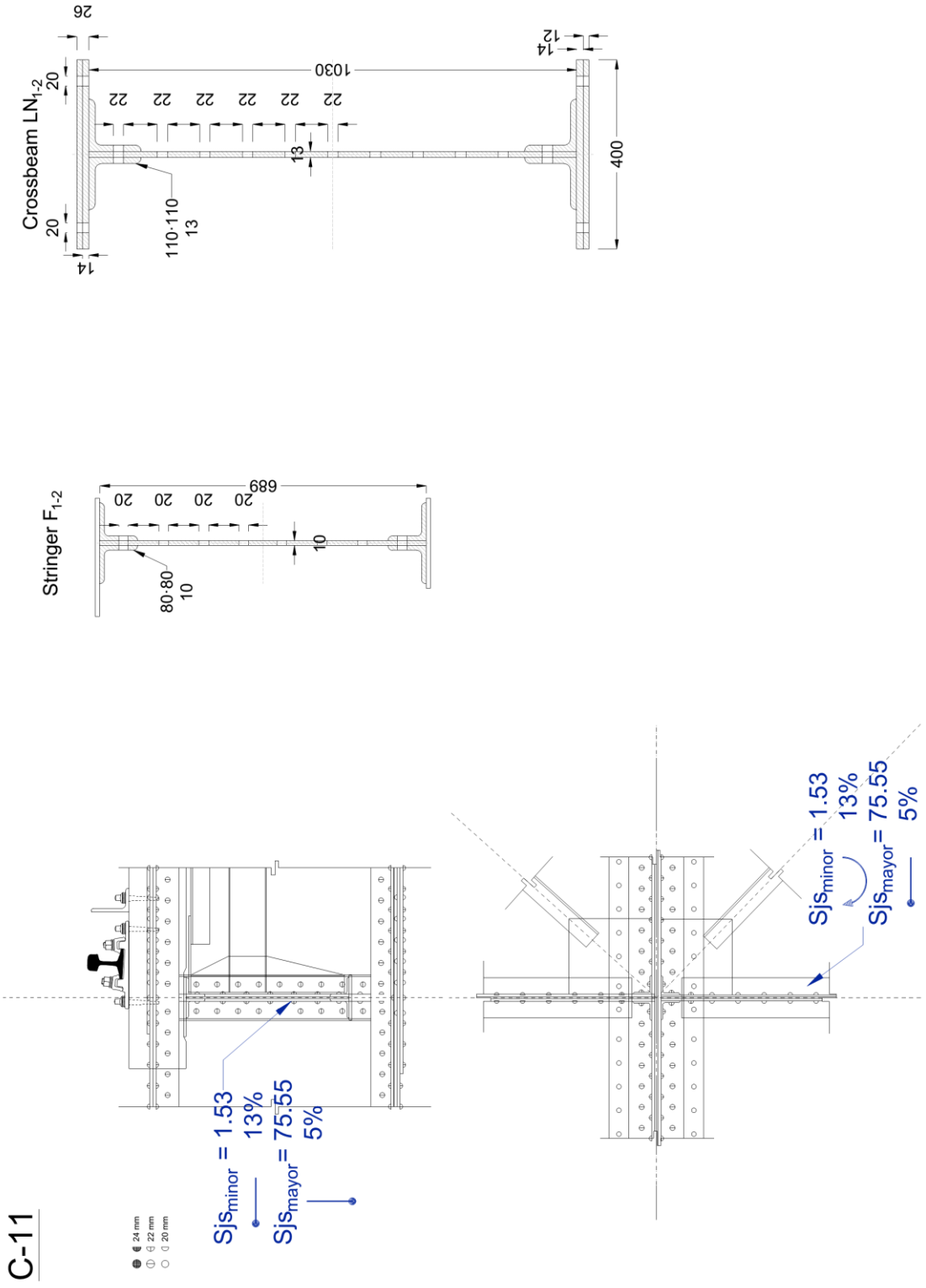
Crossbeam LN1-2
26
20
20
14
22 22 22 22 22 22
1030
13
400
110·110
13
12
14
Stringer F1-2
689
20 20 20 20
10
80·80
10
C-11
Sjsminor = 1.53
13%
Sjsmayor = 75.55
5%
Sjsminor = 1.53
13%
Sjsmayor = 75.55
5%
24 mm
22 mm
20 mm